Journal of
Medicinal Chemistry

Article

Discovery of (1H-Pyrazolo[3,4-c]pyridin-5-yl)sulfonamide Analogs as Hepatitis B Virus Capsid Assembly Modulators by Conformation Constraint

Chunting Wang, Yameng Pei, Lin Wang, Shuo Li, Chao Jiang, Xu Tan, Yi Dong, Ye Xiang, Yao Ma, and Gang Liu

J. Med. Chem., **Just Accepted Manuscript** • DOI: 10.1021/acs.jmedchem.0c00292 • Publication Date (Web): 18 May 2020

is published by the American Chemical Society. 1155 Sixteenth Street N.W., Washington, DC 20036

Discovery of (1*H*-Pyrazolo[3,4-c]pyridin-5-yl)sulfonamide Analogs as Hepatitis B Virus Capsid Assembly Modulators by Conformation Constraint

Chunting Wang[1,#], Yameng Pei[1,3#], Lin Wang[4], Shuo Li[5], Chao Jiang[5], Xu Tan[5], Yi Dong[2], Ye Xiang[4,],Yao Ma[2,*], Gang Liu[1,*]*

1, School of Pharmaceutical Sciences, Tsinghua University, Beijing 100084, China.

2, Institute of Materia Medica, Chinese Academy of Medical Sciences & Peking Union Medical College, Beijing 100050, China.

3, Tsinghua-Peking Center for Life Sciences, Tsinghua University, Beijing 100084, China.

4, Beijing Advanced Innovation Center for Structural Biology, Collaborative Innovation Center for Diagnosis and Treatment of Infectious Diseases, Center for Global Health and Infectious Diseases, Department of Basic Medical Sciences, School of Medicine, Tsinghua University, Beijing 100084, China.

5, Beijing Advanced Innovation Center for Structural Biology, Beijing Frontier Research Center for Biological Structure, School of Pharmaceutical Sciences, Center for Infectious Disease Research, School of Medicine, Tsinghua University, Beijing 100084, China.

Key words: Hepatitis B; capsid assembly; conformation constraint; pro-drug

Abstract: Hepatitis B virus (HBV) capsid assembly modulators (CAMs) have been suggested to be effective anti-HBV agents in both preclinical and clinical studies. In addition to blocking HBV replication, CAMs could reduce the formation of covalently closed circular DNA (cccDNA), which accounts for the persistence of HBV infection. Here, we describe the discovery of (1*H*-indazole-5-yl)sulfonamides and (1*H*-pyrazolo[3,4-c]pyridin-5-yl)sulfonamides as new CAM chemotypes by constraining the conformation of the sulfamoylbenzamide derivatives. Lead optimization resulted in compound **56** with an EC_{50} value of 0.034 μM and good metabolic stability in mouse liver microsomes. To increase the solubility, the amino acid prodrug (**65**) and its citric acid salt (**67**) were prepared. Compound **67** dose-dependently inhibited HBV replication in a hydrodynamic injection-based mouse model of HBV infection, while **56** did not show *in vivo* anti-HBV activity, likely owing to its sub-optimal solubility. This class of compounds may serve as a starting point to develop novel anti-HBV drugs.

Introduction

Chronic hepatitis B (CHB), caused by infection of the hepatitis B virus (HBV), is one of the major infectious diseases in the world, leading to approximately 887,000 deaths in 2015.[1] Although the worldwide application of efficient HBV vaccines greatly decreased morbidity, approximately 257 million people still live with CHB. CHB tremendously increases the risk of developing cirrhosis and hepatic carcinoma, which are the leading causes of mortality for CHB patients.[1] Two classes of drugs, nucleos(t)ide analogs (NAs) and interferon (IFN), have been approved for the treatment of CHB. For most patients, entecavir and two prodrugs of tenofovir, namely tenofovir

disoproxil fumarate and tenofovir alafenamide, are recommended as the first-line treatment because of their high potency, good safety profile and very low probability of developing resistance after long-term treatment.[2] However, these NAs only inhibit the replication of HBV and cannot disturb its persistence in hepatocytes. HBV surface antigen (HBsAg) loss, which is considered as a functional cure, is only achieved in less than 10% of patients after five years of treatment.[3] The major reason for HBV persistence is the formation of covalently closed circular DNA (cccDNA) in the nucleus of host cells, which is very stable and acts as a template for HBV transcription.[4, 5] IFN has been reported to decrease the amount of cccDNA[6] and result in HBsAg seroclearance more frequently than NAs with a 58% cure rate in genotype A infection.[7, 2] However, the severe side effects and limited efficiency of other genotypes of HBV infection have hindered its use in the clinic.[2]

Capsid assembly modulators (CAMs) have recently been proven to be effective for blocking HBV replication in preclinical and clinical studies.[8] The HBV capsid comprises 120 core protein (Cp) dimers arranged with icosahedral T4 symmetry.[9] Core nucleation is the rate limiting step of the self-assembly,[10] during which three core protein dimers interact with HBV polymerase and pregenomic RNA (pgRNA) to form a precursor complex.[11, 12] Then, the Cp dimers are rapidly added to this precursor and interact with each other through hydrophobic interactions to form the capsid. The weak interaction between the subunits enables error correction in the capsid assembly, which is important for correct assembly.[13, 14] The HBV genome is synthesized only in the properly formed capsid via reverse transcription using pgRNA as the template.[15] In

addition to enabling reverse transcription, capsid assembly or core proteins regulate almost every step in the HBV life cycle, e.g., transporting the HBV genome to the nucleus and epigenetic regulation of HBV gene expression,[16, 17] making capsid assembly one of the most attractive targets in anti-HBV drug discovery.[18]

The weak interaction between Cps also provides opportunities for regulation of the capsid assembly process by small molecules. CAMs, through kinetically and thermodynamically modulating capsid assembly, could disturb the proper formation of capsids and regulate the distribution and accessibility of Cps,[19] which affords additional therapeutic benefits besides blocking HBV replication. Several CAMs have been reported to inhibit the *de novo* establishment of cccDNA by modulating the stability of the capsid.[20-24] Long-term treatment with CAMs could inhibit the expression of HBV e antigen (HBeAg) and HBsAg, and the clearance of the latter has been considered a functional cure of CHB.[21] Thus, CAMs could potentially increase the functional cure rate for CHB by modulating multiple steps in the HBV life cycle.

Several chemotypes of CAMs have been discovered, among which phenylpropenamides (PPAs, e.g., AT130),[25] sulfamoylbenzamide (SBA, e.g., DVR-23)[26] and heteroarylpyrimidines (HAPs, e.g., BAY41-4109)[27] (**Figure 1**) are the most studied. Although they each have different chemical structures, all these CAMs bind to the same binding pocket at the Cp dimer-dimer interface.[28-30] They act as molecular glues to enhance the interaction between the Cps, thus accelerating the self-assembly of Cps and decreasing the formation of functional capsids. However, DVR-23 and AT130 promote the formation of morphologically normal but empty capsids (type II

CAMs, CAM-II), while BAY41-4109 misdirects core proteins to form aberrant structures (type I CAMs, CAM-I). This indicates that the difference in the interaction with Cp accounts for the varying effects of CAMs. Both CAM-II (JNJ-6379, Phase II trial; AB-423, Phase I trial) and CAM-I (GLS4, Phase II trial) have been evaluated in clinical trials.[18]. However, no compounds have been approved. Discovery of new chemotypes of CAMs would provide additional candidates, promoting the development of CAMs for new CHB therapeutics. In addition, different chemotypes could differentially modulate the kinetics or thermodynamics of capsid assembly,[31] providing variable effects against HBV compared with present CAMs. Here, we describe the discovery of (1*H*-indazole-5-yl)sulfonamide and (1*H*-pyrazolo[3,4-c]pyridin-5-yl)sulfonamide as new chemotypes of CAMs by constraining the conformation of SBAs. The (1*H*-pyrazolo[3,4-c]pyridin-5-yl)sulfonamide analogs **56** and **59** are less cytotoxic and approximately 10-fold more potent than SBA analogs with good metabolic stability in mouse liver microsomes. The citric acid salt (**67**) of *N*,*N*-dimethylglysine prodrug of **56** has good solubility at various pHs, and dose dependently inhibits in vivo HBV replication in a hydrodynamic injection-based mouse model.

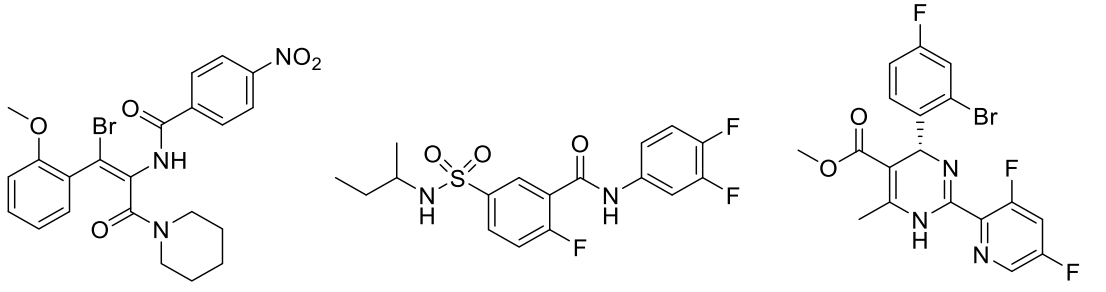

Figure 1. Structures of CAMs.

Results

1. Compound design and optimization

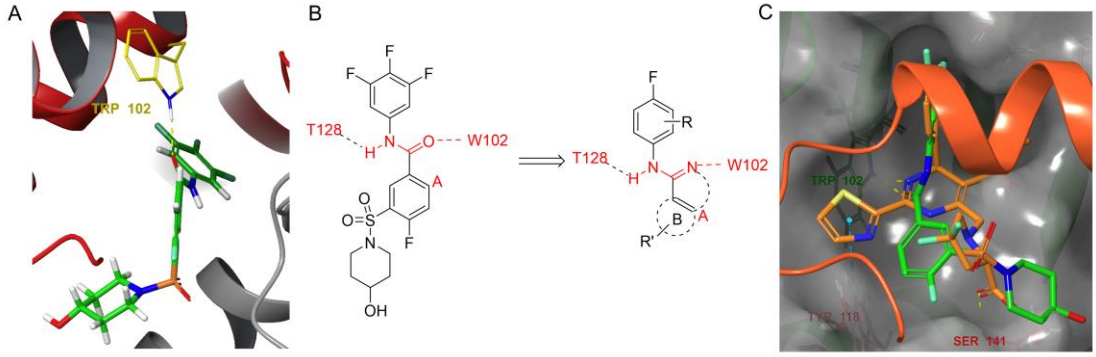

Figure 2. Design of novel CAMs through conformation constraint. (A) Crystal structure of Cps binding with SBA-R01 (PDB: 5T2P); (B) Rational design of CAMs; (C) Merging of SBA-R01 and HAP-R01 (PDB: 5WRE) in the binding site.

Sulfamoylbenzamide (SBA) was recently discovered as a new CAM chemotype from high-throughput screening.[26] Different from heteroarylpyrimidines (HAPs), SBA treatment induced the formation of morphologically normal capsids, which is characteristic of type II CAMs.[19] SBAs bind to the same pocket as HAP at the Cp dimer-dimer interface (**Figure 2C**). The halogen-substituted aniline moiety occupies a hydrophobic pocket. The amide forms hydrogen bonds with W102 and T128 (**Figure 2A** and **2B**),[30] which are essential for the inhibitory activity.[32] The sulfonamide moiety was exposed to the solvent and can tolerate various substituents.[32, 33] In addition to SBA and HAP, the PPA compound AT-130[28] and several other recently discovered CAMs[34, 35] have been reported to bind to the same pocket, indicating that various chemical scaffolds can be accommodated in this pocket. In the active conformation of SBA, the oxygen atom of the amide and carbon **A** in the central phenyl are close in space, as

shown in **Figure 2A**. To constrain this conformation, we considered whether C=O and carbon **A** could be cyclized to obtain a new scaffold in which the N atom in the aromatic heterocycle was designed to interact with W102 by hydrogen bonding in place of the C=O (**Figure 2B**). Various rings, such as phenyl or heterocycles, could be included in the ring A position, which enables structural diversity in lead discovery and optimization. To prove our idea, compounds with indazole or quinazoline scaffold were synthesized. Quinazoline derivatives did not inhibit HBV replication. Compound **1** with indazole scaffold (**Table 1**) inhibited extracellular HBV DNA in HepAD38 cells with an EC_{50} value of 1.28 μM. We proposed that the 2-*N* atom at indazole scaffold could form a proper hydrogen bond with W102 of HBV core protein. In addition, the 1-*N* atom provided an additional site for structure optimization, which distinguishes indazole from other scaffolds. The 1*H*-indazole-5-sulfonamide compounds were once reported as anti-HBV agents in a patent,[36] which increases our confidence in the design concept. However, the SAR and mechanism of this class of compounds are yet to be elucidated.

The effect of substitution at the 1-position was first explored (**Table 1**). *N*-methylation resulted in compound **2** with similar anti-HBV activity (EC_{50}=1.38 μM). However, the selectivity index (SI) of compound **2** increased compared with that of **1**. *N*-cyclopropanation greatly increased the potency compared to **1** by approximately 5-fold (**3**, EC_{50}=0.19 μM). The increase in activity may result from the occupation of a small hydrophobic pocket, which is close to carbon **A** and occupied by the 2-substituent of HAP derivatives (**Figure 1C**).[30] *N*-methylation of the aniline moiety (**4**) and

replacement of the aniline with phenol (**5**), which prevents the hydrogen bond interaction with T128, completely abolished the activity.

Table 1. Anti-HBV activity and cytotoxicity of 1*H*-indazole-5-sulfonamide analogs.

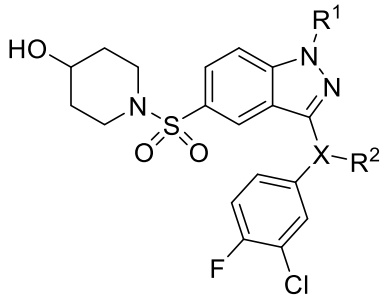

Compd.	R^1	X	R^2	EC_{50} (μM)[a]	CC_{50} (μM)[b]	SI[c]
1	H	N	H	1.28	24	18.75
2	CH_3	N	H	1.38	>100	>72
3	▷---	N	H	0.19±0.10	18.3	96
4	▷---	N	CH_3	>10	>100	-
5	▷---	O	-	>10	75	<7.5
AB-423	-	-	-	0.31±0.092	39.85±5.11[d]	129
GLS4	-	-	-	0.013±0.0045	49.2±1.30[d]	3785

a The concentration of 50% inhibition for HBV DNA in HepAD38 cell supernatant; *b* The concentration that kills 50% HepAD38 cells; *c* selectivity index, SI=CC_{50}/EC_{50}; *d* CC_{50} in HepG2 cells.

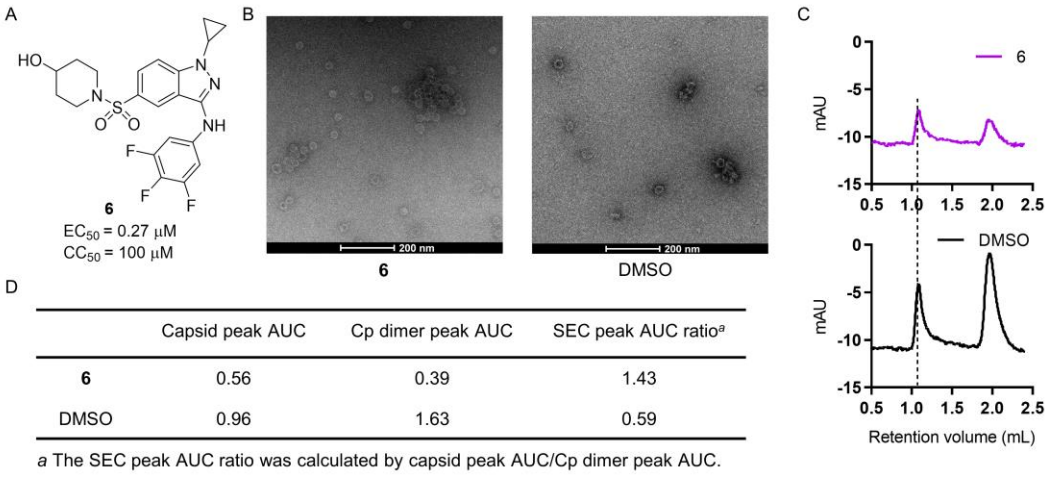

D

	Capsid peak AUC	Cp dimer peak AUC	SEC peak AUC ratio[a]
6	0.56	0.39	1.43
DMSO	0.96	1.63	0.59

a The SEC peak AUC ratio was calculated by capsid peak AUC/Cp dimer peak AUC.

Figure 3. Compound **6** and its effect on capsid assembly. (A) Structure of compound **6**; (B) and (C) Compound **6** accelerated capsid assembly as detected by EM (B) and SEC (C); (D) Calculation of the peak AUC and SEC peak AUC ratio in Figure 3C. Cp149 protein (5 μM) was incubated with **6** (10 μM) in a buffer containing 150 mM NaCl and 50 mM HEPES (pH 7.4) at 37 °C overnight prior to EM or SEC detection.

Although potent inhibition activity was achieved, the selective index of these derivatives was relatively low (**Table 1**). Interestingly, replacement of 3-chloro-4-fluoroaniline moiety with 3,4,5-trifluoroaniline greatly decreased cytotoxicity (**6**, **Figure 3A**). To detect the effect of compound **6** on capsid assembly, electron microscopy (EM) and size exclusion chromatography (SEC) analyses were performed. The *N*-terminal domain of the core protein (aa 1-149, 5 μM) was incubated with **6** (10 μM) in a buffer containing 150 mM NaCl. EM images showed that more capsids were formed after treatment with **6** compared with DMSO (**Figure 3B**). Two peaks of the DMSO treated core protein appeared in the SEC analysis (**Figure 3C**), indicating the co-existence of the capsids (left peak, elution volume: 1.08 mL, early fraction) and the core protein dimers (right peak, elution volume: 1.97 mL, late fraction).The ratio

between the left and right peak area under the curve (AUC) (capsid peak AUC/core protein dimers peak AUC) was used to evaluate the ability of compound **6** to accelerate the capsid assembly. As shown in **Figure 3D**, the SEC peak AUC ratio of compound **6** was 1.43 while DMSO was 0.59, indicating that compound **6** promoted more core protein dimers to assemble into capsids than DMSO did, consistent with the EM results. The morphology and size of the capsid formed after treatment with **6** was the same as that of the normal capsid, which was characteristic of type II CAMs.

Table 2. Anti-HBV activity and cytotoxicity of the compounds generated by scaffold modification.

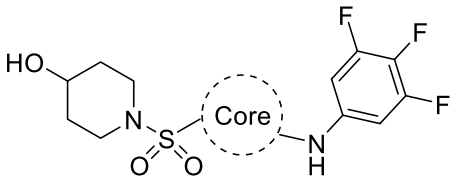

Compd.	Core		EC_{50} (μM)	CC_{50} (μM)	SI
7	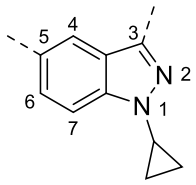	7-F	2.0	>100	>50
8		6-F	0.13	>100	>769
9		4-F	>20	>100	-
10	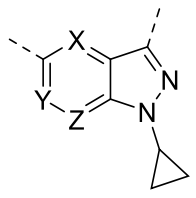	X=Y=CH Z=N	>20	-	-
11		X=Z=CH Y=N	0.24	>100	>417
12		Y=Z=CH X=N	>5	-	-

To explore the structural diversity of ring A (**Figure 2B**), we optimized the scaffold by fluorine scan and *N*-walking strategy, which is widely applied in lead optimization.[37, 38] In this article, fluorination and *N*-replacement were performed on the three positions of the indazole scaffold (**Table 2**, **7-12**). Compounds **8** and **11** were comparable in

potency and cytotoxicity to **6**, with EC_{50} values of 0.13 and 0.24 μM, respectively, while modification at the other positions was not tolerable. Compounds **8** and **11** were thus considered a proper starting point for structure optimization for the potential improvement in drug-like property. Due to its facile synthesis compared to **8** and **11**, indazole analog **6** was used as a template for the SAR study. The SAR information was then applied to **8** and **11**, as we proposed that modification of the scaffold should not influence the interaction between the other parts of the molecule and Cp.

R^4 (Table 3) was supposed to bind to the hydrophobic pocket at Cp dimer interface as the halogen-substituted phenyl in SBA analogs does. Thus, the steric match, which is determined by the substituents on the phenyl group, is vital to the interaction between R^4 and this hydrophobic pocket.[39] Removal of the fluorine at the *meta* position (**13**, EC_{50}=0.22 μM, **Table 3**) was tolerable and maintained potency compared with **6**. The 4-fluorophenyl group is a common fragment in several chemotypes of CAMs.[26, 32-34] In this case, replacement of the *p*-fluorine with a larger group, such as chlorine (**15**) and methyl (**14**), led to a ten-fold decrease or even a loss in activity, probably due to steric hindrance. Removal of the *para* fluorine (**16**) also resulted in diminished activity compared with **13**. These data suggested that the *para* fluorine-substituted aniline is essential for ligand-target interactions. Introducing chlorine and methyl groups at the 2-position reduced the activity by more than five-fold (**17** and **18**). The addition of another fluorine or chlorine at the 3-position, which was expected to enhance hydrophobic interactions, did not significantly influence the anti-HBV activity (**19** in **Table 3, 3** in **Table 1**), suggesting that a 3-fluorine or 3-chlorine group did not cause

steric hindrance and was not perfectly matched with the target. Inspired by the above result, we replaced the 3-substituents with a larger group, such as methyl, leading to **20**, which was approximately ten-fold more potent than **13** with an EC_{50} value of 0.032 μM. Although Cl and CH_3 are isosteres with a similar size, the Van der Waals radius of CH_3 (2 Å) is slightly larger than Cl (1.75 Å). As F, an electron withdrawing atom like Cl, significantly contributed to the increase in potency, we proposed that the lower potency of **3** compared to **20** is, if not all, partly due to the smaller volume of Cl than CH_3 instead of the electron withdrawing effect of Cl. Replacing the phenyl with a pyridinyl (**22**, **23** and **24**) or introducing a polar group (CN in **21**) resulted in a loss of activity, consistent with the hydrophobic nature of the pocket accommodating the aniline moiety. To increase the flexibility of the compound, a methylene was inserted between the phenyl and the NH (**25** and **26**). The benzyl amine fragment was also present in other SBA analogs.[26] However, benzyl amine substituents were not tolerable with the indazole scaffold (**Table 3**). Aliphatic substituents also resulted in a great decrease in potency (**27** and **28**). Although **20** was the most potent compound obtained from the optimization of R^4, it was somewhat more cytotoxic than the others.

Table 3. Effect of aniline substituents on anti-HBV activity and cytotoxicity.

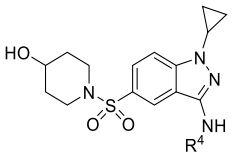

Compd	R_4				EC_{50} (μM)	CC_{50} (μM)	SI
		R_5	R_6	R_7			
3	-				0.19±0.10	18.3	96
13	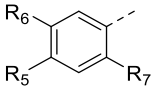	F	H	H	0.22	>100	>455
14		CH_3	H	H	>5	ND	-
15		Cl	H	H	3.14	6.9	2.2
16		H	H	H	0.74	32.2	44
17		F	H	CH_3	1.15	>100	>87
18		F	H	Cl	4	>100	>25
19		F	F	H	0.12	75	625
20		F	CH_3	H	0.032	11.0	343
21		F	CN	H	>10	ND	-
22	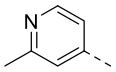				>20	46.6	<23
23	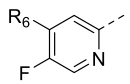	---	H	---	>10	ND	-
24		---	CH_3		>10	ND	-
25	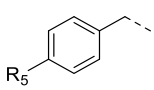	H	---	---	>10	ND	-
26		F	---	---	>10	ND	-
27					>10	100.2	<10
28					>10	>100	-

To reduce the LogP value of the compounds, the cyclopropane was replaced with trimethylene oxide (**29**, **Table 4**). This led to a loss in activity, suggesting the requirement of hydrophobic substituents at R^1. Replacement of the cyclopropane with a smaller (ethyl, **30**) or larger (isopropyl in **31** or cyclobutyl in **32**) group significantly diminished anti-HBV activity with EC_{50} values >1 μM. As the sulfonamide moiety was supposed to bind in the solvent exposed region and interact with the target through a water-mediated network,[30] fragments containing hydrophilic groups, which enable the interaction with water, were included. Similar anti-HBV activity but varied cytotoxicity was achieved with various substitutions at the R^3 position. Replacement of the 4-hydroxyl piperidine with morpholine led to compound **33** with similar potency (EC_{50}=0.43 μM). Moving the hydroxyl group from the 4-position to the 3-position of piperidine did not affect the activity (EC_{50}=0.25 μM) but greatly increased the cytotoxicity (**34**). Carboxylic acid at R^3 was detrimental to anti-HBV activity (**35**). Replacement of the piperidine with pyrrolidine (**36**) or insertion of one carbon atom between the hydroxyl and piperidine (**37**) reduced the potency by 10-fold and increased the cytotoxicity. Other groups containing oxygen at the 4-position of piperidine (**38** and **39**) were well-tolerated.

Table 4. Effects of R^1 and R^3 on anti-HBV activity and cytotoxicity.

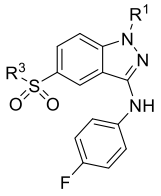

Compd.	R^1	R^3	EC_{50} (μM)	CC_{50} (μM)	SI
14	cyclopropanyl	4-hydroxypiperidinyl	0.22	>100	>455
29		4-hydroxypiperidinyl	>10	ND	-
30	ethyl	4-hydroxypiperidinyl	1.26	>100	>79
31	isopropanyl	4-hydroxypiperidinyl	>10	ND	-
32	cyclobutanyl	4-hydroxypiperidinyl	≈8	10.79	≈1.3
33	cyclopropanyl	morpholinyl	0.43	>100	>232
34	cyclopropanyl	3-hydroxypiperidinyl	0.25	19.06	76.24
35	cyclopropanyl	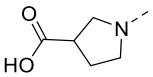	>10	>100	-
36	cyclopropanyl	3-hydroxypyrrolidinyl	2.1	≈60	≈28
37	cyclopropanyl	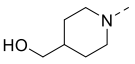	1.1	24.77	23
38	cyclopropanyl	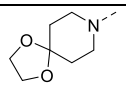	0.25	>100	>400
39	cyclopropanyl	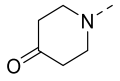	0.33	14.25	43

Considering both HBV inhibition activity and cytotoxicity, we combined the optimal substituents from **Tables 3** and **4**. As described above, the introduction of a 3-methyl group on the aniline moiety (**20**, **Table 3**) greatly improved the antiviral activity. We also found that different substitutes on the sulfonamide moiety resulted in variations in cytotoxicity. Compound **40** (**Table 5**), designed by combining 3-methyl-4-fluorophenyl

at the R^4 position with morpholinyl at the R^3 position, inhibited HBV replication with an EC_{50} value of 0.057 μM without cytotoxicity (CC_{50}>100 μM). Introduction of these two substitutes into the scaffold of **11** but not **8** improved the antiviral activity by 5-fold without increasing cytotoxicity (**42** and **41**, **Table 5**). Compound **42** inhibited HBV replication with an EC_{50} value of 0.042 μM, without cytotoxicity (CC_{50}>100 μM). Therefore, compounds **40** and **42** were selected for further optimization.

Table 5. Anti-HBV activity and cytotoxicity of compounds generated by combining the optimal substituents with different scaffolds.

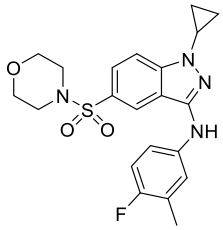

40

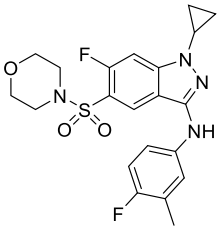

41

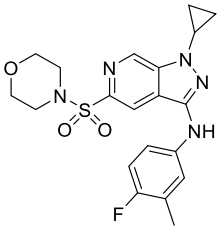

42

Compd.	EC_{50} (μM)	CC_{50} (μM)	HLM/MLM Clint (μL/min/mg)[a]
20	0.032	11.0	ND[b]
40	0.057	>100	41.0/26.9
41	0.21	>100	ND
42	0.042	>100	38.0/53.5

a The intrinsic clearance of compounds by human or mouse liver microsome (HLM/MLM). *b* ND, not determined.

Table 6. Structural modifications to improve the metabolic stability.

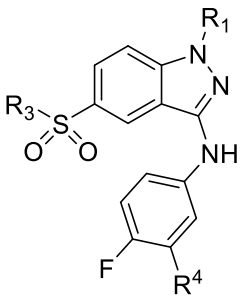

A

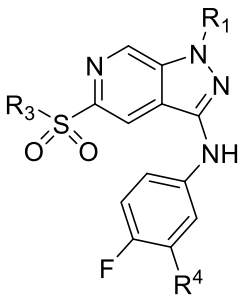

B

Compd.	Class	R^1	R^3	R^4	cLogP[a]	EC_{50} (μM)	CC_{50} (μM)	SI
43	A		morpholinyl	F	3.51	0.22±0.17	>100	>454
46			morpholinyl	CF_3	-	0.29±0.16	8.42	29
47			4-hydroxypiperidinyl	CF_3	-	6.00	≈7.52	1.3
49			4-hydroxypiperidinyl		3.83	0.68	≈5.86	8.6
54			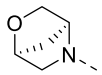	CH_3	3.06	0.045±0.021	19.0	422
57			4-hydroxypiperidinyl	CF_2H	3.22	0.29	13.55	47
58			morpholinyl	CF_2H	3.55	0.12	50	417
50		CF_3CH_2	morpholinyl	CH_3	-	0.24	>100	>417
51		CF_2HCH_2	morpholinyl	CH_3	3.40	0.23	>100	>435
52		CFH_2CH_2	morpholinyl	CH_3	3.15	0.41	>100	>244
53		CF_2H	morpholinyl	CH_3	3.27	>10	>100	≈10
55		H	morpholinyl	CH_3	2.84	0.29±0.14	50.0	172
44	B		4-hydroxypiperidinyl	F	2.93	0.25±0.11	>100	>400
45			morpholinyl	F	3.23	0.22	>100	>454
48			morpholinyl	CF_3	-	0.34	>100	>294
56			4-hydroxypiperidinyl	CH_3	2.78	0.034±0.012	>100	2941
59			4-hydroxypiperidinyl	CF_2H	3.04	0.071±0.035	>100	1408
60			morpholinyl	CF_2H	3.12	0.23	>100	435

a Calculated by the ACD/Percepta platform.

The metabolic stability in liver microsomes of **40** and **42** was low (**Table 5**). To improve the metabolic stability, we replaced the methyl group at R^4 in **40** and **42**, which is prone to be oxidized by CYP450,[39] with a F (**43-45**, **Table 6**), CF_3 (**46-48**) or cyclopropanyl group (**49**). These modifications resulted in a 5- to 100-fold decrease in potency compared with **40** and **42** (**Table 6**). This was most likely because of the

improper steric match of these groups with Cp. The cyclopropanyl group at the 1-position is another site prone to metabolism through *N*-dealkylation mediated by CYP450.[39] We replaced cyclopropanyl with fluorine-substituted methyl or ethyl groups, which are less liable to CYP450-mediated oxidation due to the electron-withdrawing effects of fluorine and the higher strength of the C-F bond.[37] Although less potent than **40**, compounds **50**-**52** inhibited HBV replication with submicromolar EC_{50} values. However, difluoromethyl substitution (**53**) significantly decreased the anti-HBV activity, probably because the strong electron-withdrawing effect of the difluoromethyl group reduced the hydrogen bond acceptor ability of the N atom at the 2-position. All these attempts to block metabolism sites were discontinued due to the accompanying decreases in potency. Another popular approach to improve metabolic stability is to reduce the lipophilicity of the compound.[40, 41] Replacing the morpholine with its one-carbon bridged analog (**54**), which has been reported to have lower lipophilicity,[42] reduced the cLogP by 0.85 units compared to **40**. Compound **54** inhibited HBV replication with an EC_{50} value of 0.045 μM, similar to **40**. However, the cytotoxicity greatly increased compared to **40** (CC_{50} 19.0 *vs*. >100 μM). The 3-methyl group at R^4 in compounds **40** and **42** was found to significantly contribute to the increased anti-HBV activity (**Table 3**). We intended to investigate the contribution of cyclopropane in **40**. The removal of cyclopropane resulted in a 1.07-unit reduction in cLogP (**55**, **Table 6**). Compound **55** inhibited HBV replication at an EC_{50} of 0.25 μM, which is less potent than **40**, indicating that both the cyclopropane and 3-methyl groups significantly contribute to the anti-HBV activity. Optimization of the solvent-exposed sulfonamide

group was another approach to reduce the lipophilicity without significantly decreasing potency. Unfortunately, most analogs of **40** with various substituents at the R^3 position were cytotoxic with CC_{50} values < 30 μM (**Supplementary Table S1**). Compound **56**, designed by replacing the morpholine in compound **42** with the more hydrophilic 4-hydroxypiperidine, inhibited HBV replication with an EC_{50} value of 0.042 μM, without cytotoxicity at 100 μM in HepAD38 cells. Interestingly, the metabolic stability of **56** in mouse liver microsome (MLM)s was significantly improved compared to **42** (**Table 7**). To block metabolism at the benzyl site, we replaced methyl with a difluoromethyl (**57-60**), a less lipophilic bioisostere of the methyl group.[43] The antiviral activity of these compounds decreased slightly. Indazole derivatives **57** and **58** were found to be more cytotoxic than the 1*H*-pyrazolo[3,4-c]pyridine derivatives **59** and **60** (**Table 6**), consistent with the above result of the matched pair compounds **20** and **56**. Although replacement of methyl with difluoromethyl did not reduce the lipophilicity, we observed that the metabolic stability of **59** increased compared with **56** (**Table 7**).

Table 7. Mouse liver microsome metabolism of **56** and **59**.

Compd.	EC_{50} (μM)	CC_{50} (μM)	MLM Clint (μL/min/mg)[a]
56	0.034±0.012	>100	10.3
59	0.071±0.035	>100	6.90

a The intrinsic clearance of compounds by mouse liver microsome (MLM).

2. *In vitro* effects of compounds 56 and 59 in HepAD38 and HepG2.2.15 cells

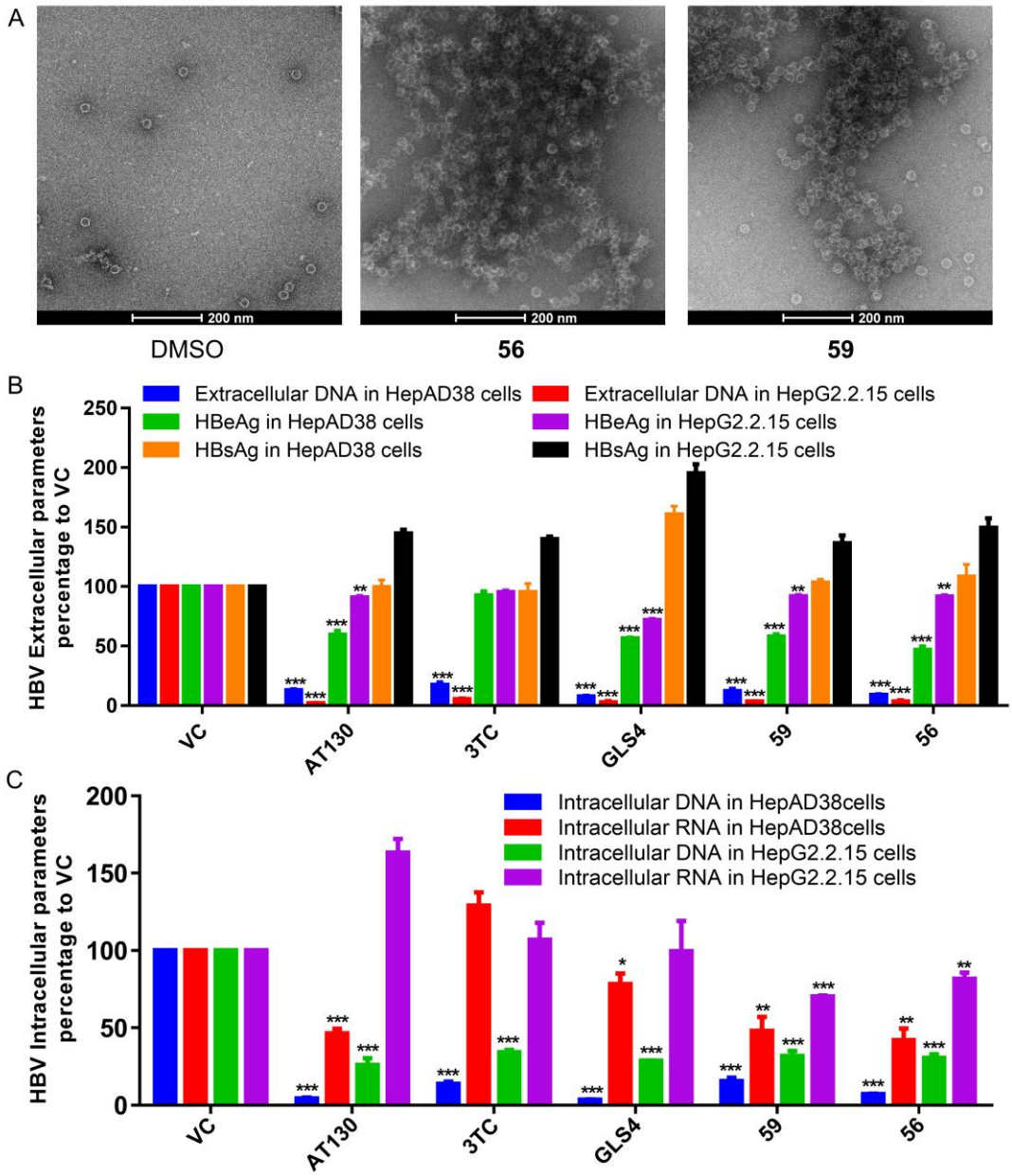

Figure 4. *In vitro* effects of compounds **56** and **59** in HepAD38 and HepG2.2.15 cells. (A) EM analysis of the effects on capsid assembly. (B) and (C) Changes of HBV extracellular and intracellular parameters in HepAD38 and HepG2.2.15 cells after treatment with AT130, 3TC, GLS4, **56** and **59** at 2 μM. Cells were treated with compounds or DMSO for 4 days. The medium was replaced every 2 days. DNA and RNA were quantified with qPCR or qRT-PCR. HBeAg and HBsAg were quantified by ELISA. VC, vehicle control. The results are presented as the means ± SD. Statistics were determined by two-tailed t-test. *, $P < 0.05$; **, $P < 0.01$; ***, $P < 0.001$.

As shown in **Figure 4A**, compounds **56** and **59** accelerated the capsid assembly and

behaved as type II CAMs. To clarify their effect on the HBV life cycle, we treated HepAD38 and HepG2.2.15 cells with **56**, **59**, positive control CAMs (AT130 and GLS4) and Lamivudine (3TC) at 2 μM for four days. At the extracellular level, all these compounds inhibited HBV replication in both cell lines, reducing extracellular HBV DNA by approximately 90% at 2 μM (**Figure 4B**). None of the compounds, including the positive controls, could inhibit the secretion of HBsAg in either cell line. The inhibition of HBsAg secretion by CAMs was only observed in the *de novo* infection models after long-term treatment,[20, 21] resulting from the inhibition of *de novo* synthesis of cccDNA. The secretion of HBeAg by HepAD38 cells was reduced by approximately 50% after treating with 4 CAMs. However, only GLS4 could weakly decrease HBeAg in HepG2.2.15 cells (**Figure 4B**). Inhibition of HBeAg was most probably due to the decrease in intracellular RNA accumulation (**Figure 4C**) or a direct effect on HBeAg by CAMs, which could inhibit HBeAg secretion by inducing precore protein self-assembly,[44] as CAMs did not inhibit cccDNA in such cell lines after short-term treatment.

CAMs inhibit reverse transcription by reducing the encapsulation of pgRNA into the capsid. Thus, intracellular DNA levels in both cell lines were significantly reduced after treatment with CAMs (**Figure 4C**). AT130, **56** and **59** decreased intracellular total RNA in HepAD38 cells by 50%. GLS4 also induced a weak but significant decrease in the total intracellular RNA in HepAD38 cells. We proposed that the reduction of intracellular RNA may be due to the increased exposure to the cytoplasm as reduced encapsulation into the capsid. However, more details about which RNA decreased are

needed to fully understand this phenomenon. The reverse transcriptase (RT) inhibitor 3TC slightly induced intracellular RNA accumulation due to the inhibition of reverse transcription. In HepG2.2.15 cells, only **56** and **59** could significantly reduce intracellular RNA, probably due to the different properties of each cell type.

3. Compounds 56 and 59 suppressed viral replication of both lamivudine-resistant and multidrug-resistant HBV strains

Table 8. Anti-HBV activity in wild type (HepAD38 and HepG2.2.15 cells), lamivudine-resistant (HepG2.A64 cells) and multidrug-resistant (HepG2.1403F cells) HBV strains.

	HepG2.2.15	HepAD38	HepG2.A64	HepG2.1403F	HepG2
	EC_{50} (μM)				CC_{50} (μM)
3TC	0.0038±0.0033	0.070±0.019	>10	>10	>100
TDF	6.4E-05±7.62E-06	0.010±0.0017	0.84±0.36	2.52±1.04	15.04±3.88
ETV	2.2E-06±3.71E-07	0.011±0.011	>10	>10	42.07±2.92
56	0.0035±0.0012	0.034±0.012	0.00025±3.06E-05	0.00033±1.5E-04	>100
59	0.042±0.010	0.071±0.035	0.0022±0.00087	0.013±0.0032	>100
AB-423	0.28±0.074	0.31±0.092	0.048±0.028	0.074±0.011	39.85±5.11
GLS4	0.0066±0.0020	0.013±0.0045	0.0063±0.0017	0.042±0.012	49.2±1.30

As CAMs have different action mechanisms with NAs, they should be effective against HBV that is resistant to RT inhibitors. We then tested the effects of the compounds on HBV DNA in a lamivudine/entecavir (3TC/ETV)-resistant cell line (HepG2.A64) containing rtL180M+rtT184L+rtM204V mutations, and a multidrug-resistant (MDR) cell line (HepG2.1403F) containing rtL180M+rtM204V+rtS202G+ rtN236T mutations.[45] As shown in **Table 8**, compounds **56** and **59** inhibited HBV replication in the HepG2.A64, HepG2.1403F, HepG2.2.15, and HepAD38 cell lines with EC_{50} values well below 0.1 μM. Both compounds did not influence the viability

of HepG2 cells with CC_{50} values >100 μM. Although 3TC and ETV potently inhibited HBV replication in HepG2.2.15 and HepAD38 cells, they did not show a significant inhibitory effect even at 10 μM in HepG2.A64 and HepG2.1403F cells. The activity of tenofovir (TDF) on the resistant strains was also more than 100-fold weaker than that on HepG2.2.15 and HepAD38 cells. These results further proved the potential of CAMs in CHB therapy.

4. Design of amino acid prodrugs to improve anti-HBV activity *in vivo*

The rigid and planar structure together with a high fraction of sp2 carbons led to the poor solubility of compound **56** and its analogs (as shown in **Table 10**). Salt formation is an efficient method to increase compound solubility.[46] However, **56** and the related analogs are weak bases, which are not ideal for salt formation. Thus, amino acid prodrugs were designed, whose amino group was utilized for salt formation (**Table 9**). Several amino acids, including *N*,*N*-dimethylglycine, *L*-valine, *L*-alanine and glycine, were attached to the hydroxyl group of **56** through an ester bond. Different alpha substituents were selected to modulate the stability of the prodrug. To evaluate the stability of these prodrugs, the percent of remaining compound after incubation in plasma and different buffers was determined by HPLC. Except for **62**, all the other prodrugs were rapidly hydrolyzed in plasma (**Table 9**). The steric hindrance of the *i*-Pr in **62** may account for the resistance to hydrolysis. However, a significant portion of compounds **63** and **64** was hydrolyzed in the aqueous buffers, indicating that they are unstable in the digestive tract. Compound **61** was chosen for salt screening to increase solubility.

Table 9. Stability of the prodrugs in plasma and buffers.

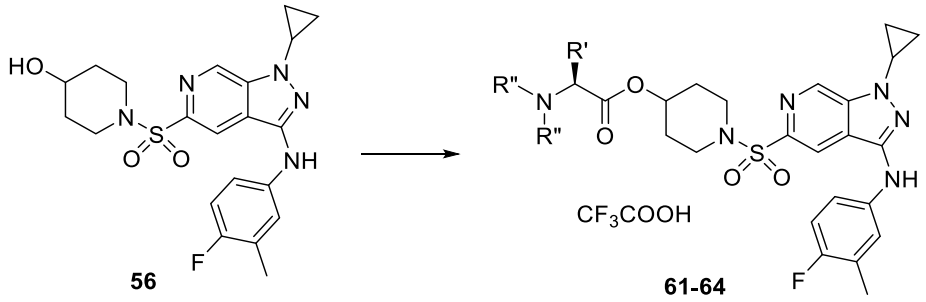

56 61-64

Compound	R’	R”	Half-life in plasma	Percent remaining			
				pH 7.4	pH 6.8	pH 5.8	0.1 M HCl
61	H	CH_3	47.2 min	stable[a]	--[b]	--	stable
62	*i*-Pr	H	18 h	stable	--	--	--
63	CH_3	H	31.2 min	55.6%[c]	80.2%	85.7%	--
64	H	H	77.5 min	74.2%	67.6%	88.3%	--

* Compounds were incubated in buffer at 37 °C; *a* No hydrolysis after 2 h at 37 °C; *b* Not detected; *c* Percent remaining of the compound after 3 h.

Introduction of the amino acid moiety indeed improved the solubility in water (**65**, **Table 10**), probably by increasing the fraction of sp3 carbons and the basicity. The TFA salt further increased the solubility (**61**, **Table 10**). However, the solubility of **61** in pH 6.8 and 7.4 buffer were very low, which indicates poor solubility in the digestive tract. To increase the solubility at various pH values, other salts with acetic acid, citric acid, maleic acid, methanesulfonic acid and hydrochloric acid were prepared (**66-70**, **Table 10**). As excess salt in the detection samples would change the pH of the dissolvent, 1 mg of compound in 100 μL of buffer was used to determine the solubility (**Table 10**). The more acidic acids used in the salt led to increased solubility (**66** *vs*. **68** and **69**). Hydrophilic groups on the acid also increased the solubility (**67** *vs.* **70**). The solubility

decreased with increasing pH (**Table 10**). The citric acid salt **66** was selected as the acceptable solubility in various buffers and a low degree of hygroscopicity.

Table 10. Solubility of the prodrugs.

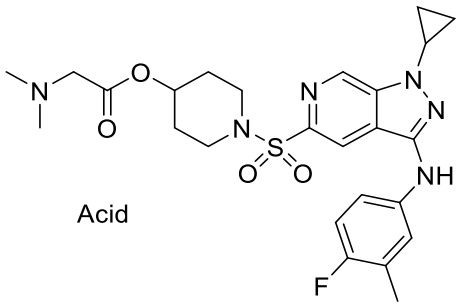

Compd.	Acid	Solubility (mg/mL)[a]			
		water	pH 5.8	pH 6.8	pH 7.4
56	-	ND	ND	ND	ND
61	TFA	1.51	0.29	ND	-
65	-	0.71	-	-	-
66	AcOH	1.11	ND	ND	ND
67	Citric Acid	8.13	7.60	6.65	0.031
68	$(MeSO_3H)_2$	7.90	7.08	7.69	0.23
69	HCl	6.90	6.75	0.040	0.016
70	Maleic acid	4.20	7.93	ND	ND

a Solubility in water or 0.067 M phosphate buffer; ND Not detectable, below the detection limit.

5. Anti-HBV activity of 56 and 67 in the hydrodynamic injection (HDI) HBV mouse model

To evaluate the anti-HBV activity of **56** and **67**, a hydrodynamic injection-based mouse model of HBV infection was used. In this mouse model, the HBV genome was transiently transduced into the hepatocytes of C57BL/6 mice under high pressure conditions, and inhibition of HBV replication could be evaluated during the transient time of about 7 days.[47] Although this animal model cannot mimic the full cycle of HBV infection, it was commonly used to evaluate the inhibition of HBV replication and liver

exposure of the compounds. Compounds **56** and **67** were chosen for *in vivo* anti-HBV evaluation in HDI model as the higher potency and metabolic stability of **56** and the increased solubility of **67**. Oral administration once a day at doses of 50 mg/kg and 100 mg/kg were performed. Once daily oral dose of 100 mg/kg AB-423 and 0.03 mg/kg ETV were used as positive controls. However, neither **56** nor **67** as well as AB-423 significantly inhibited HBV replication in mice (**Supplementary Figure S1**). In the preclinical study, 100 mg/kg AB-423 was orally administrated twice daily for *in vivo* anti-HBV evaluation. Thus, we adopt the administration frequency of twice a day, to elucidate the therapeutic potential of this class of CAMs of AB-423. After 7 days treatment, 100 mg/kg **67** achieved significant inhibition of both serum (**Figure 5A**) and liver (**Figure 5B**) HBV DNA levels compared to vehicle control, whereas 50 mg/kg **67** only achieved weak inhibition of liver HBV DNA levels. Both doses of **56** did not lead to a significant anti-HBV effect (**Figure 5**), which probably resulted from poor absorption due to poor solubility.

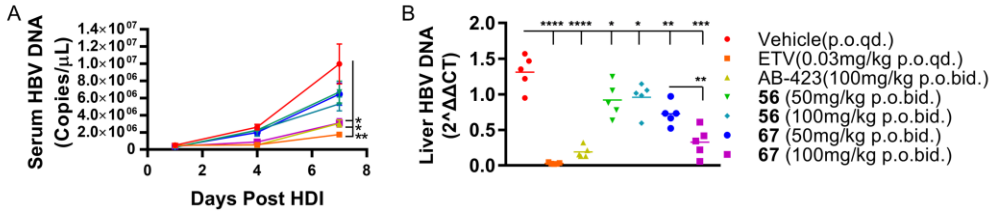

Figure 5. Anti-HBV activity in an HDI HBV mouse model. (A) Serum HBV DNA copies after hydrodynamic injection; (B) Liver HBV DNA on the 7th day after hydrodynamic injection. N=5; *, $P < 0.05$; **, $P < 0.01$; ***, $P < 0.001$; ****, $P < 0.0001$.

The dose-dependent inhibition of *in vivo* HBV replication inspired us to further evaluate

the *in vivo* anti-HBV activity of **67**. As the molecular weight of **67** is nearly twice that of AB-423, we increased the dose to 200 mg/kg. However, no significant improvement in the inhibition of HBV replication was observed (**Supplementary Figure S2**). This may result from a limited absorption rate, induction of the expression of metabolic enzymes etc. Blood and liver concentration of **56** after oral administration of **56** and its pro-drug **67** were investigated. It was indicated that **56** was quickly eliminated in mice with a clearance of 0.14 L/h and a short half-life time of 0.63 hour (**Figure 6A**, **Table 11**). Oral bioavailability of **56** was calculated as 12%. Blood concentration (1.19 μM) of **56** reached maximum (*Cmax*) at 30 min after administration of 100 mg/kg parent compound **56** (**Table 11**). At the dose of 100 mg/kg, oral bioavailability of **67** reached 87.6% (**Table 11**), much higher than that of parent compound **56** (12%). At the dose of 200 mg/kg, the oral bioavailability of **67** was increased to 132%, which might be resulted from a phenomenon of saturated metabolic enzyme.[48] Blood concentration of **56** reached *Cmax* of 3.73 μM and 8.84 μM at 1h after administrating **67** with the dose of 100mg/kg and 200 mg/kg, respectively (**Table 11**). It was noted that very low level of the pro-drug **67** in blood of mice was observed (data not shown). Considering the fact that the half-life time of **67** in mice plasma was 47 min, we speculated that **67** could be hydrolyzed by additional enzymes in small intestine and liver besides plasma.

Parent compound **56** distributed fast to liver after either intravascular or oral administration of **56** or pro-drug **67** (**Figure 6B**). More than 10 nmol/g in liver was detectable at 5 min after oral administration of **56** or **67**. The liver *Cmax* of **56** reached 32 nmol/g at 0.5 h (*Tmax*) after oral administration of **56**, corresponding with the *Tmax*

of **56** in blood. Fortunately, liver *Cmax* of **56** after oral administration of pro-drug **67** with the dose of 100 mg/kg and 200 mg/kg reached 40 nmol/g at 2 h and 59 nmol/g at 4 h, respectively, much higher than that after oral administration of parent compound **56** (**Table 11**). Correspondingly, liver exposure of **56** achieved by oral administrating 100 mg/kg **67** was two-fold higher than that achieved by oral administrating 100 mg/kg **56**. Unexpectedly, 1.5-fold increase in liver exposure of **56** was observed at the dose of 200 mg/kg of **67** comparing with that at 100 mg/kg (**Table 11**). One possibility was that high concentration of compound induced the metabolic enzyme overexpression.[49] These results proved the advantage of amino acid pro-drug in improving the exposure and in vivo anti-HBV efficacy of (1*H*-Pyrazolo[3,4-c]pyridin-5-yl)sulfonamide derivative **56**.

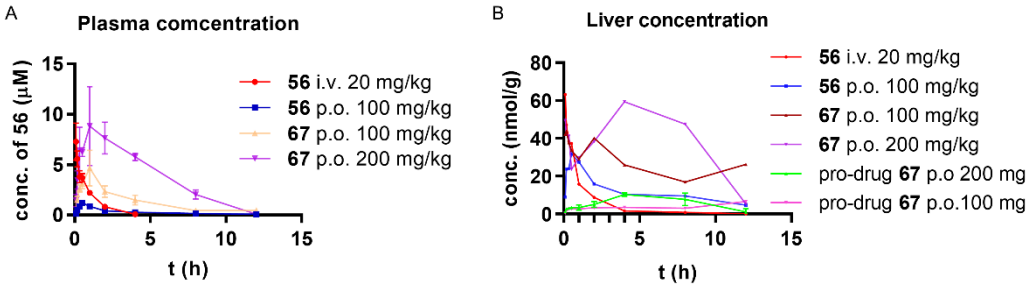

Figure 6. Pharmacokinetics of compound **56** and **67** in male C57BL/6 mice. (A) Plasma concentration of **56** after administration of **56** and its prodrug **67**; (B) Liver concentration of **56** and its pro-drug. N=3.

Table 11. Pharmacokinetics of **56** and **67** in mice.

Dose	$t_{1/2}$ (h)	CL (L/h)	AUC_{plasma} (μg*h/L)	AUC_{Liver} (nmol*h/g)	Blood T_{max} (h)	Blood C_{max} (μM)	Liver T_{max} (h)	Liver C_{max} (nmol/g)	F (%)
56 i.v. 20mg/kg	0.63	0.14	2597	62	-	-	-	-	-
56 p.o. 100mg/kg	-	-	1580	142	0.5	1.19	0.5	32	12
67 p.o. 100mg/kg	-	-	7013.2	306	1.0	3.73	2	40	87.6
67 p.o. 200mg/kg	-	-	21106	482	1.0	8.84	4	59	132

6. Molecule modeling

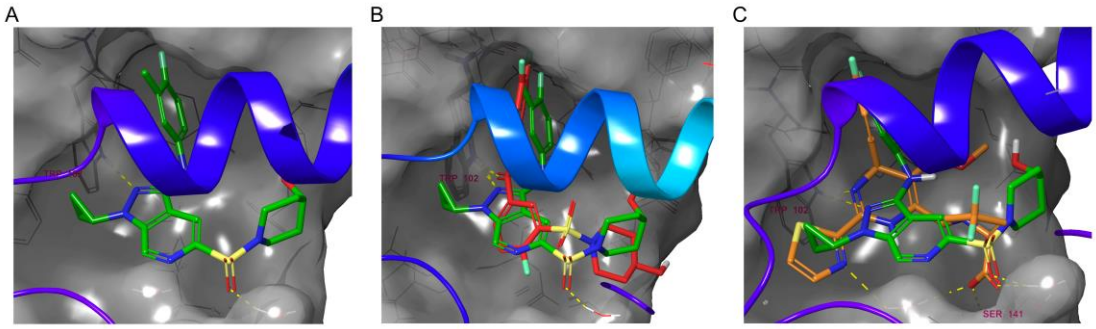

Figure 7. Predicted binding mode of **56**. (A) Docking of **56** with HBV core protein crystal structure (PDB code: 5WRE); (B) Merging of **56** and NVR 3-778 at the binding site; (C) Merging of **56** and HAP-R01 at the binding site.

To gain insight of the interaction between **56** and HBV core protein, molecule modeling was performed. We carried out docking based on the co-crystal structure of HAP-R01 and core protein (PDB code: 5WRE). The results showed that compound **56** binds to the core protein dimer-dimer interface with a similar interaction mode as that of SBAs and HAPs (**Figure 7**). The modeling results show the formation of a hydrogen bond between 2-*N* and W102. The aniline moiety pointed to a hydrophobic pocket formed by the two core protein dimers, which is occupied by a halogen substituted

phenyl group of SBA or HAP derivatives (**Figure 7B** and **7C**). The fluorine atom and methyl group of **56** were in tight contacts with core protein, consistent with the SAR study. Sulfonamide moiety pointed to the solvent exposing region. The oxygen of sulfonamide formed another hydrogen bond with a water molecule (**Figure 7A**). The cyclopropanyl group of **56** bound to the pocket where the thiazolyl group of HAP-R01 binds (**Figure 7C**), which should contribute to the increased potency of **56**.

Chemistry

The preparation of (1*H*-indazol-5-yl)sulfonamide derivatives began with the cross coupling of benzyl mercaptan and 5-bromo-1*H*-indazol analogs (**A**, **Scheme 1**), whose preparation is described in the supporting information, using a reported method.[50] Oxidative chlorination[51] and reaction with the corresponding amines afforded sulfonamide derivatives (**C**). Intermediate **D** was prepared by bromination of **C** using NBS or 1,3-dibromo-5,5-dimethylhydantoin in a mixture of acetonitrile and acetic acid at room temperature or 40 °C. The target compounds (**E**) were synthesized by Buchwald-Hartwig cross coupling under the catalysis of $Pd(OAc)_2$ and xantphos (**Scheme 1**).

Scheme 1. General synthetic route for the indazole derivatives.

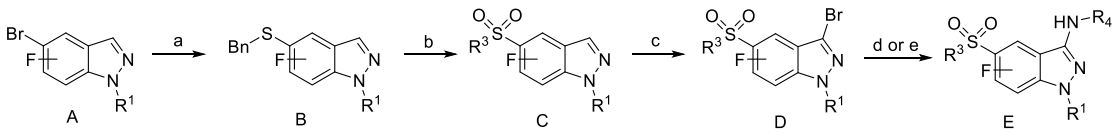

Reagents and conditions: (a) BnSH (1.5 eq), $Pd_2(dba)_3$ (5% mol), xantphos (10% mol), DIPEA (2 eq), 1,4-dioxane, 90 °C; (b) i. 1,3-dibromo-5,5-dimethylhydantoin (2 eq), -30 °C, CH_3CN, H_2O, AcOH; ii. 4-hydroxypiperidine (2 eq), Et_3N (3 eq), DCM, rt; (c) NBS (1.5 eq), or 1,3-dibromo-5,5-dimethylhydantoin, CH_3CN/AcOH; (d) corresponding aniline (1.5 eq), $Pd(OAc)_2$ (5% mol), xantphos (10% mol), Cs_2CO_3 (2 eq), 1,4-dioxane, 130 °C; (e) corresponding aniline (1.5 eq), $Pd(OAc)_2$ (5% mol),

xantphos (10% mol), Cs_2CO_3 (2 eq), 1,4-dioxane, 130 °C; ii. LiOH (3 eq), THF, H_2O, rt.

The preparation of **1** began with the cross coupling of benzyl mercaptan and 5-bromo-1*H*-indazol, followed by oxidative chlorination, coupling with 4-hydroxypiperidine, and bromination as described above. Compound **75** was afforded by protecting the hydroxyl group and 1-position N-atom using acetyl and tetrahydropyran, respectively. After cross coupling with 3-chloro-4-fluoroaniline and deprotection, **1** was obtained (**Scheme 2**).

Scheme 2. Synthesis of compound **1**.

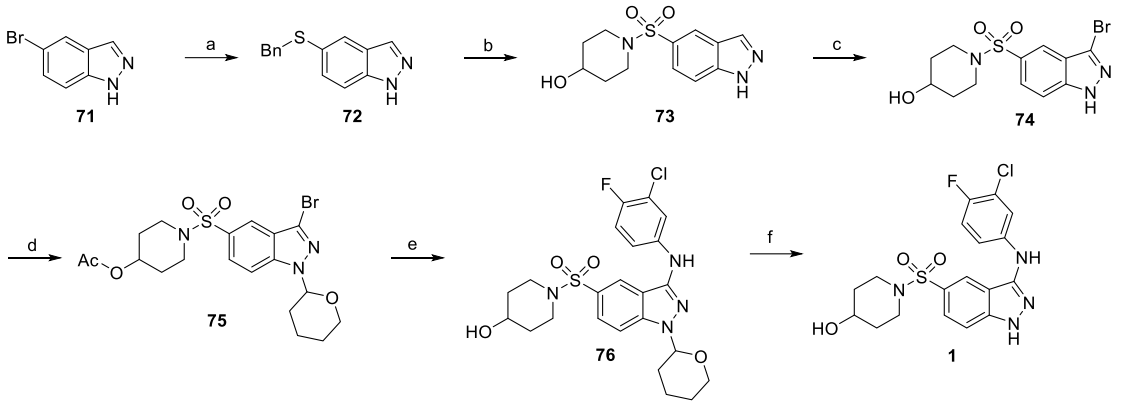

Reagents and conditions: (a) BnSH (1.5 eq), $Pd_2(dba)_3$ (5% mol), xantphos (10% mol), DIPEA (2 eq), 1,4-dioxane, 90 °C, 92%; (b) i. 5,5-dimethylhydantoin (2 eq), -30 °C, CH_3CN, H_2O, AcOH; ii. 4-hydroxypiperidine (2 eq), Et_3N (3 eq), DCM, rt, 41%; (c) NBS (1.1 eq), $CHCl_3$, 60 °C; (d) i. DHP (2 eq), TsOH H_2O (0.3 eq), EA, reflux; ii. Ac_2O (1 eq), 86% for three steps; (e) i. 3-chloro-4-fluoroaniline (1.5 eq), $Pd(OAc)_2$ (5% mol), xantphos (10% mol), Cs_2CO_3 (2 eq), 1,4-dioxane, 110 °C; ii. LiOH (3 eq), THF, H_2O, rt, 89%; (f) HCl, EtOH, rt, quantitative.

Synthesis of 1*H*-pyrazolo[3,4-c]pyridine derivatives started from the reduction of the nitro group in **77** using Raney Ni and hydrogen, followed by acylation of the amino group. Then, **79** reacted with isoamyl nitrite to afford **80** (**Scheme 3**). The target compounds were prepared following the protocol described in **Scheme 1**.

Scheme 3. Synthetic route of 1*H*-pyrazolo[3,4-c]pyridine derivatives.

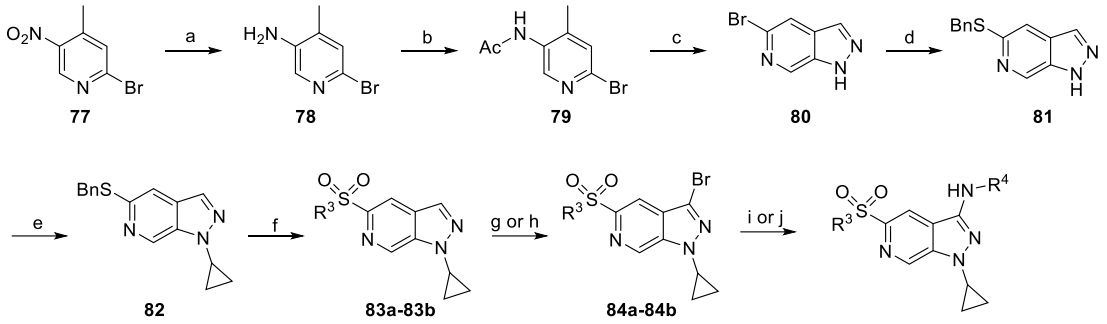

Reagents and conditions: (a) Raney Ni, H_2, methanol, rt, quantitative; (b) Ac_2O (3 eq), $PhCH_3$, 100 °C, 85%; (c) isoamyl nitrite (2.5 eq), Ac_2O (2 eq), KOAc (2 eq), 18-crown-6 (0.1 eq), $PhCH_3$, 80 °C, then NaOH (4 eq), rt, 63%; (d) BnSH (1.5 eq), $Pd_2(dba)_3$ (5% mol), xantphos (5% mol), DIPEA (2 eq), 1,4-dioxane, 90 °C, 87%; (e) cyclopropylboronic acid (2 eq), $Cu(OAc)_2$ (1 eq), 2,2'-bipyridine (1 eq), Na_2CO_3 (2 eq), 1,2-DCE, 70 °C, 51%; (f) i. 5,5-dimethylhydantoin (2 eq), -15 °C, CH_3CN, H_2O (1% v/v), AcOH (1% v/v); ii. 4-hydroxypiperidine (for **83a**, 2 eq) or morpholine (for **83b**, 2 eq), Et_3N (3 eq), DCM, rt; (g) for **84a** i. Ac_2O (5 eq), pyridine (4 eq), ethyl acetate, reflux; ii. NBS (1.5 eq), TFA/AcOH (1:1), 50 °C, 50% for 2 steps; (h) for **84b** 1,3-dibromo-5,5-dimethylhydantoin (1.5 eq), CH_3CN/AcOH (1:1), 50 °C, 59% for 2 steps; (i) corresponding aniline (1.5 eq), $Pd(OAc)_2$ (5% mol), xantphos (10% mol), Cs_2CO_3 (2 eq), 1,4-dioxane, 130 °C; (j) corresponding aniline (1.5 eq), $Pd(OAc)_2$ (5% mol), xantphos (10% mol), Cs_2CO_3 (2 eq), 1,4-dioxane, 130 °C; ii. LiOH (3 eq), THF, H_2O, rt.

Compound **5** was prepared by the CuI-catalyzed cross coupling of 3,4,5-trifluorophenol and **85**, which was synthesized by iodination of 1-((1-cyclopropyl-1H-indazol-5-yl)sulfonyl)piperidin-4-yl acetate (supporting information) using NIS in the mixture of CH_3CN and H_2SO_4. Compounds **27** and **28** were also synthesized using CuI-catalyzed cross-coupling between **85** and cyclohexylamine or cyclopentylamine (**Scheme 4**).

Scheme 4. Synthesis of compounds **5**, **27** and **28**.

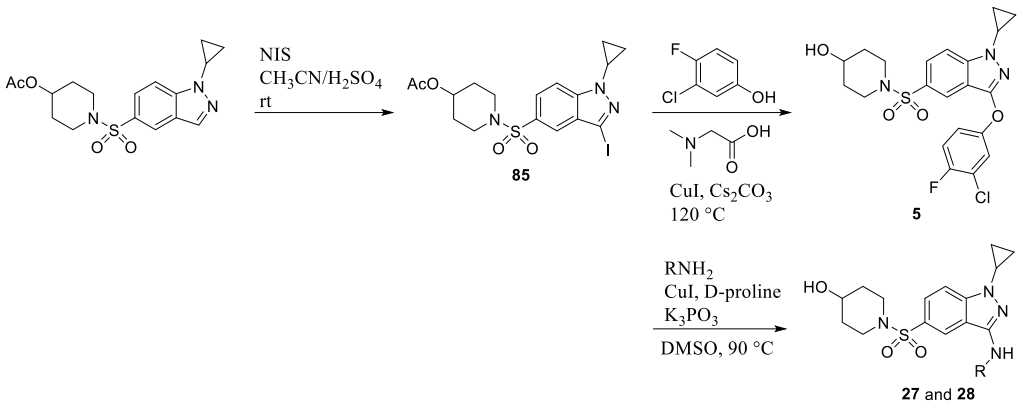

Four amino acids were selected for the preparation of prodrugs. *N*,*N*-dimethylglycine or the *N*-Boc-*L*-amino acid were attached to **56** through an ester bond under DCC and DMAP conditions. Compounds **61**-**64** were afforded by removing the Boc group in **86**-**87** using TFA. The other salts **66**-**70** were prepared by mixing **65** with the corresponding acid in the proper solvent (**Scheme 5**).

Scheme 5. Synthesis of the prodrugs and preparation of the salt form.

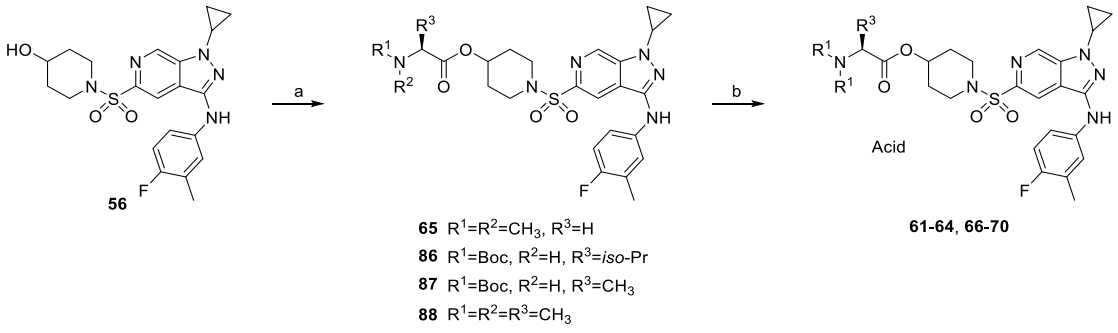

Reagents and conditions: (a) amino acid (3 eq), DCC (3 eq), DMAP (1.2 eq), DCM, 40 °C, ~90%; (b) for **61**-**64**, TFA/DCM (1/1), rt; for **66**-**70**, the corresponding acid, DCM or ethyl acetate.

Discussion and Conclusion

HBV genome is a 3.2 kbp relaxed circular DNA, expressing only seven proteins. To compensate for the limited number of viral proteins, each HBV protein plays multiple essential roles in the HBV life cycle.[17] The core protein could self-assemble to form the

shell of HBV and enable the synthesis of the viral genome via reverse transcription in the capsid. In addition, Cps could bind to CpG island 2 to positively regulate HBV transcription by maintaining the hypomethylation of CpG island 2.[16] Capsids containing mature HBV genome are able to release the viral genome into the nucleus[52] in the initial infection and amplification of the cccDNA pool, which is vital to the establishment and persistence of chronic infection. Thus, targeting the multifunctional core protein and capsid represents a promising strategy for HBV therapy.

Sustained and prolonged suppression of HBV is required to prevent the progression of the disease. However, current therapeutics only inhibit virus replication and seldom achieve complete elimination of HBV. Lifelong treatment is usually required to suppress HBV replication. cccDNA, which is the template of transcription, is the major cause of HBV persistence. New therapies, especially those that could clear cccDNA, are needed to shorten the treatment period and improve the outcome. Various CAM chemotypes have been reported to inhibit the formation of cccDNA.[20, 21, 23] However, the inhibition of cccDNA was achieved only when CAM treatment began before or together with the infection, meaning that the already established cccDNA in cells is not influenced by CAMs. In addition, a much higher concentration of compound is needed to inhibit cccDNA formation than to block HBV replication. CAMs have been reported to directly target the mature capsid.[24] This interaction between CAMs and capsids may disturb the morphology and disassembly of the capsid, which is important for the importing of the genome into the nucleus.[51] To evaluate the effect on cccDNA, the establishment of an HBV infection model is required, which is ongoing in our lab.

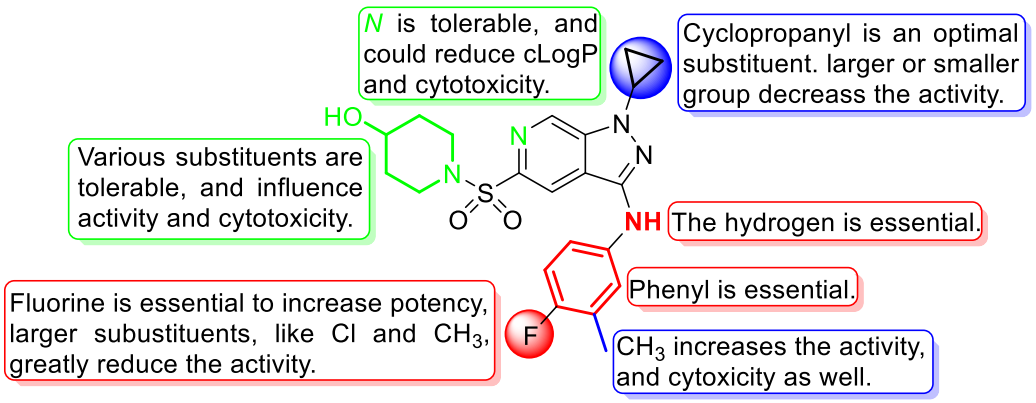

Figure 8. Summary of the structure-activity relationship (SAR).

As proven in both preclinical and clinical studies, capsid assembly modulators (CAMs), which could interfere with the HBV life cycle in multiple steps, have great potential to be developed into new anti-HBV therapies. However, no CAMs have currently been approved. Through constraining the conformation of SBAs, we designed indazole as a new chemotype of CAMs. The indazole analog **6** accelerates the formation of morphologically normal (**Figure 3**) but empty capsids as SBAs do. In the subsequent SAR study, we discovered (1*H*-pyrazolo[3,4-c]pyridin-5-yl)sulfonamide (**Table 2**) analog **56 (Table 6)** through scaffold hopping and substituents modification (**Figure 8**). The lipophilicity of (1*H*-pyrazolo[3,4-c]pyridin-5-yl)sulfonamide analogs is lower than that of indazoles, due to the replacement of the phenyl with a pyridinyl. Matched molecular pair comparison (**46**, **57** and **58** *vs.* **48**, **59** and **60**, **Table 6**) revealed that the cytotoxicity of (1*H*-pyrazolo[3,4-c]pyridin-5-yl)sulfonamides is much lower than that of indazoles. Compound **56** potently inhibited HBV replication in HepAD38 cells with an EC_{50} of 0.034 μM, approximately 10-fold lower than that of SBAs. However, the poor solubility of **56** diminished its *in vivo* anti-HBV activity (**Figure 5**). Compound **67** is the citric acid salt of the prodrug of **56**. It has good aqueous solubility and is

hydrolyzed quickly to release **56** in plasma. The *in vivo* exposure of **56** after oral administration of **67** was much higher compared to oral administration of **56** (**Figure 6**). Compound **67** dose-dependently inhibited *in vivo* HBV replication in an HDI HBV mouse model. These results highlight (1*H*-pyrazolo[3,4-c]pyridin-5-yl)sulfonamide as a new chemotype of CAMs and provide a starting point to develop new therapeutics for HBV infection.

Experimental section

Chemistry method.

All the reactions were stirred magnetically unless otherwise noted. Reagents and solvents were purchased from commercial suppliers and used directly unless otherwise specified. Reactions were monitored using the Waters UPLC-MS system equipped with an autosampler, a PDA detector and a SQ mass detector. The eluent was the mixture of acetonitrile and water containing 0.05% (v/v) HCOOH. TLC was performed using thin layer chromatography silica gel plate (HSGF254) from Yantai Institute of chemical industry and were visualized with UV light. The column chromatography was performed with silica gel 60 (200−300 mesh) from Qingdao Haiyang Chemical Factory. ^{1}H and ^{13}C NMR spectrum were collected using a Bruker Advance 400 MHz spectrometer. Chemical shifts are given in parts per million (ppm), and coupling constants (J values) are reported in hertz (Hz). Multiplicities are described using the following abbreviations: s (singlet), d (doublet), dd (double doublet), dt (double triplet), t (triplet), q (quartet), br s (broad singlet), m (multiplet). Accurate molecular weight and chemical formula were determined using HRMS, which was conducted by Agilent

LC/MSD TOF The ion source was electrospray ionization (ESI). All compounds submitted for biological test were >95% purity detected by Agilent HPLC system equipped with an autosampler and a PDA detector. The eluent was the mixture of acetonitrile and water containing 0.05% (v/v) HCOOH.

Synthesis of the target compounds.

*1-((3-((3-Chloro-4-fluorophenyl)amino)-1H-indazol-5-yl)sulfonyl)piperidin-4-ol (**1**).* The mixture of **75** (0.27 mmol), 3-chloro-5-fluroaniline (0.4 mmol), $Pd(OAc)_2$ (0.014 mmol), Xantphos (0.027 mmol) and Cs_2CO_3 (0.54 mmol) in 1.5 mL 1,4-dioxane was stirred at 110 ℃ under argon atmosphere for 3h. After that, the solution was diluted with DCM and filtered. The filtrate was concentrated under vacuum and dissolved in THF (2 mL) and H_2O (2 mL). To the mixture was added LiOH (0.84 mmol). The mixture was stirred at room temperature for 1 h and extracted with ethyl acetate (15 mL). The organic layer was washed with brine, dried with anhydrous Na_2SO_4, and concentrated. The residue was purified with silico column chromatography (petro ether/ ethyl acetate, v/v, 1/1) to afford 122 mg **76**, 89% yield. The mixture of **76** in ethanol (5 mL) and hydrochloric acid (1 mL) was stirred at room temperature for 30 min, neutralize with 2N NaOH to pH 8-9, and filtered. The solid was washed with methanol to afford compound **1** with quantitative yield. ^{1}H NMR (400 MHz, DMSO-d_6) δ 12.63 (s, 1H), 9.53 (s, 1H), 8.56 (s, 1H), 8.11 (s, 1H), 7.92 – 7.45 (m, 3H), 7.35 (t, J = 9.3 Hz, 1H), 4.65 (s, 1H), 3.49 (s, 1H), 3.16 (s, 2H), 2.71 (s, 2H), 1.74 (s, 2H), 1.44 (s, 2H). ^{13}C NMR (100 MHz, DMSO-d_6) δ 151.2 (d, J = 237.9 Hz), 146.2, 141.7, 140.0, 126.0, 125.6, 122.4, 119.5 (d, J = 18.1 Hz), 117.4 (d, J = 21.6 Hz), 117.0, 116.5 (d, J = 6.1 Hz),

113.8, 110.8, 64.2, 43.7, 33.3. HRMS (ESI) calculated for $C_{18}H_{19}ClFN_4O_3S$ $[M+H]^+$ 425.0845, found 425.0831.

Procedure for synthesis of the title compounds.

Method I (for compounds **2-26**, **29-32**, **34-37**, **44, 47**, **49**, **56-57** and **59**): The mixture of the 3-bromoindazole derivatives (0.1 mmol), the corresponding aniline (0.2 mmol), $Pd(OAc)_2$ (0.01 mmol), Xantphos (0.01 mmol) and Cs_2CO_3 (0.2 mmol) in 1.5 mL 1,4-dioxane was stirred at 130 ℃ under argon atmosphere for 3h. After that, the solution was diluted with DCM and filtered. The filtrate was concentrated under vacuum and dissolved in THF (2 mL) and H_2O (2 mL). To the mixture was added LiOH (0.5 mmol). The mixture was stirred at room temperature for 1 h and extracted with ethyl acetate (15 mL). The organic layer was washed with brine, dried with anhydrous Na_2SO_4, and concentrated. The residue was purified with column chromatography on silico gel.

Method II (for compounds **33**, **38**, **40-42**, **43**, **45-46**, **48**, **50-55**, **58** and **60**): The mixture of the 3-bromoindazole derivatives (0.1 mmol), the corresponding aniline (0.2 mmol), $Pd(OAc)_2$ (0.01 mmol), Xantphos (0.01 mmol) and Cs_2CO_3 (0.2 mmol) in 1.5 mL 1,4-dioxane was stirred at 130 ℃ under argon atmosphere for 3h. The insoluble matters were removed by filtration and the filtrate was concentrated under vacuum. The residue was purified with column chromatography on silico gel.

*1-((3-((3-Chloro-4-fluorophenyl)amino)-1-methyl-1H-indazol-5-yl)sulfonyl)piperidin-4-ol (**2**)*. 25% yield. ^{1}H NMR (400 MHz, DMSO-d_6) δ 9.56 (s, 1H), 8.56 (d, J = 1.5 Hz, 1H), 8.04 (dd, J = 6.6, 2.7 Hz, 1H), 7.76 – 7.65 (m, 2H), 7.60 (ddd, J = 9.1, 4.1, 2.7 Hz, 1H), 7.37 (t, J = 9.1 Hz, 1H), 4.65 (s, 1H), 3.99 (s, 3H), 3.51 (dt, J = 7.9, 4.0 Hz, 1H),

3.23 – 3.10 (m, 2H), 2.72 (ddd, *J* = 11.8, 8.5, 3.4 Hz, 2H), 1.76 (ddd, *J* = 13.1, 6.9, 3.5 Hz, 2H), 1.44 (dtd, *J* = 12.2, 8.0, 3.5 Hz, 2H). ^{13}C NMR (100 MHz, DMSO-d_6) δ 150.9 (d, *J* = 238.4 Hz), 144.9, 140.8, 139.3 (d, *J* = 2.3 Hz), 125.5, 125.1, 122.1, 119.1 (d, *J* = 18.1 Hz), 117.0 (d, *J* = 21.7 Hz), 116.7, 116.1 (d, *J* = 6.5 Hz), 113.7, 109.7, 63.8, 43.3, 35.4, 32.9. HRMS (ESI) calculated for $C_{19}H_{21}O_3N_4ClFS$ $[M+H]^+$ 439.0986, found 439.1001.

*1-((3-((3-Chloro-4-fluorophenyl)amino)-1-cyclopropyl-1H-indazol-5-yl)sulfonyl)piperidin-4-ol (**3**)*. 39% yield, ^{1}H NMR (400 MHz, DMSO-d_6) δ 9.57 (d, *J* = 1.9 Hz, 1H), 8.55 (s, 1H), 8.01 (dd, *J* = 5.8, 3.0 Hz, 1H), 7.72 (s, 2H), 7.62 (ddt, *J* = 9.0, 4.5, 2.3 Hz, 1H), 7.37 (td, *J* = 9.1, 1.9 Hz, 1H), 4.66 (t, *J* = 2.7 Hz, 1H), 3.76 – 3.61 (m, 1H), 3.52 (dt, *J* = 9.1, 4.5 Hz, 1H), 3.23 – 3.07 (m, 2H), 2.73 (t, *J* = 9.8 Hz, 2H), 1.83 – 1.68 (m, 2H), 1.53 – 1.37 (m, 3H), 1.18 – 1.09 (m, 4H). ^{13}C NMR (101 MHz, DMSO-d_6) δ 151.4 (d, *J* = 238.5 Hz), 145.1, 142.0, 139.7 (d, *J* = 2.5 Hz), 126.3, 126.3, 122.6, 119.6 (d, *J* = 18.2 Hz), 117.5, 117.3, 116.6 (d, *J* = 6.5 Hz), 115.0, 110.4, 64.2, 43.7, 33.4, 29.6, 6.8. HRMS (ESI) calculated for $C_{21}H_{23}O_3N_4ClFS$ $[M+H]^+$ 465.1143, found 465.1158.

*1-((3-((3-Chloro-4-fluorophenyl)(methyl)amino)-1-cyclopropyl-1H-indazol-5-yl) sulfonyl) piperidin-4-ol (**4**)*. 10% yield, ^{1}H NMR (400 MHz, DMSO-d_6) δ 7.81 (d, *J* = 8.9 Hz, 1H), 7.66 (dd, *J* = 8.9, 1.6 Hz, 1H), 7.38 (t, *J* = 9.0 Hz, 1H), 7.31 (dd, *J* = 6.6, 2.8 Hz, 1H), 7.23 – 7.10 (m, 2H), 4.65 (d, *J* = 3.8 Hz, 1H), 3.72 (p, *J* = 6.0 Hz, 1H), 3.48 (dd, *J* = 10.0, 6.0 Hz, 1H), 3.44 (s, 3H), 3.01 (dd, *J* = 11.2, 5.3 Hz, 2H), 2.63 – 2.53 (m, 2H), 1.79 – 1.66 (m, 2H), 1.42 (dtd, *J* = 11.9, 8.0, 3.5 Hz, 2H), 1.16 (d, *J* = 3.3

Hz, 4H). ^{13}C NMR (101 MHz, DMSO-d_6) δ 151.4 (d, J = 238.5 Hz), 145.1, 142.0, 139.7 (d, J = 2.5 Hz), 126.3, 126.3, 122.6, 119.6 (d, J = 18.2 Hz), 117.5, 117.3, 116.6 (d, J = 6.5 Hz), 115.0, 110.4, 64.2, 43.7, 33.4, 29.6, 6.8. HRMS (ESI) calculated for $C_{22}H_{25}O_3N_4ClFS$ $[M+H]^+$ 479.1298, found 479.1314.

*1-((3-(3-Chloro-4-fluorophenoxy)-1-cyclopropyl-1H-indazol-5-yl)sulfonyl)piperidin-4-ol (**5**)*. To the solution of **85** (28 mg, 0.057 mmol) in 1,4-dioxane was added CuI (1.0 mg, 0.0057 mmol), *N*,*N*-dimethylglycine (1.5 mg, 0.014 mmol) and Cs_2CO_3 (46 mg, 0.14 mmol). The mixture was stirred at 120 ℃ under argon atmosphere for 20 h. The insoluble matter was removed through filtration and filtrate was concentrated under vacuum. The residue was dissolved in THF (2 mL) and H_2O (2 mL). To the mixture was added LiOH (0.5 mmol). The mixture was stirred at room temperature for 1 h and extracted with ethyl acetate (15 mL). The organic layer was washed with brine, dried with anhydrous Na_2SO_4, and concentrated. The residue was purified with column chromatography on C18 silico gel to afford compound **5**. Yield: 40%. ^{1}H NMR (400 MHz, DMSO-d_6) δ 7.88 (d, J = 8.9 Hz, 1H), 7.83 (d, J = 1.5 Hz, 1H), 7.77 (dd, J = 8.9, 1.7 Hz, 1H), 7.64 (dd, J = 6.2, 3.0 Hz, 1H), 7.49 (t, J = 9.0 Hz, 1H), 7.36 (dt, J = 9.1, 3.5 Hz, 1H), 4.65 (s, 1H), 3.72 (tt, J = 6.8, 4.1 Hz, 1H), 3.49 (dq, J = 7.7, 4.0 Hz, 1H), 3.11 (ddd, J = 11.2, 7.1, 3.7 Hz, 2H), 2.69 (ddd, J = 11.7, 8.3, 3.4 Hz, 2H), 1.73 (ddt, J = 13.9, 7.2, 3.5 Hz, 2H), 1.42 (dtd, J = 12.2, 8.1, 3.7 Hz, 2H), 1.11 (dq, J = 7.7, 2.5 Hz, 4H). ^{13}C NMR (101 MHz, DMSO-d_6) δ 154.5 (d, J = 243.2 Hz), 153.0, 152.1 (d, J = 2.9 Hz), 143.2, 128.4, 126.3, 121.2, 120.9, 120.5 (d, J = 19.6 Hz), 119.7 (d, J = 7.3 Hz),

118.1 (d, *J* = 23.1 Hz), 112.4, 111.8, 64.1, 43.6, 33.3, 29.9, 6.9. HRMS (ESI) calculated for $C_{21}H_{21}O_4N_3F_3S$ $[M+H]^+$ 468.1184, found 468.1199.

*1-((1-Cyclopropyl-3-((3,4,5-trifluorophenyl)amino)-1H-indazol-5-yl)sulfonyl)piperidin-4-ol (**6**)*. 52% yield, ^{1}H NMR (400 MHz, DMSO-d_6) δ 9.77 (s, 1H), 8.52 (s, 1H), 7.74 (d, *J* = 1.8 Hz, 2H), 7.57 (dt, *J* = 10.9, 5.0 Hz, 2H), 4.66 (d, *J* = 3.9 Hz, 1H), 3.69 (ddd, *J* = 10.6, 6.9, 4.3 Hz, 1H), 3.51 (tq, *J* = 7.5, 3.7 Hz, 1H), 3.29 – 3.09 (m, 2H), 2.73 (ddd, *J* = 11.6, 8.4, 3.4 Hz, 2H), 1.76 (ddt, *J* = 13.9, 7.2, 3.6 Hz, 2H), 1.45 (dtd, *J* = 12.0, 8.0, 3.6 Hz, 2H), 1.24 – 1.09 (m, 4H). ^{13}C NMR (101 MHz, DMSO-d_6) δ 150.8 (ddd, *J* = 242.6, 9.9, 6.1 Hz), 144.7, 141.9, 139.3 – 138.3 (m), 132.7 (dt, *J* = 239.8, 16.1 Hz), 126.5, 126.3, 122.4, 114.8, 110.5, 100.4 (d, *J* = 24.7 Hz), 64.2, 43.6, 33.3, 29.6, 6.8. HRMS (ESI) calculated for $C_{21}H_{22}O_3N_4F_3S$ $[M+H]^+$ 467.1339, found 467.1359.

*1-((1-Cyclopropyl-7-fluoro-3-((3,4,5-trifluorophenyl)amino)-1H-indazol-5-yl)sulfonyl)piperidin-4-ol (**7**)*. 31% yield, ^{1}H NMR (400 MHz, DMSO-d_6) δ 9.75 (s, 1H), 8.34 (s, 1H), 7.58 – 7.44 (m, 3H), 4.68 (d, *J* = 3.9 Hz, 1H), 3.83 (tt, *J* = 7.2, 3.7 Hz, 1H), 3.51 (tq, *J* = 7.6, 3.6 Hz, 1H), 3.19 (ddd, *J* = 10.6, 6.2, 3.4 Hz, 2H), 2.75 (ddd, *J* = 11.8, 8.3, 3.4 Hz, 2H), 1.76 (ddt, *J* = 13.8, 7.3, 3.6 Hz, 2H), 1.45 (dtd, *J* = 12.3, 8.3, 3.7 Hz, 2H), 1.25 – 1.19 (m, 2H), 1.15 – 1.09 (m, 2H). ^{13}C NMR (101 MHz, DMSO-d_6) δ 150.8 (ddd, *J* = 242.8, 10.0, 6.0 Hz), 147.5 (d, *J* = 252.4 Hz), 144.9 (d, *J* = 2.2 Hz), 138.6 – 138.2 (m), 134.4 – 131.5 (m), 131.4 (d, *J* = 13.6 Hz), 127.0 (d, *J* = 4.4 Hz), 118.6 (d, *J* = 6.0 Hz), 118.4 (d, *J* = 3.7 Hz), 111.4 (d, *J* = 20.7 Hz), 100.5 (d, *J* = 24.9

Hz), 64.2, 43.8, 33.4, 32.0 (d, *J* = 2.6 Hz), 7.8 (d, *J* = 3.0 Hz). HRMS (ESI) calculated for $C_{21}H_{21}O_3N_4F_4S$ $[M+H]^+$ 485.1265, found 485.1244.

*1-((1-Cyclopropyl-6-fluoro-3-((3,4,5-trifluorophenyl)amino)-1H-indazol-5-yl)sulfonyl)piperidin-4-ol (**8**)*. 21% yield, ^{1}H NMR (400 MHz, DMSO-d_6) δ 9.81 (s, 1H), 8.59 (d, *J* = 6.6 Hz, 1H), 7.60 (d, *J* = 11.2 Hz, 1H), 7.53 (dd, *J* = 11.0, 6.2 Hz, 2H), 4.71 (d, *J* = 4.0 Hz, 1H), 3.66 (p, *J* = 5.3 Hz, 1H), 3.62 – 3.51 (m, 1H), 2.89 (ddd, *J* = 12.0, 8.3, 3.2 Hz, 2H), 1.76 (ddt, *J* = 13.4, 7.1, 3.5 Hz, 2H), 1.43 (dtd, *J* = 12.5, 8.3, 3.7 Hz, 2H), 1.13 (d, *J* = 5.3 Hz, 4H). ^{13}C NMR (101 MHz, DMSO-d_6) δ 158.3 (d, *J* = 251.3 Hz), 150.8 (ddd, *J* = 243.0, 10.1, 6.4 Hz), 144.9, 142.4 (d, *J* = 12.5 Hz), 138.5 (t, *J* = 12.6 Hz), 132.8 (d, *J* = 240.9 Hz), 125.6 (d, *J* = 3.1 Hz), 117.5 (d, *J* = 19.1 Hz), 111.5, 100.5 (d, *J* = 24.4 Hz), 97.5 (d, *J* = 27.7 Hz), 64.5, 43.3, 33.7, 29.8, 6.8. HRMS (ESI) calculated for $C_{21}H_{21}O_3N_4F_4S$ $[M+H]^+$ 485.1265, found 485.1243.

*1-((1-Cyclopropyl-4-fluoro-3-((3,4,5-trifluorophenyl)amino)-1H-indazol-5-yl)sulfonyl)piperidin-4-ol (**9**)*. 12% yield, ^{1}H NMR (400 MHz, DMSO-d_6) δ 9.06 (s, 1H), 7.68 (dd, *J* = 8.9, 6.2 Hz, 1H), 7.59 (dd, *J* = 11.2, 6.3 Hz, 2H), 7.55 (d, *J* = 8.9 Hz, 1H), 4.71 (d, *J* = 4.0 Hz, 1H), 3.73 (tt, *J* = 7.0, 4.0 Hz, 1H), 3.56 (dq, *J* = 8.1, 4.1 Hz, 1H), 3.28 (dt, *J* = 11.3, 4.7 Hz, 2H), 2.88 (ddd, *J* = 11.9, 8.8, 3.2 Hz, 2H), 1.82 – 1.71 (m, 2H), 1.45 (dtd, *J* = 12.3, 8.1, 3.7 Hz, 2H), 1.20 – 1.11 (m, 4H). ^{13}C NMR (101 MHz, DMSO-d_6) δ 153.3 (d, *J* = 263.6 Hz), 152.0 – 149.0 (m), 145.4 (d, *J* = 8.7 Hz), 142.5 (d, *J* = 2.2 Hz), 139.0, 129.3, 113.4 (d, *J* = 11.3 Hz), 106.8 (d, *J* = 3.9 Hz), 105.1 (d, *J* = 20.1 Hz), 101.1 (d, *J* = 24.9 Hz), 64.3, 43.5, 33.5, 29.9, 6.9. HRMS (ESI) calculated for $C_{21}H_{21}O_3N_4F_4S$ $[M+H]^+$ 485.1265, found 485.1243.

*1-((1-Cyclopropyl-3-((3,4,5-trifluorophenyl)amino)-1H-pyrazolo[3,4-b]pyridin-5-yl)sulfonyl)piperidin-4-ol (**10**)*. 27% yield, ^{1}H NMR (400 MHz, DMSO-d_6) δ 9.91 (s, 1H), 8.82 (d, *J* = 2.1 Hz, 1H), 8.80 (d, *J* = 2.1 Hz, 1H), 7.49 (dd, *J* = 10.8, 6.2 Hz, 2H), 4.68 (d, *J* = 4.0 Hz, 1H), 3.82 (tt, *J* = 7.3, 3.7 Hz, 1H), 3.51 (tq, *J* = 7.5, 3.6 Hz, 1H), 3.20 (ddd, *J* = 13.1, 6.1, 3.0 Hz, 2H), 2.76 (ddd, *J* = 11.8, 8.6, 3.3 Hz, 2H), 1.77 (ddt, *J* = 13.5, 6.6, 3.5 Hz, 2H), 1.45 (dtd, *J* = 12.3, 8.0, 3.5 Hz, 2H), 1.25 – 1.18 (m, 2H), 1.18 – 1.10 (m, 2H). ^{13}C NMR (101 MHz, DMSO-d_6) δ 151.1, 150.8 (ddd, *J* = 243.0, 10.0, 5.8 Hz), 148.6, 143.6, 138.2 (td, *J* = 12.3, 2.8 Hz), 133.0 (dt, *J* = 240.5, 15.9 Hz), 131.5, 123.8, 107.3, 100.7 (d, *J* = 24.3 Hz), 64.2, 43.7, 33.4, 29.2, 6.6. HRMS (ESI) calculated for $C_{20}H_{21}O_3N_5F_3S$ $[M+H]^+$ 468.1312, found 468.1291.

*1-((1-Cyclopropyl-3-((3,4,5-trifluorophenyl)amino)-1H-pyrazolo[3,4-c]pyridin-5-yl)sulfonyl)piperidin-4-ol (**11**)*. 47% yield, ^{1}H NMR (400 MHz, DMSO-d_6) δ 9.86 (s, 1H), 9.15 (s, 1H), 8.62 (s, 1H), 7.48 (dd, *J* = 10.9, 6.1 Hz, 2H), 4.69 (d, *J* = 3.9 Hz, 1H), 3.84 (dq, *J* = 6.9, 3.5, 3.0 Hz, 1H), 3.63 – 3.48 (m, 2H), 3.41 (dt, *J* = 11.4, 4.5 Hz, 2H), 2.94 (ddd, *J* = 12.2, 8.8, 3.4 Hz, 2H), 1.83 – 1.67 (m, 2H), 1.52 – 1.33 (m, 2H), 1.23 – 1.16 (m, 4H). ^{13}C NMR (101 MHz, DMSO-d_6) δ 150.8 (ddd, *J* = 242.6, 10.0, 5.8 Hz), 144.6, 143.9, 138.9 – 137.9 (m), 137.5, 134.8, 132.9 (d, *J* = 240.7 Hz), 118.8, 116.4, 100.5 (d, *J* = 24.7 Hz), 64.8, 44.2, 33.8, 30.3, 7.0. HRMS (ESI) calculated for $C_{20}H_{21}O_3N_5F_3S$ $[M+H]^+$ 468.1312, found 468.1289.

*1-((1-Cyclopropyl-3-((3,4,5-trifluorophenyl)amino)-1H-pyrazolo[4,3-b]pyridin-5-yl)sulfonyl)piperidin-4-ol (**12**)*. 21% yield, ^{1}H NMR (400 MHz, DMSO-d_6) δ 9.67 (s, 1H), 8.25 (d, *J* = 8.8 Hz, 1H), 7.94 (d, *J* = 8.8 Hz, 1H), 7.72 (dd, *J* = 11.2, 6.2 Hz, 2H),

4.69 (d, *J* = 4.0 Hz, 1H), 3.81 – 3.67 (m, 1H), 3.59 – 3.46 (m, 1H), 3.41 (dd, *J* = 12.4, 5.6 Hz, 2H), 2.95 (ddd, *J* = 12.2, 8.8, 3.3 Hz, 2H), 1.73 (ddt, *J* = 13.6, 7.0, 3.6 Hz, 2H), 1.40 (dtd, *J* = 12.6, 8.6, 3.8 Hz, 2H), 1.15 (d, *J* = 5.2 Hz, 4H). ^{13}C NMR (101 MHz, DMSO-d_6) δ 151.7 – 148.8 (m), 148.3, 143.6, 138.2 (t, *J* = 12.5 Hz), 134.0, 133.9 – 131.1 (m), 131.9, 120.8, 119.2, 100.7 (d, *J* = 24.7 Hz), 64.2, 43.6, 33.3, 29.6, 6.2. HRMS (ESI) calculated for $C_{20}H_{21}O_3N_5F_3S$ $[M+H]^+$ 468.1312, found 468.1291.

1-((1-Cyclopropyl-3-((4-fluorophenyl)amino)-1H-indazol-5-yl)sulfonyl)piperidin-4-ol ***(13)***. 11% yield, ^{1}H NMR (400 MHz, DMSO-d_6) δ 9.39 (s, 1H), 8.58 (d, *J* = 1.3 Hz, 1H), 7.79 – 7.72 (m, 2H), 7.70 (d, *J* = 1.2 Hz, 2H), 7.21 – 7.13 (m, 2H), 4.69 (s, 1H), 3.65 (p, *J* = 5.3 Hz, 1H), 3.51 (tt, *J* = 7.6, 3.6 Hz, 1H), 3.18 – 3.11 (m, 2H), 2.72 (ddd, *J* = 11.8, 8.4, 3.4 Hz, 2H), 1.76 (ddt, *J* = 13.5, 6.8, 2.9 Hz, 2H), 1.45 (dtd, *J* = 12.0, 7.8, 3.6 Hz, 2H), 1.13 (d, *J* = 5.2 Hz, 4H). ^{13}C NMR (101 MHz, DMSO-d_6) δ 156.5 (d, *J* = 235.7 Hz), 145.7, 142.1, 139.0 (d, *J* = 2.1 Hz), 126.1 (d, *J* = 26.0 Hz), 122.8, 117.8 (d, *J* = 7.4 Hz), 115.9, 115.6, 115.1, 110.2, 64.2, 43.7, 33.4, 29.6, 6.9. HRMS (ESI) calculated for $C_{21}H_{24}O_3N_4FS$ $[M+H]^+$ 431.1548, found 431.1528.

1-((1-Cyclopropyl-3-(p-tolylamino)-1H-indazol-5-yl)sulfonyl)piperidin-4-ol ***(14)***. 49% yield, ^{1}H NMR (400 MHz, DMSO-d_6) δ 9.24 (s, 1H), 8.60 (t, *J* = 1.3 Hz, 1H), 7.72 – 7.67 (m, 2H), 7.67 – 7.61 (m, 2H), 7.12 (d, *J* = 8.3 Hz, 2H), 4.68 (d, *J* = 3.3 Hz, 1H), 3.64 (p, *J* = 5.3 Hz, 1H), 3.52 (d, *J* = 8.6 Hz, 1H), 3.16 (ddd, *J* = 11.1, 6.9, 3.7 Hz, 2H), 2.72 (ddd, *J* = 11.8, 8.4, 3.4 Hz, 2H), 2.26 (s, 3H), 1.76 (ddt, *J* = 13.5, 6.8, 2.9 Hz, 2H), 1.46 (dtd, *J* = 12.0, 7.9, 3.5 Hz, 2H), 1.13 (d, *J* = 5.2 Hz, 4H). ^{13}C NMR (101 MHz, DMSO-d_6) δ 145.8, 142.1, 140.1, 129.7, 128.7, 126.1, 125.8, 122.9, 116.6, 115.3,

110.08, 64.3, 43.7, 33.4, 29.6, 20.8, 6.9. HRMS (ESI) calculated for $C_{23}H_{27}O_3N_4S$ $[M+H]^+$ 427.1798, found 427.1779.

*1-((3-((4-Chlorophenyl)amino)-1-cyclopropyl-1H-indazol-5-yl)sulfonyl)piperidin-4-ol **(15)***. 36% yield, ^{1}H NMR (400 MHz, DMSO) δ 9.51 (s, 1H), 8.58 (s, 1H), 7.74 (dd, *J* = 14.7, 10.6 Hz, 4H), 7.45 – 7.30 (m, 2H), 4.66 (d, *J* = 3.6 Hz, 1H), 3.72 – 3.59 (m, 1H), 3.51 (s, 1H), 3.15 (s, 2H), 2.71 (d, *J* = 8.1 Hz, 2H), 1.75 (s, 2H), 1.53 – 1.38 (m, 2H), 1.13 (d, *J* = 4.6 Hz, 4H). ^{13}C NMR (101 MHz, DMSO-d_6) δ 145.2, 142.0, 141.3, 129.1, 126.2, 126.0, 123.4, 122.7, 118.0, 115.2, 110.3, 64.2, 43.7, 33.4, 29.6, 6.9. HRMS (ESI) calculated for $C_{21}H_{24}O_3N_4ClS$ $[M+H]^+$ 447.1252, found 447.1232.

*1-((1-Cyclopropyl-3-(phenylamino)-1H-indazol-5-yl)sulfonyl)piperidin-4-ol (**16**)*. 31% yield, ^{1}H NMR (400 MHz, DMSO) δ 9.34 (s, 1H), 8.61 (s, 1H), 7.83 – 7.64 (m, 4H), 7.32 (t, *J* = 7.9 Hz, 2H), 6.87 (t, *J* = 7.3 Hz, 1H), 4.66 (d, *J* = 3.8 Hz, 1H), 3.66 (dt, *J* = 10.4, 5.3 Hz, 1H), 3.59 – 3.45 (m, 1H), 3.16 (s, 2H), 2.72 (t, *J* = 8.3 Hz, 2H), 1.76 (dd, *J* = 12.3, 3.4 Hz, 2H), 1.46 (dd, *J* = 8.2, 3.8 Hz, 2H), 1.14 (d, *J* = 5.2 Hz, 4H). ^{13}C NMR (101 MHz, DMSO-d_6) δ 145.6, 142.5, 142.0, 129.3, 126.1, 125.8, 122.8, 120.1, 116.5, 115.3, 110.2, 64.2, 43.7, 33.4, 29.6, 6.9. HRMS (ESI) calculated for $C_{21}H_{25}O_3N_4S$ $[M+H]^+$ 413.1642, found 413.1623.

*1-((1-Cyclopropyl-3-((4-fluoro-2-methylphenyl)amino)-1H-indazol-5-yl)sulfonyl)piperidin-4-ol (**17**)*. 20% yield, ^{1}H NMR (400 MHz, DMSO-d_6) δ 8.41 (s, 1H), 8.16 (s, 1H), 7.81 – 7.61 (m, 3H), 7.07 (dd, *J* = 9.7, 2.9 Hz, 1H), 7.02 – 6.93 (m, 1H), 4.65 (d, *J* = 3.8 Hz, 1H), 3.65 – 3.54 (m, 1H), 3.54 – 3.45 (m, 1H), 3.14 (td, *J* = 11.1, 10.7, 5.0 Hz, 2H), 2.78 – 2.64 (m, 2H), 2.32 (s, 3H), 1.85 – 1.66 (m, 2H), 1.54 –

1.36 (m, 2H), 1.14 – 0.97 (m, 4H). ^{13}C NMR (101 MHz, DMSO-d_6) δ 157.8 (d, J = 237.9 Hz), 146.7, 142.6, 137.0 (d, J = 2.5 Hz), 131.6 (d, J = 7.7 Hz), 125.9, 123.1, 122.0 (d, J = 8.3 Hz), 117.2 (d, J = 22.0 Hz), 115.1, 112.9 (d, J = 21.6 Hz), 110.3, 64.2, 43.6, 33.4, 29.4, 18.7, 6.8. HRMS (ESI) calculated for $C_{22}H_{26}O_3N_4FS$ $[M+H]^+$ 445.1704, found 445.1684.

*1-((3-((2-Chloro-4-fluorophenyl)amino)-1-cyclopropyl-1H-indazol-5-yl)sulfonyl)piperidin-4-ol (**18**)*. 43% yield, ^{1}H NMR (400 MHz, DMSO-d_6) δ 8.57 (s, 1H), 8.54 (d, J = 1.5 Hz, 1H), 8.03 (dd, J = 9.2, 5.6 Hz, 1H), 7.80 – 7.64 (m, 2H), 7.47 (dd, J = 8.5, 3.0 Hz, 1H), 7.22 (td, J = 8.6, 3.0 Hz, 1H), 4.66 (d, J = 3.8 Hz, 1H), 3.71 – 3.60 (m, 1H), 3.53 (tq, J = 7.6, 3.7 Hz, 1H), 3.16 (ddt, J = 11.2, 7.3, 4.5 Hz, 2H), 2.74 (ddd, J = 11.8, 8.5, 3.4 Hz, 2H), 1.86 – 1.68 (m, 2H), 1.46 (dtd, J = 12.1, 8.0, 3.6 Hz, 2H), 1.15 – 1.05 (m, 4H). ^{13}C NMR (100 MHz, DMSO-d_6) δ 156.7 (d, J = 240.9 Hz), 145.4, 142.5, 136.0 (d, J = 3.0 Hz), 126.4, 126.0, 123.4 (d, J = 10.5 Hz), 123.3, 121.8 (d, J = 8.2 Hz), 117.0 (d, J = 25.7 Hz), 115.3, 115.0 (d, J = 21.8 Hz), 110.4, 64.2, 43.7, 33.4, 29.6, 6.9. HRMS (ESI) calculated for $C_{21}H_{23}O_3N_4ClFS$ $[M+H]^+$ 465.1158, found 465.1139.

*1-((1-Cyclopropyl-3-((3,4-difluorophenyl)amino)-1H-indazol-5-yl)sulfonyl)piperidin-4-ol (**19**)*. 11% yield, ^{1}H NMR (400 MHz, DMSO-d_6) δ 9.63 (s, 1H), 8.56 (d, J = 1.2 Hz, 1H), 7.96 – 7.82 (m, 1H), 7.71 (s, 2H), 7.48 – 7.31 (m, 2H), 4.66 (s, 1H), 3.76 – 3.60 (m, 1H), 3.50 (s, 1H), 3.14 (dt, J = 11.2, 4.0 Hz, 2H), 2.72 (ddd, J = 11.7, 8.4, 3.4 Hz, 2H), 1.82 – 1.67 (m, 2H), 1.44 (dtd, J = 12.1, 8.1, 3.7 Hz, 2H), 1.18 – 1.05 (m, 4H). ^{13}C NMR (100 MHz, DMSO-d_6) δ 151.4 – 146.8 (m), 145.2, 143.4 (dd, J = 237.0, 12.4

Hz), 142.0, 139.6 (dd, *J* = 9.7, 2.2 Hz), 126.3, 126.2, 122.6, 118.0 (d, *J* = 17.7 Hz), 115.0, 112.6 (dd, *J* = 5.3, 2.8 Hz), 110.4, 105.1 (d, *J* = 22.3 Hz), 64.2, 43.7, 33.4, 29.6, 6.9. HRMS (ESI) calculated for $C_{21}H_{23}O_3N_4F_2S$ $[M+H]^+$ 449.1453, found 449.1432.

*1-((1-Cyclopropyl-3-((4-fluoro-3-methylphenyl)amino)-1H-indazol-5-yl)sulfonyl)piperidin-4-ol (**20**)*. 9% yield, ^{1}H NMR (400 MHz, DMSO-d_6) δ 9.27 (s, 1H), 8.56 (s, 1H), 7.68 (s, 2H), 7.63 (dt, *J* = 8.2, 3.6 Hz, 1H), 7.53 (dd, *J* = 6.9, 2.8 Hz, 1H), 7.09 (t, *J* = 9.2 Hz, 1H), 4.66 (s, 1H), 3.64 (p, *J* = 5.3 Hz, 1H), 3.50 (tt, *J* = 7.9, 3.6 Hz, 1H), 3.22 – 3.07 (m, 2H), 2.71 (ddd, *J* = 11.9, 8.6, 3.5 Hz, 2H), 2.24 (s, 3H), 1.74 (ddd, *J* = 13.9, 7.3, 3.6 Hz, 2H), 1.44 (dtd, *J* = 12.3, 8.2, 3.6 Hz, 2H), 1.12 (d, *J* = 5.2 Hz, 4H). ^{13}C NMR (100 MHz, DMSO-d_6) δ 155.2 (d, *J* = 234.8 Hz), 145.7, 142.1, 138.7 (d, *J* = 2.2 Hz), 126.0 (d, *J* = 29.0 Hz), 124.5 (d, *J* = 18.0 Hz), 122.8, 119.2 (d, *J* = 4.0 Hz), 115.5, 115.2 (d, *J* = 4.1 Hz), 115.2, 115.2, 110.2, 64.2, 43.7, 33.4, 29.6, 15.1 (d, *J* = 2.9 Hz), 6.9. HRMS (ESI) calculated for $C_{22}H_{26}O_3N_4FS$ $[M+H]^+$ 445.1704, found 445.1686.

*5-((1-Cyclopropyl-5-((4-hydroxypiperidin-1-yl)sulfonyl)-1H-indazol-3-yl)amino)-2-fluorobenzonitrile (**21**)*. 46% yield, ^{1}H NMR (400 MHz, DMSO-d_6) δ 9.75 (s, 1H), 8.54 (s, 1H), 8.18 (dd, *J* = 5.5, 2.9 Hz, 1H), 8.02 – 7.87 (m, 1H), 7.72 (s, 2H), 7.48 (t, *J* = 9.1 Hz, 1H), 4.64 (d, *J* = 3.8 Hz, 1H), 3.68 (p, *J* = 5.4 Hz, 1H), 3.51 (tt, *J* = 7.7, 3.6 Hz, 1H), 3.15 (tt, *J* = 7.0, 3.2 Hz, 2H), 2.73 (ddd, *J* = 11.8, 8.5, 3.5 Hz, 2H), 1.84 – 1.66 (m, 2H), 1.45 (dtd, *J* = 12.3, 8.2, 3.7 Hz, 2H), 1.15 (d, *J* = 6.4 Hz, 4H). ^{13}C NMR (100 MHz, DMSO-d_6) δ 156.5 (d, *J* = 248.2 Hz), 144.9, 142.0, 139.6 (d, *J* = 2.2 Hz), 126.5, 126.4, 123.5 (d, *J* = 7.5 Hz), 122.5, 119.1, 117.6 (d, *J* = 20.5 Hz), 115.0, 114.9, 110.5, 100.2

(d, *J* = 16.0 Hz), 64.2, 43.7, 33.4, 29.7, 6.9. HRMS (ESI) calculated for $C_{22}H_{23}O_3N_5FS$ $[M+H]^+$ 456.1500, found 456.1477.

*1-((1-Cyclopropyl-3-((2-methylpyridin-4-yl)amino)-1H-indazol-5-yl)sulfonyl)piperidin-4-ol (**22**)*. 32% yield, ^{1}H NMR (400 MHz, DMSO) δ 9.82 (s, 1H), 8.59 (s, 1H), 8.23 (d, *J* = 5.7 Hz, 1H), 7.74 (q, *J* = 8.9 Hz, 2H), 7.50 (d, *J* = 4.3 Hz, 1H), 7.44 (s, 1H), 4.71 (s, 1H), 3.72 (dt, *J* = 10.2, 5.2 Hz, 1H), 3.51 (s, 1H), 3.15 (s, 2H), 2.72 (t, *J* = 8.4 Hz, 2H), 2.42 (s, 3H), 1.83 – 1.68 (m, 2H), 1.45 (d, *J* = 8.4 Hz, 2H), 1.16 (d, *J* = 4.8 Hz, 4H). ^{13}C NMR (100 MHz, DMSO-d_6) δ 158.4, 149.9, 148.6, 144.4, 142.0, 126.5, 126.2, 122.7, 115.2, 110.6, 109.9, 108.7, 64.2, 43.7, 33.4, 29.7, 25.0, 6.9. HRMS (ESI) calculated for $C_{21}H_{26}O_3N_5S$ $[M+H]^+$ 428.1751, found 428.1736.

*1-((1-Cyclopropyl-3-((5-fluoropyridin-2-yl)amino)-1H-indazol-5-yl)sulfonyl)piperidin-4-ol (**23**)*. 70% yield, ^{1}H NMR (400 MHz, DMSO-d_6) δ 10.19 (s, 1H), 8.71 (d, *J* = 1.2 Hz, 1H), 8.23 (d, *J* = 3.0 Hz, 1H), 8.05 (dd, *J* = 9.2, 3.9 Hz, 1H), 7.78 – 7.66 (m, 3H), 4.65 (d, *J* = 3.8 Hz, 1H), 3.69 (tt, *J* = 6.6, 4.5 Hz, 1H), 3.52 (tq, *J* = 7.4, 3.6 Hz, 1H), 3.18 – 3.10 (m, 2H), 2.73 (ddd, *J* = 11.8, 8.4, 3.4 Hz, 2H), 1.76 (ddt, *J* = 14.0, 7.2, 3.5 Hz, 2H), 1.46 (dtd, *J* = 11.9, 7.9, 3.6 Hz, 2H), 1.19 – 1.07 (m, 4H). ^{13}C NMR (100 MHz, DMSO-d_6) δ 154.5 (d, *J* = 243.3 Hz), 151.5, 144.2, 142.2, 135.2 (d, *J* = 24.7 Hz), 126.5, 126.1, 125.9 (d, *J* = 19.9 Hz), 123.7, 115.4, 111.1 (d, *J* = 4.0 Hz), 110.3, 64.3, 43.7, 33.4, 29.6, 6.8. HRMS (ESI) calculated for $C_{20}H_{23}O_3N_5FS$ $[M+H]^+$ 432.1500, found 432.1484.

*1-((1-Cyclopropyl-3-((5-fluoro-4-methylpyridin-2-yl)amino)-1H-indazol-5-yl)sulfonyl)piperidin-4-ol (**24**)*. 43% yield, ^{1}H NMR (400 MHz, DMSO-d_6) δ 10.02 (s,

1H), 8.66 (s, 1H), 8.10 (s, 1H), 7.86 (d, *J* = 5.6 Hz, 1H), 7.78 – 7.66 (m, 2H), 4.64 (d, *J* = 3.8 Hz, 1H), 3.71 (td, *J* = 6.3, 3.2 Hz, 1H), 3.52 (tq, *J* = 7.6, 3.7 Hz, 1H), 3.16 (ddt, *J* = 11.2, 7.2, 4.2 Hz, 2H), 2.73 (ddd, *J* = 11.7, 8.2, 3.3 Hz, 2H), 2.31 (s, 3H), 1.76 (ddt, *J* = 14.0, 7.2, 3.5 Hz, 2H), 1.46 (dtd, *J* = 12.1, 8.1, 3.6 Hz, 2H), 1.19 – 1.07 (m, 4H). ^{13}C NMR (100 MHz, DMSO-d_6) δ 153.9 (d, *J* = 242.1 Hz), 151.4 (d, *J* = 1.9 Hz), 144.2, 142.3, 135.9 (d, *J* = 16.1 Hz), 134.5 (d, *J* = 25.7 Hz), 126.5, 126.0, 123.8, 115.5, 112.1, 110.2, 64.3, 43.7, 33.4, 29.7, 15.0 (d, *J* = 2.8 Hz), 6.8. HRMS (ESI) calculated for $C_{21}H_{25}O_3N_5FS$ $[M+H]^+$ 446.1657, found 446.1638.

*1-((3-(Benzylamino)-1-cyclopropyl-1H-indazol-5-yl)sulfonyl)piperidin-4-ol (**25**)*. 28% yield, ^{1}H NMR (400 MHz, DMSO-d_6) δ 8.34 (d, *J* = 1.6 Hz, 1H), 7.65 – 7.50 (m, 2H), 7.42 (d, *J* = 7.2 Hz, 2H), 7.34 (t, *J* = 7.4 Hz, 2H), 7.25 (t, *J* = 7.3 Hz, 1H), 7.07 (t, *J* = 5.8 Hz, 1H), 4.66 (s, 1H), 4.45 (d, *J* = 5.8 Hz, 2H), 3.48 (qt, *J* = 6.8, 3.8 Hz, 2H), 3.11 (ddd, *J* = 11.2, 6.9, 3.7 Hz, 2H), 2.66 (ddd, *J* = 11.8, 8.5, 3.4 Hz, 2H), 1.73 (ddt, *J* = 13.9, 7.2, 3.5 Hz, 2H), 1.43 (dtd, *J* = 12.2, 8.2, 3.7 Hz, 2H), 1.03 (dt, *J* = 8.3, 2.8 Hz, 4H). ^{13}C NMR (100 MHz, DMSO-d_6) δ 150.4, 143.2, 140.4, 128.6, 128.3, 127.2, 125.84, 124.9, 123.1, 114.5, 109.7, 64.3, 47.0, 43.7, 33.4, 29.2. HRMS (ESI) calculated for $C_{22}H_{27}O_3N_4S$ $[M+H]^+$ 427.1798, found 427.1786.

*1-((1-Cyclopropyl-3-((4-fluorobenzyl)amino)-1H-indazol-5-yl)sulfonyl)piperidin-4-ol (**26**)*. 16% yield, ^{1}H NMR (400 MHz, DMSO-d_6) δ 8.31 (s, 1H), 7.64 – 7.57 (m, 1H), 7.55 (d, *J* = 8.9 Hz, 1H), 7.45 (dd, *J* = 8.4, 5.6 Hz, 2H), 7.16 (t, *J* = 8.7 Hz, 2H), 7.07 (t, *J* = 5.9 Hz, 1H), 4.64 (d, *J* = 3.8 Hz, 1H), 4.42 (d, *J* = 5.7 Hz, 2H), 3.61 – 3.42 (m, 2H), 3.10 (t, *J* = 8.8 Hz, 2H), 2.75 – 2.59 (m, 2H), 1.84 – 1.64 (m, 2H), 1.53 – 1.32 (m,

2H), 1.02 (t, *J* = 6.4 Hz, 4H). ^{13}C NMR (100 MHz, DMSO-d_6) δ 161.6 (d, *J* = 242.0 Hz), 150.3, 143.2, 136.6 (d, *J* = 2.9 Hz), 130.2 (d, *J* = 8.0 Hz), 125.9, 124.9, 123.0, 115.3 (d, *J* = 21.2 Hz), 114.5, 109.8, 64.3, 46.3, 43.7, 33.4, 29.2, 6.7. HRMS (ESI) calculated for $C_{22}H_{26}O_3N_4FS$ $[M+H]^+$ 445.1704, found 445.1687.

General Procedure for synthesis of **27** and **28**. The mixture of **85** (49 mg, 0.1 mmol), the corresponding aniline (0.15 mmol), CuI (1.9 mg, 0.01 mmol), D-proline (1.0 mg, 0.01 mmol) and K_3PO_3 (63 mg, 0.2 mmol) in 1.5 mL DMSO was stirred at 90 ℃ under argon atmosphere. After that, the solution was diluted ethyl acetate and washed with water for twice. The organic phase was concentrated under vacuum and dissolved in THF (2 mL) and H_2O (2 mL). To the mixture was added LiOH (0.5 mmol). The mixture was stirred at room temperature for 1 h and extracted with ethyl acetate (15 mL). The organic layer was washed with brine, dried with anhydrous Na_2SO_4, and concentrated. The residue was purified with column chromatography on C18 silico gel.

1-((3-(Cyclohexylamino)-1-cyclopropyl-1H-indazol-5-yl)sulfonyl)piperidin-4-ol ***(27)***. 17% yield, ^{1}H NMR (400 MHz, DMSO-d_6) δ 8.34 (d, *J* = 1.6 Hz, 1H), 7.58 (dd, *J* = 8.8, 1.7 Hz, 1H), 7.51 (d, *J* = 8.8 Hz, 1H), 6.40 (d, *J* = 7.3 Hz, 1H), 4.64 (d, *J* = 3.8 Hz, 1H), 3.51 (qt, *J* = 7.3, 4.2 Hz, 2H), 3.44 (tt, *J* = 6.9, 3.8 Hz, 1H), 3.12 (ddd, *J* = 11.1, 7.1, 3.8 Hz, 2H), 2.68 (ddd, *J* = 11.7, 8.4, 3.4 Hz, 2H), 2.11 – 2.01 (m, 2H), 1.80 – 1.70 (m, 4H), 1.61 (dt, *J* = 12.7, 3.8 Hz, 1H), 1.45 (ddt, *J* = 12.7, 8.3, 4.0 Hz, 2H), 1.37 – 1.22 (m, 5H), 1.09 – 0.98 (m, 4H). ^{13}C NMR (100 MHz, DMSO-d_6) δ 149.8, 143.0, 125.8, 124.5, 123.1, 114.8, 109.5, 64.3, 51.6, 43.7, 33.4, 33.0, 29.2, 26.2, 25.1, 6.8.

1-((3-(Cyclopentylamino)-1-cyclopropyl-1H-indazol-5-yl)sulfonyl)piperidin-4-ol ***(28)***. 57% yield, ^{1}H NMR (400 MHz, DMSO-d_6) δ 8.32 (d, *J* = 1.5 Hz, 1H), 7.58 (dd, *J* = 8.9, 1.7 Hz, 1H), 7.52 (d, *J* = 8.8 Hz, 1H), 6.51 (d, *J* = 6.4 Hz, 1H), 4.64 (d, *J* = 3.6 Hz, 1H), 3.97 (p, *J* = 6.3 Hz, 1H), 3.49 (dtt, *J* = 16.8, 6.8, 3.8 Hz, 2H), 3.12 (ddd, *J* = 11.1, 7.1, 3.7 Hz, 2H), 2.68 (ddd, *J* = 11.7, 8.4, 3.4 Hz, 2H), 2.05 – 1.90 (m, 2H), 1.80 – 1.65 (m, 4H), 1.63 – 1.50 (m, 4H), 1.44 (dtd, *J* = 12.1, 8.0, 3.5 Hz, 2H), 1.03 (t, *J* = 5.1 Hz, 4H). ^{13}C NMR (100 MHz, DMSO-d_6) δ 150.3, 143.0, 125.7, 124.6, 123.1, 114.8, 109.5, 64.3, 54.5, 43.7, 33.38, 32.9, 29.2, 24.0, 6.8. HRMS (ESI) calculated for $C_{20}H_{29}O_3N_4S$ $[M+H]^+$ 405.1955, found 405.1939.

1-((3-((4-Fluorophenyl)amino)-1-(oxetan-3-yl)-1H-indazol-5-yl)sulfonyl)piperidin-4-ol ***(29)***. 7% yield, ^{1}H NMR (400 MHz, DMSO-d_6) δ 9.49 (s, 1H), 8.61 (s, 1H), 7.84 (dd, *J* = 8.9, 4.8 Hz, 2H), 7.75 (d, *J* = 8.9 Hz, 1H), 7.69 (d, *J* = 9.0 Hz, 1H), 7.21 (t, *J* = 8.7 Hz, 2H), 6.04 (p, *J* = 7.2 Hz, 1H), 5.12 (t, *J* = 6.4 Hz, 2H), 4.97 (t, *J* = 7.0 Hz, 2H), 4.63 (d, *J* = 3.8 Hz, 1H), 3.50 (dt, *J* = 8.2, 3.9 Hz, 1H), 3.16 (dt, *J* = 11.2, 4.6 Hz, 2H), 2.72 (ddd, *J* = 12.0, 8.9, 3.3 Hz, 2H), 1.83 – 1.67 (m, 2H), 1.44 (dtd, *J* = 12.5, 8.4, 3.7 Hz, 2H). ^{13}C NMR (100 MHz, DMSO-d_6) δ 156.6 (d, *J* = 236.2 Hz), 146.6, 141.1, 138.9, 126.2, 126.1, 122.8, 117.9 (d, *J* = 7.3 Hz), 115.8 (d, *J* = 22.1 Hz), 115.0, 110.1, 76.9, 64.2, 51.4, 43.7, 33.4. HRMS (ESI) calculated for $C_{21}H_{24}O_4N_4FS$ $[M+H]^+$ 447.1497, found 447.1476.

1-((1-Ethyl-3-((4-fluorophenyl)amino)-1H-indazol-5-yl)sulfonyl)piperidin-4-ol ***(30)***. 48 % yield, ^{1}H NMR (400 MHz, DMSO-d_6) δ 9.38 (s, 1H), 8.59 (d, *J* = 1.6 Hz, 1H), 7.81 – 7.73 (m, 2H), 7.72 – 7.62 (m, 2H), 7.16 (t, *J* = 8.9 Hz, 2H), 4.66 (d, *J* = 3.9 Hz,

1H), 4.36 (q, *J* = 7.1 Hz, 2H), 3.52 (tt, *J* = 7.8, 3.9 Hz, 1H), 3.18 (ddd, *J* = 11.1, 7.0, 3.7 Hz, 2H), 2.73 (ddd, *J* = 11.8, 8.6, 3.4 Hz, 2H), 1.76 (ddt, *J* = 14.0, 7.3, 3.6 Hz, 2H), 1.52 – 1.36 (m, 5H). ^{13}C NMR (100 MHz, DMSO-d_6) δ 156.4 (d, *J* = 235.7 Hz), 146.0, 140.5, 139.1 (d, *J* = 2.2 Hz), 125.9, 125.3, 122.9, 117.7 (d, *J* = 7.3 Hz), 115.7 (d, *J* = 22.0 Hz), 114.4, 109.8, 64.3, 43.8, 43.3, 33.4, 15.1. HRMS (ESI) calculated for $C_{20}H_{24}O_3N_4FS$ $[M+H]^+$ 419.1548, found 419.1530.

1-((3-((4-Fluorophenyl)amino)-1-isopropyl-1H-indazol-5-yl)sulfonyl)piperidin-4-ol ***(31)***. 44% yield, ^{1}H NMR (400 MHz, DMSO-d_6) δ 9.38 (s, 1H), 8.58 (d, *J* = 1.6 Hz, 1H), 7.82 – 7.74 (m, 2H), 7.72 (d, *J* = 9.0 Hz, 1H), 7.64 (dd, *J* = 8.9, 1.7 Hz, 1H), 7.17 (t, *J* = 8.9 Hz, 2H), 4.92 (p, *J* = 6.5 Hz, 1H), 4.66 (d, *J* = 3.9 Hz, 1H), 3.52 (tt, *J* = 7.6, 3.7 Hz, 1H), 3.17 (ddd, *J* = 11.1, 7.0, 3.8 Hz, 2H), 2.73 (ddd, *J* = 11.7, 8.5, 3.4 Hz, 2H), 1.77 (ddt, *J* = 13.7, 7.1, 3.2 Hz, 2H), 1.54 – 1.41 (m, 8H). ^{13}C NMR (100 MHz, DMSO-d_6) δ 156.4 (d, *J* = 235.4 Hz), 145.7, 140.0, 139.2 (d, *J* = 1.9 Hz), 125.7, 125.2, 122.84, 117.6 (d, *J* = 7.4 Hz), 115.7 (d, *J* = 22.2 Hz), 114.4, 109.8, 64.3, 49.6, 43.8, 33.4, 22.3. HRMS (ESI) calculated for $C_{21}H_{26}O_3N_4FS$ $[M+H]^+$ 433.1704, found 433.1687.

1-((1-Cyclobutyl-3-((4-fluorophenyl)amino)-1H-indazol-5-yl)sulfonyl)piperidin-4-ol ***(32)***. 41% yield, ^{1}H NMR (400 MHz, DMSO-d_6) δ 9.42 (d, *J* = 2.6 Hz, 1H), 8.57 (s, 1H), 7.81 (dt, *J* = 8.0, 3.6 Hz, 2H), 7.72 (dd, *J* = 9.0, 2.6 Hz, 1H), 7.64 (d, *J* = 8.5 Hz, 1H), 7.19 (td, *J* = 9.0, 2.7 Hz, 2H), 5.22 (p, *J* = 9.0 Hz, 1H), 4.66 (t, *J* = 3.3 Hz, 1H), 3.49 (tt, *J* = 7.4, 3.8 Hz, 1H), 3.24 – 3.08 (m, 2H), 2.69 (q, *J* = 9.5, 8.6 Hz, 4H), 2.47 – 2.34 (m, 2H), 1.95 – 1.80 (m, 2H), 1.75 (ddd, *J* = 13.6, 7.0, 3.5 Hz, 2H), 1.45 (ddt, *J* = 16.7, 11.9, 5.6 Hz, 2H). ^{13}C NMR (100 MHz, DMSO-d_6) δ 156.5 (d, *J* = 235.6 Hz),

146.0, 140.2, 139.1 (d, *J* = 1.9 Hz), 125.9, 125.55, 122.8, 117.7 (d, *J* = 7.4 Hz), 115.8 (d, *J* = 22.1 Hz), 114.6, 111.0, 64.3, 51.7, 43.8, 33.4, 29.9, 14.9. HRMS (ESI) calculated for $C_{22}H_{26}O_3N_4S$ $[M+H]^+$ 445.1704, found 445.1684.

1-Cyclopropyl-N-(4-fluorophenyl)-5-(morpholinosulfonyl)-1H-indazol-3-amine (***33***). 24% yield, ^{1}H NMR (400 MHz, DMSO-d_6) δ 9.39 (s, 1H), 8.60 (d, *J* = 1.4 Hz, 1H), 7.75 (dd, *J* = 9.1, 4.7 Hz, 2H), 7.73 – 7.67 (m, 2H), 7.17 (t, *J* = 8.9 Hz, 2H), 3.74 – 3.59 (m, 5H), 2.97 – 2.80 (m, 4H), 1.14 (d, *J* = 5.3 Hz, 4H). ^{13}C NMR (100 MHz, DMSO-d_6) δ 156.5 (d, *J* = 235.7 Hz), 145.7, 142.2, 138.9 (d, *J* = 2.0 Hz), 126.2, 124.8, 123.2, 117.8 (d, *J* = 7.4 Hz), 115.8 (d, *J* = 22.0 Hz), 115.2, 110.4, 65.7, 46.4, 29.6, 6.9. HRMS (ESI) calculated for $C_{20}H_{21}O_3N_4FS$ $[M+H]^+$ 417.1391, found 417.1375.

1-((1-Cyclopropyl-3-((4-fluorophenyl)amino)-1H-indazol-5-yl)sulfonyl)piperidin-3-ol (***34***). 28% yield, ^{1}H NMR (400 MHz, DMSO-d_6) δ 9.38 (s, 1H), 8.58 (d, *J* = 1.2 Hz, 1H), 7.80 – 7.72 (m, 2H), 7.70 (d, *J* = 1.7 Hz, 2H), 7.24 – 7.10 (m, 2H), 4.98 (d, *J* = 4.8 Hz, 1H), 3.65 (p, *J* = 5.3 Hz, 1H), 3.55 (tq, *J* = 8.8, 4.1 Hz, 1H), 3.46 (dd, *J* = 10.9, 4.2 Hz, 1H), 3.30 (s, 1H), 2.31 (td, *J* = 11.1, 2.5 Hz, 1H), 2.18 – 2.07 (m, 1H), 1.81 – 1.65 (m, 2H), 1.47 (qd, *J* = 11.7, 10.6, 3.7 Hz, 1H), 1.13 (d, *J* = 5.3 Hz, 4H), 1.11 – 1.00 (m, 1H). ^{13}C NMR (100 MHz, DMSO-d_6) δ 156.5 (d, *J* = 235.5 Hz), 145.6, 142.1, 139.0 (d, *J* = 2.0 Hz), 126.1, 126.0, 122.7, 117.8 (d, *J* = 7.3 Hz), 115.7 (d, *J* = 22.1 Hz), 115.1, 110.3, 65.5, 53.1, 46.3, 32.4, 29.6, 22.7, 6.9. HRMS (ESI) calculated for $C_{21}H_{24}O_3N_4FS$ $[M+H]^+$ 431.1548, found 431.1534.

1-((1-Cyclopropyl-3-((4-fluorophenyl)amino)-1H-indazol-5-yl)sulfonyl)pyrrolidine-3-carboxylic acid (***35***). 43% yield, ^{1}H NMR (400 MHz, DMSO-d_6) δ 12.52 (s, 1H), 9.37

(s, 1H), 8.66 (s, 1H), 7.77 (dt, *J* = 8.9, 5.7 Hz, 3H), 7.69 (d, *J* = 8.9 Hz, 1H), 7.17 (t, *J* = 8.8 Hz, 2H), 3.65 (p, *J* = 5.3 Hz, 1H), 3.43 – 3.28 (m, 2H), 3.28 – 3.12 (m, 2H), 2.94 (p, *J* = 7.3 Hz, 1H), 1.97 (dd, *J* = 13.0, 7.1 Hz, 1H), 1.88 (td, *J* = 14.6, 12.8, 7.9 Hz, 1H), 1.14 (d, *J* = 5.3 Hz, 4H). ^{13}C NMR (100 MHz, DMSO-d_6) δ 174.3, 156.5 (d, *J* = 235.7 Hz), 145.7, 142.1, 139.0 (d, *J* = 2.1 Hz), 126.2, 126.0, 122.9, 117.8 (d, *J* = 7.5 Hz), 115.7 (d, *J* = 22.0 Hz), 115.1, 110.3, 50.2, 47.9, 42.5, 29.6, 28.4, 6.9. HRMS (ESI) calculated for $C_{21}H_{22}O_4N_4FS$ $[M+H]^+$ 445.1340, found 445.1323.

*1-((1-Cyclopropyl-3-((4-fluorophenyl)amino)-1H-indazol-5-yl)sulfonyl)pyrrolidin-3-ol (**36**)*. 26% yield, ^{1}H NMR (400 MHz, DMSO-d_6) δ 9.41 (s, 1H), 8.64 (s, 1H), 7.85 – 7.71 (m, 3H), 7.67 (d, *J* = 8.8 Hz, 1H), 7.17 (t, *J* = 8.7 Hz, 2H), 4.91 (s, 1H), 4.14 (s, 1H), 3.64 (p, *J* = 5.2 Hz, 1H), 3.25 (ddd, *J* = 15.8, 9.8, 6.2 Hz, 3H), 3.01 (dd, *J* = 10.4, 2.4 Hz, 1H), 1.72 (dtd, *J* = 13.3, 8.6, 4.9 Hz, 1H), 1.61 (ddt, *J* = 13.3, 7.0, 3.6 Hz, 1H), 1.13 (d, *J* = 5.4 Hz, 4H). ^{13}C NMR (100 MHz, DMSO-d_6) δ 156.5 (d, *J* = 235.5 Hz), 145.7, 142.1, 139.0 (d, *J* = 2.2 Hz), 126.7, 126.2, 122.6, 117.8 (d, *J* = 7.4 Hz), 115.7 (d, *J* = 22.2 Hz), 115.1, 110.2, 69.4, 56.3, 46.6, 34.1, 29.6, 6.8. HRMS (ESI) calculated for $C_{20}H_{22}O_3N_4FS$ $[M+H]^+$ 417.1391, found 417.1370.

*(1-((1-Cyclopropyl-3-((4-fluorophenyl)amino)-1H-indazol-5-yl)sulfonyl)piperidin-4-yl)methanol (**37**)*. 25% yield, ^{1}H NMR (400 MHz, DMSO-d_6) δ 9.39 (s, 1H), 8.57 (d, *J* = 1.4 Hz, 1H), 7.84 – 7.70 (m, 3H), 7.68 (d, *J* = 1.2 Hz, 2H), 7.16 (t, *J* = 8.9 Hz, 2H), 4.49 (t, *J* = 5.1 Hz, 1H), 3.75 – 3.58 (m, 3H), 3.27 – 3.10 (m, 2H), 2.17 (td, *J* = 11.7, 2.4 Hz, 2H), 1.70 (dd, *J* = 12.9, 3.3 Hz, 2H), 1.20 – 1.07 (m, 6H). ^{13}C NMR (101 MHz, DMSO-d_6) δ 156.5 (d, *J* = 235.9 Hz), 145.7, 142.1, 139.0 (d, *J* = 2.2 Hz), 126.1 (d, *J* =

8.7 Hz), 122.8, 117.8 (d, *J* = 7.3 Hz), 115.8, 115.6, 115.1, 110.2, 65.7, 46.4, 37.7, 29.6, 28.3, 6.9. HRMS (ESI) calculated for $C_{22}H_{26}O_3N_4FS$ $[M+H]^+$ 445.1704, found 445.1688.

*5-((1,4-Dioxa-8-azaspiro[4.5]decan-8-yl)sulfonyl)-1-cyclopropyl-N-(4-fluorophenyl)-1H-indazol-3-amine (**38**)*. 25% yield, ^{1}H NMR (400 MHz, DMSO-d_6) δ 9.36 (s, 1H), 8.60 (s, 1H), 7.75 (dd, *J* = 8.9, 4.8 Hz, 2H), 7.71 (s, 2H), 7.17 (t, *J* = 8.8 Hz, 2H), 3.78 (s, 4H), 3.65 (dq, *J* = 6.8, 4.5, 3.5 Hz, 1H), 3.00 (t, *J* = 5.5 Hz, 4H), 1.69 (t, *J* = 5.6 Hz, 4H), 1.20 – 1.05 (m, 4H). ^{13}C NMR (101 MHz, DMSO-d_6) δ 156.5 (d, *J* = 235.9 Hz), 145.7, 142.09, 139.0 (d, *J* = 2.1 Hz), 126.1, 125.6, 122.8, 117.8 (d, *J* = 7.4 Hz), 115.8 (d, *J* = 22.2 Hz), 115.1, 110.3, 105.6, 64.2, 45.0, 34.1, 29.6, 6.8. HRMS (ESI) calculated for $C_{23}H_{26}O_4N_4FS$ $[M+H]^+$ 473.1653, found 473.1636.

*1-((1-Cyclopropyl-3-((4-fluorophenyl)amino)-1H-indazol-5-yl)sulfonyl)piperidin-4-one (**39**)*. To the solution of **38** (0.05 mmol, 23 mg) in 1 mL acetone was added HCl (conc., 1 mL). The mixture was stirred at room temperature. Upon completion, acetone was evaporated under vacuum. The residue was neutralized with 1 N NaOH. The product was collected by filtration and dried under vacuum at 40 ℃. 80% yield, ^{1}H NMR (400 MHz, DMSO-d_6) δ 9.40 (s, 1H), 8.67 (s, 1H), 7.82 – 7.66 (m, 4H), 7.16 (t, *J* = 8.7 Hz, 2H), 3.66 (p, *J* = 5.4 Hz, 1H), 3.33 (d, *J* = 6.6 Hz, 4H), 2.44 (t, *J* = 6.1 Hz, 4H), 1.19 – 1.07 (m, 4H). ^{13}C NMR (100 MHz, DMSO-d_6) δ 206.0, 156.50 (d, *J* = 235.6 Hz), 145.7, 142.2, 139.0 (d, *J* = 2.1 Hz), 126.3, 126.0, 122.9, 117.8 (d, *J* = 7.4 Hz), 115.7 (d, *J* = 22.2 Hz), 115.2, 110.4, 45.6, 29.6, 6.9. HRMS (ESI) calculated for $C_{21}H_{22}O_3N_4FS$ $[M+H]^+$ 429.1391, found 429.1376.

*1-Cyclopropyl-N-(4-fluoro-3-methylphenyl)-5-(morpholinosulfonyl)-1H-indazol-3-amine (**40**)*. 58% yield, ^{1}H NMR (400 MHz, DMSO-d_6) δ 9.29 (s, 1H), 8.59 (d, *J* = 1.5 Hz, 1H), 7.78 – 7.67 (m, 2H), 7.67 – 7.60 (m, 1H), 7.54 (dd, *J* = 6.9, 2.8 Hz, 1H), 7.10 (t, *J* = 9.2 Hz, 1H), 3.75 – 3.59 (m, 5H), 2.87 (dd, *J* = 5.6, 3.4 Hz, 4H), 2.25 (s, 3H), 1.14 (d, *J* = 5.3 Hz, 4H). ^{13}C NMR (100 MHz, DMSO-d_6) δ 155.2 (d, *J* = 235.1 Hz), 145.7, 142.2, 138.6 (d, *J* = 2.2 Hz), 126.2, 124.7, 124.5 (d, *J* = 18.1 Hz), 123.2, 119.2 (d, *J* = 4.0 Hz), 110.3, 65.7, 46.4, 29.6, 15.1 (d, *J* = 3.0 Hz), 6.8. HRMS (ESI) calculated for $C_{21}H_{24}O_3N_4FS$ $[M+H]^+$ 431.1548, found 431.1530.

1-Cyclopropyl-6-fluoro-N-(4-fluoro-3-methylphenyl)-5-(morpholinosulfonyl)-1H-indazol-3-amine (***41***). 56% yield, ^{1}H NMR (400 MHz, DMSO-d_6) δ 9.36 (s, 1H), 8.66 (d, *J* = 6.7 Hz, 1H), 7.61 (ddd, *J* = 8.9, 4.4, 2.9 Hz, 1H), 7.55 (d, *J* = 11.3 Hz, 1H), 7.52 (dd, *J* = 6.8, 2.8 Hz, 1H), 7.08 (t, *J* = 9.2 Hz, 1H), 3.77 – 3.55 (m, 5H), 3.03 (dd, *J* = 5.7, 3.5 Hz, 4H), 2.24 (d, *J* = 1.8 Hz, 3H), 1.11 (td, *J* = 5.2, 4.6, 3.1 Hz, 4H). ^{13}C NMR (101 MHz, DMSO-d_6) δ 157.7 (d, *J* = 250.6 Hz), 154.8 (d, *J* = 235.3 Hz), 145.5, 142.2 (d, *J* = 12.5 Hz), 138.0 (d, *J* = 2.2 Hz), 125.9 (d, *J* = 3.2 Hz), 124.0 (d, *J* = 18.1 Hz), 118.8 (d, *J* = 4.0 Hz), 115.1 (d, *J* = 11.7 Hz), 114.9 (d, *J* = 6.2 Hz), 114.8 (d, *J* = 2.1 Hz), 111.6, 96.8 (d, *J* = 27.7 Hz), 65.6, 45.6, 29.2, 14.6 (d, *J* = 3.0 Hz), 6.3. HRMS (ESI) calculated for $C_{21}H_{23}O_3N_4F_2S$ $[M+H]^+$ 449.1453, found 449.1438.

*1-Cyclopropyl-N-(4-fluoro-3-methylphenyl)-5-(morpholinosulfonyl)-1H-pyrazolo[3,4-c]pyridin-3-amine (**42**)*. ^{1}H NMR (400 MHz, DMSO-d_6) δ 9.44 (s, 1H), 9.13 (s, 1H), 8.73 (s, 1H), 7.61 (dt, *J* = 8.4, 3.6 Hz, 1H), 7.52 (dd, *J* = 6.8, 2.8 Hz, 1H), 7.11 (t, *J* = 9.2 Hz, 1H), 3.83 (tt, *J* = 7.0, 3.8 Hz, 1H), 3.64 (t, *J* = 4.7 Hz, 4H), 3.13 (t, *J* = 4.7 Hz,

4H), 2.26 (d, *J* = 1.8 Hz, 3H), 1.31 – 1.12 (m, 4H). ^{13}C NMR (100 MHz, DMSO-d_6) δ 155.4 (d, *J* = 235.5 Hz), 145.6, 142.6, 138.3 (d, *J* = 2.2 Hz), 137.7, 134.7, 124.6 (d, *J* = 18.0 Hz), 119.3 (d, *J* = 4.2 Hz), 119.0, 117.4, 115.7 – 115.4 (m), 115.3, 66.1, 46.9, 30.2, 15.1 (d, *J* = 2.9 Hz), 7.0. ^{13}C NMR (100 MHz, DMSO-d_6) δ 155.4 (d, *J* = 235.5 Hz), 145.6, 142.6, 138.3 (d, *J* = 2.2 Hz), 137.7, 134.7, 124.6 (d, *J* = 18.0 Hz), 119.3 (d, *J* = 4.2 Hz), 119.0, 117.4, 115.5 (d, *J* = 23.4 Hz), 115.3, 66.1, 46.8, 30.2, 15.11 (d, *J* = 2.9 Hz), 7.0. HRMS (ESI) calculated for $C_{20}H_{23}O_3N_5FS$ $[M+H]^+$ 432.1500, found 432.1488.

1-Cyclopropyl-N-(3,4-difluorophenyl)-5-(morpholinosulfonyl)-1H-indazol-3-amine ***(43)***. 9% yield, ^{1}H NMR (400 MHz, DMSO-d_6) δ 9.63 (s, 1H), 8.57 (s, 1H), 7.89 (dd, *J* = 13.8, 7.1 Hz, 1H), 7.72 (q, *J* = 8.9 Hz, 2H), 7.45 – 7.33 (m, 2H), 3.66 (dt, *J* = 15.6, 5.0 Hz, 5H), 2.87 (t, *J* = 4.5 Hz, 4H), 1.15 (d, *J* = 5.3 Hz, 4H). ^{13}C NMR (101 MHz, DMSO-d_6) δ 149.7 (dd, *J* = 241.7, 12.9 Hz), 145.2, 143.5 (dd, *J* = 237.1, 12.9 Hz), 142.1, 139.6 (dd, *J* = 9.6, 2.2 Hz), 126.3, 125.1, 123.0, 118.0 (d, *J* = 17.8 Hz), 115.0, 112.6 (dd, *J* = 5.6, 2.9 Hz), 110.5, 105.1 (d, *J* = 22.1 Hz), 65.7, 46.4, 29.6, 6.9. HRMS (ESI) calculated for $C_{20}H_{21}O_3N_4F_2S$ $[M+H]^+$ 435.1297, found 435.1282.

1-((1-Cyclopropyl-3-((3,4-difluorophenyl)amino)-1H-pyrazolo[3,4-c]pyridin-5-yl)sulfonyl)piperidin-4-ol ***(44)***. 47% yield, ^{1}H NMR (400 MHz, DMSO-d_6) δ 9.59 (s, 1H), 8.64 (s, 1H), 7.97 – 7.81 (m, 2H), 7.74 (d, *J* = 8.9 Hz, 1H), 7.46 – 7.31 (m, 2H), 4.47 (s, 2H), 3.76 – 3.63 (m, 2H), 3.61 (d, *J* = 7.5 Hz, 1H), 3.23 (d, *J* = 10.0 Hz, 1H), 3.12 (d, *J* = 9.9 Hz, 1H), 1.57 (d, *J* = 9.8 Hz, 1H), 1.15 (d, *J* = 6.3 Hz, 4H), 0.97 (d, *J* = 10.0 Hz, 1H). ^{13}C NMR (101 MHz, DMSO-d_6) δ 149.7 (dd, *J* = 241.8, 13.0 Hz), 145.3 , 143.5 (dd, *J* = 237.1, 12.8 Hz), 142.0, 139.6 (dd, *J* = 9.5, 2.2 Hz), 128.3, 126.0, 122.6,

117.9 (d, *J* = 17.6 Hz), 114.9, 112.6 (dd, *J* = 5.6, 3.0 Hz), 110.7, 105.0 (d, *J* = 22.1 Hz), 76.1, 73.6, 60.3, 56.2, 35.4, 29.6, 6.8. HRMS (ESI) calculated for $C_{20}H_{22}O_3N_2F_2S$ $[M+H]^+$ 450.1406, found 450.1388.

*1-Cyclopropyl-N-(3,4-difluorophenyl)-5-(morpholinosulfonyl)-1H-pyrazolo[3,4-c]pyridin-3-amine (**45**).* 30% yield, ^{1}H NMR (400 MHz, DMSO) δ 9.75 (s, 1H), 9.17 (s, 1H), 8.71 (s, 1H), 7.85 (dd, *J* = 12.8, 6.6 Hz, 1H), 7.41 (dd, *J* = 17.8, 7.7 Hz, 2H), 3.85 (d, *J* = 3.7 Hz, 1H), 3.64 (s, 4H), 3.13 (s, 4H), 1.34 – 1.08 (m, 4H). ^{13}C NMR (101 MHz, DMSO-d_6) δ 149.7 (dd, *J* = 242.0, 13.3 Hz), 145.1, 143.7 (dd, *J* = 237.7, 12.8 Hz), 142.8, 139.2 (dd, *J* = 9.5, 2.1 Hz), 137.6, 134.9, 118.8, 118.1 (d, *J* = 17.8 Hz), 117.2, 112.7 (dd, *J* = 5.7, 3.0 Hz), 105.1 (d, *J* = 22.2 Hz), 66.1, 46.8, 30.3, 7.0. HRMS (ESI) calculated for $C_{19}H_{20}O_3N_5F_2S$ $[M+H]^+$ 436.1249, found 436.1234.

*1-Cyclopropyl-N-(4-fluoro-3-(trifluoromethyl)phenyl)-5-(morpholinosulfonyl)-1H-indazol-3-amine (**46**).* 68% yield, ^{1}H NMR (400 MHz, DMSO-d_6) δ 9.77 (s, 1H), 8.58 (d, *J* = 1.5 Hz, 1H), 8.18 (dd, *J* = 6.3, 2.8 Hz, 1H), 8.01 (dt, *J* = 8.9, 3.6 Hz, 1H), 7.77 (d, *J* = 8.9 Hz, 1H), 7.72 (dd, *J* = 8.8, 1.7 Hz, 1H), 7.49 (t, *J* = 9.8 Hz, 1H), 3.73 (p, *J* = 5.3 Hz, 1H), 3.65 (dd, *J* = 5.8, 3.6 Hz, 4H), 2.97 – 2.80 (m, 4H), 1.15 (d, *J* = 5.3 Hz, 4H). ^{13}C NMR (101 MHz, DMSO-d_6) δ 152.6 (dd, *J* = 244.9, 2.6 Hz), 145.1, 142.1, 139.2 (d, *J* = 2.3 Hz), 126.3, 125.2, 123.3 (q, *J* = 271.8 Hz), 123.0, 121.8 (d, *J* = 7.7 Hz), 118.1 (d, *J* = 21.5 Hz), 116.9 (qd, *J* = 31.8, 13.1 Hz), 115.0, 113.8 (q, *J* = 5.0 Hz), 110.5, 65.7, 46.4, 29.7, 6.7. HRMS (ESI) calculated for $C_{21}H_{21}O_3N_4F_4S$ $[M+H]^+$ 485.1265, found 485.1247.

*1-((1-Cyclopropyl-3-((4-fluoro-3-(trifluoromethyl)phenyl)amino)-1H-indazol-5-yl)sulfonyl)piperidin-4-ol (**47**)*. 56% yield, ^{1}H NMR (400 MHz, DMSO-d_6) δ 9.74 (s, 1H), 8.56 (s, 1H), 8.17 (dd, *J* = 6.3, 2.8 Hz, 1H), 8.01 (dt, *J* = 9.1, 3.6 Hz, 1H), 7.81 – 7.69 (m, 2H), 7.49 (t, *J* = 9.8 Hz, 1H), 4.65 (d, *J* = 3.9 Hz, 1H), 3.72 (p, *J* = 5.3 Hz, 1H), 3.51 (dh, *J* = 7.8, 3.7 Hz, 1H), 3.25 – 3.07 (m, 2H), 2.74 (ddd, *J* = 11.8, 8.5, 3.4 Hz, 2H), 1.76 (ddt, *J* = 10.6, 6.9, 3.5 Hz, 2H), 1.45 (dtd, *J* = 11.9, 7.9, 3.5 Hz, 2H), 1.15 (d, *J* = 5.3 Hz, 4H). ^{13}C NMR (101 MHz, DMSO-d_6) δ 154.3 – 150.9 (m), 145.0, 142.0, 139.2 (d, *J* = 2.2 Hz), 126.3 (d, *J* = 3.3 Hz), 123.3 (q, *J* = 271.8 Hz), 122.6, 121.7 (d, *J* = 7.5 Hz), 118.2, 118.0, 116.9 (qd, *J* = 32.0, 13.0 Hz), 115.0, 113.8 (q, *J* = 5.3, 4.8 Hz), 110.4, 64.2, 43.7, 33.4, 29.7, 6.7. HRMS (ESI) calculated for $C_{22}H_{23}O_3N_4F_4S$ $[M+H]^+$ 499.1421, found 499.1403.

*1-Cyclopropyl-N-(4-fluoro-3-(trifluoromethyl)phenyl)-5-(morpholinosulfonyl)-1H-indazol-3-amine (**48**)*. 37% yield, ^{1}H NMR (400 MHz, DMSO-d_6) δ 9.91 (s, 1H), 9.19 (d, *J* = 1.1 Hz, 1H), 8.70 (d, *J* = 1.1 Hz, 1H), 8.15 (dd, *J* = 6.2, 2.9 Hz, 1H), 7.96 (dt, *J* = 9.0, 3.6 Hz, 1H), 7.51 (t, *J* = 9.8 Hz, 1H), 3.94 – 3.83 (m, 1H), 3.64 (dd, *J* = 5.9, 3.5 Hz, 4H), 3.25 – 3.00 (m, 4H), 1.21 (ddt, *J* = 12.7, 9.3, 5.0 Hz, 4H). ^{13}C NMR (101 MHz, DMSO-d_6) δ 152.8 (d, *J* = 245.9 Hz), 145.0, 142.9, 138.8 (d, *J* = 2.5 Hz), 137.6, 135.0, 128.9 – 123.6 (m), 121.9 (d, *J* = 8.5 Hz), 118.8, 118.3 (d, *J* = 21.3 Hz), 117.1, 117.2 – 116.6 (m), 113.8 (d, *J* = 5.2 Hz), 66.1, 46.8, 30.3, 6.8. HRMS (ESI) calculated for $C_{20}H_{20}O_3N_5F_4S$ $[M+H]^+$ 486.1218, found 486.1201.

*1-((1-Cyclopropyl-3-((3-cyclopropyl-4-fluorophenyl)amino)-1H-indazol-5-yl)sulfonyl)piperidin-4-ol (**49**)*. 47% yield, ^{1}H NMR (400 MHz, DMSO-d_6) δ 9.26 (s,

1H), 8.55 (s, 1H), 7.70 (s, 2H), 7.62 – 7.52 (m, 1H), 7.31 (dd, *J* = 6.8, 2.8 Hz, 1H), 7.09 (t, *J* = 9.5 Hz, 1H), 4.65 (d, *J* = 3.8 Hz, 1H), 3.75 – 3.61 (m, 1H), 3.51 (tt, *J* = 7.6, 3.9 Hz, 1H), 3.15 (ddd, *J* = 11.2, 6.7, 3.5 Hz, 2H), 2.72 (dd, *J* = 20.2, 3.4 Hz, 2H), 2.07 (dp, *J* = 8.5, 5.1 Hz, 1H), 1.75 (ddd, *J* = 11.3, 7.4, 3.6 Hz, 2H), 1.45 (dtd, *J* = 12.3, 8.2, 3.6 Hz, 2H), 1.12 (d, *J* = 2.3 Hz, 4H), 1.03 (dt, *J* = 8.7, 3.2 Hz, 2H), 0.78 – 0.66 (m, 2H). ^{13}C NMR (101 MHz, DMSO-d_6) δ 155.6 (d, *J* = 235.3 Hz), 145.6, 142.0, 139.0 (d, *J* = 2.0 Hz), 130.4 (d, *J* = 15.3 Hz), 126.2, 125.8, 122.7, 115.4 (d, *J* = 23.1 Hz), 115.1, 114.5 (d, *J* = 7.5 Hz), 113.4 (d, *J* = 3.4 Hz), 110.1, 64.2, 43.7, 33.4, 29.6, 8.9 (d, *J* = 4.7 Hz), 8.5, 6.7. HRMS (ESI) calculated for $C_{24}H_{28}O_3N_4FS$ $[M+H]^+$ 471.1861, found 471.1846.

*N-(4-Fluoro-3-methylphenyl)-5-(morpholinosulfonyl)-1-(2,2,2-trifluoroethyl)-1H-indazol-3-amine (**50**)*. 51% yield, ^{1}H NMR (400 MHz, DMSO-d_6) δ 9.44 (s, 1H), 8.68 (s, 1H), 7.89 (d, *J* = 8.8 Hz, 1H), 7.78 (d, *J* = 9.0 Hz, 1H), 7.65 (dt, *J* = 8.2, 3.6 Hz, 1H), 7.59 (d, *J* = 6.9 Hz, 1H), 7.11 (t, *J* = 9.2 Hz, 1H), 5.39 (q, *J* = 9.0 Hz, 2H), 3.66 (t, *J* = 4.6 Hz, 4H), 2.90 (t, *J* = 4.6 Hz, 4H), 2.26 (s, 3H). ^{13}C NMR (101 MHz, DMSO-d_6) δ 155.4 (d, *J* = 235.5 Hz), 147.2, 142.6, 138.3 (d, *J* = 2.2 Hz), 126.9 , 126.2 (q, *J* = 281.5 Hz), 125.7 , 124.6 (d, *J* = 18.0 Hz), 123.2, 119.5 (d, *J* = 4.0 Hz), 115.6, 115.5, 115.4 (d, *J* = 16.7 Hz), 110.4, 65.8, 49.2 (q, *J* = 32.8 Hz), 46.4, 15.1 (d, *J* = 3.0 Hz). HRMS (ESI) calculated for $C_{20}H_{21}O_3N_4F_4S$ $[M+H]^+$ 473.1265, found 473.1249.

*1-(2,2-Difluoroethyl)-N-(4-fluoro-3-methylphenyl)-5-(morpholinosulfonyl)-1H-indazol-3-amine (**51**)*. 57% yield, ^{1}H NMR (400 MHz, DMSO-d_6) δ 9.39 (s, 1H), 8.64 (s, 1H), 7.80 (d, *J* = 8.9 Hz, 1H), 7.71 (d, *J* = 9.0 Hz, 1H), 7.68 – 7.61 (m, 1H), 7.58 (d, *J* = 6.6 Hz, 1H), 7.09 (t, *J* = 9.2 Hz, 1H), 6.48 (t, *J* = 54.9 Hz, 1H), 4.86 (t, *J* = 14.8 Hz,

2H), 3.64 (t, *J* = 4.4 Hz, 4H), 2.87 (s, 4H), 2.25 (s, 3H). ^{13}C NMR (101 MHz, DMSO-d_6) δ 155.3 (d, *J* = 235.4 Hz), 146.8, 142.4, 138.4 (d, *J* = 2.2 Hz), 126.5, 125.1, 124.6 (d, *J* = 18.0 Hz), 123.1, 119.4 (d, *J* = 4.1 Hz), 115.3 (d, *J* = 14.7 Hz), 115.3 (d, *J* = 35.9 Hz), 115.0 (t, *J* = 241.8 Hz), 110.5, 65.8, 50.3 (t, *J* = 26.0 Hz), 46.4, 15.1 (d, *J* = 2.9 Hz). HRMS (ESI) calculated for $C_{20}H_{22}O_3N_4F_3S$ $[M+H]^+$ 455.1359, found 455.1341.

*N-(4-Fluoro-3-methylphenyl)-1-(2-fluoroethyl)-5-(morpholinosulfonyl)-1H-indazol-3-amine (**52**).* 48% yield, ^{1}H NMR (400 MHz, DMSO-d_6) δ 9.36 (s, 1H), 8.63 (s, 1H), 7.74 (d, *J* = 8.9 Hz, 1H), 7.66 (dd, *J* = 14.4, 6.3 Hz, 2H), 7.59 (dd, *J* = 6.9, 2.7 Hz, 1H), 7.09 (t, *J* = 9.2 Hz, 1H), 4.86 (dt, *J* = 47.3, 4.7 Hz, 2H), 4.68 (dt, *J* = 27.7, 4.8 Hz, 2H), 3.64 (d, *J* = 4.6 Hz, 4H), 2.89 (d, *J* = 4.6 Hz, 4H), 2.26 (s, 3H). ^{13}C NMR (101 MHz, DMSO-d_6) δ 155.2 (d, *J* = 235.1 Hz), 146.5, 142.0, 138.6 (d, *J* = 2.2 Hz), 126.1, 124.5 (d, *J* = 18.1 Hz), 124.5, 123.2, 119.2 (d, *J* = 4.2 Hz), 115.4 (d, *J* = 13.0 Hz), 115.3 (d, *J* = 2.5 Hz), 114.8, 110.24 , 82.6 (d, *J* = 167.7 Hz), 65.8, 49.0 (d, *J* = 19.9 Hz), 46.4, 15.1 (d, *J* = 2.9 Hz). HRMS (ESI) calculated for $C_{20}H_{23}O_3N_4F_2S$ $[M+H]^+$ 437.1453, found 437.1436.

*1-(Difluoromethyl)-N-(4-fluoro-3-methylphenyl)-5-(morpholinosulfonyl)-1H-indazol-3-amine (**53**).* 39% yield, ^{1}H NMR (400 MHz, DMSO-d_6) δ 9.11 (s, 1H), 8.76 (s, 1H), 8.23 (t, *J* = 58.7 Hz, 1H), 7.68 (d, *J* = 1.4 Hz, 1H), 7.29 (dd, *J* = 7.0, 2.5 Hz, 1H), 7.25 – 7.12 (m, 2H), 6.87 (d, *J* = 1.4 Hz, 1H), 3.76 – 3.53 (m, 4H), 2.92 (t, *J* = 4.7 Hz, 4H), 2.23 (d, *J* = 1.9 Hz, 3H). ^{13}C NMR (101 MHz, DMSO-d_6) δ 157.1 (d, *J* = 238.8 Hz), 144.1, 137.4 (d, *J* = 2.8 Hz), 136.8, 131.3, 127.4, 125.3 (d, *J* = 18.2 Hz), 124.9 (d, *J* = 4.8 Hz), 121.2, 121.1 (d, *J* = 7.8 Hz), 116.0 (d, *J* = 23.1 Hz), 113.2, 111.2 (t, *J* = 252.6

Hz), 100.7, 65.9, 46.4, 14.8 (d, *J* = 2.9 Hz). HRMS (ESI) calculated for $C_{19}H_{20}O_3N_4F_3S$ $[M+H]^+$ 441.1203, found 441.1185.

*5-(((1S,4S)-2-Oxa-5-azabicyclo[2.2.1]heptan-5-yl)sulfonyl)-1-cyclopropyl-N-(4-fluoro-3-methylphenyl)-1H-indazol-3-amine (**54**).* 56% yield, ^{1}H NMR (400 MHz, DMSO-d_6) δ 9.28 (s, 1H), 8.67 (d, *J* = 1.6 Hz, 1H), 7.82 (dd, *J* = 8.8, 1.7 Hz, 1H), 7.69 (d, *J* = 8.8 Hz, 1H), 7.64 (ddd, *J* = 8.9, 4.5, 3.0 Hz, 1H), 7.54 (dd, *J* = 6.9, 2.8 Hz, 1H), 7.10 (t, *J* = 9.2 Hz, 1H), 4.46 (d, *J* = 3.0 Hz, 2H), 3.72 – 3.63 (m, 2H), 3.60 (dd, *J* = 7.6, 1.8 Hz, 1H), 3.23 (d, *J* = 10.0 Hz, 1H), 3.12 (dd, *J* = 10.0, 1.6 Hz, 1H), 2.25 (d, *J* = 1.9 Hz, 3H), 1.62 – 1.49 (m, 1H), 1.19 – 1.07 (m, 4H), 0.96 (dd, *J* = 10.1, 2.3 Hz, 1H). ^{13}C NMR (101 MHz, DMSO-d_6) δ 155.17 (d, *J* = 235.1 Hz), 145.75, 142.05, 138.63 (d, *J* = 2.4 Hz), 127.89, 125.91, 124.49 (d, *J* = 18.0 Hz), 122.70, 119.16 (d, *J* = 4.1 Hz), 115.39 (d, *J* = 22.9 Hz), 115.18 (d, *J* = 7.1 Hz), 115.13, 110.53, 76.09, 73.61, 60.29, 56.24, 35.34, 29.60, 15.12 (d, *J* = 2.9 Hz), 6.82. HRMS (ESI) calculated for $C_{22}H_{24}O_3N_4FS$ $[M+H]^+$ 443.1548, found 443.1530.

*N-(4-fluoro-3-methylphenyl)-5-(morpholinosulfonyl)-1H-indazol-3-amine (**55**).* 46% yield, ^{1}H NMR (400 MHz, DMSO-d_6) δ 12.54 (s, 1H), 9.25 (s, 1H), 8.61 (s, 1H), 7.78 – 7.40 (m, 4H), 7.07 (t, *J* = 9.3 Hz, 1H), 3.65 (s, 5H), 2.88 (s, 4H), 2.25 (s, 3H). ^{13}C NMR (101 MHz, DMSO-d_6) δ 155.0 (d, *J* = 234.5 Hz), 146.9, 141.92 , 139.0, 125.9, 124.4 (d, *J* = 17.8 Hz), 124.2, 123.1, 119.0 (d, *J* = 3.9 Hz), 115.4 (d, *J* = 22.2 Hz), 115.2, 114.1, 110.7, 65.8, 46.4, 15.1 (d, *J* = 3.1 Hz). HRMS (ESI) calculated for $C_{18}H_{20}O_3N_4FS$ $[M+H]^+$ 391.1235, found 391.1217.

*1-((1-Cyclopropyl-3-((4-fluoro-3-methylphenyl)amino)-1H-pyrazolo[3,4-c]pyridin-5-yl)sulfonyl)piperidin-4-ol (**56**)*. 64% yield, ^{1}H NMR (400 MHz, DMSO-d_6) δ 9.43 (s, 1H), 9.12 (s, 1H), 8.71 (s, 1H), 7.61 (dt, *J* = 8.3, 3.6 Hz, 1H), 7.51 (dd, *J* = 6.8, 2.8 Hz, 1H), 7.11 (t, *J* = 9.2 Hz, 1H), 4.70 (d, *J* = 3.9 Hz, 1H), 3.82 (dq, *J* = 7.1, 3.5 Hz, 1H), 3.55 (tt, *J* = 8.1, 4.6 Hz, 1H), 3.48 – 3.37 (m, 2H), 2.94 (ddd, *J* = 12.2, 8.9, 3.4 Hz, 2H), 2.38 – 2.16 (m, 3H), 1.83 – 1.68 (m, 2H), 1.42 (dtd, *J* = 12.6, 8.6, 3.7 Hz, 2H), 1.28 – 1.13 (m, 4H). ^{13}C NMR (100 MHz, DMSO-d_6) δ 155.3 (d, *J* = 235.5 Hz), 145.6, 143.5, 138.3 (d, *J* = 2.3 Hz), 137.6, 134.5, 124.6 (d, *J* = 18.2 Hz), 119.3 (d, *J* = 4.3 Hz), 119.1, 116.9, 115.6, 115.4, 115.3 (d, *J* = 7.2 Hz), 64.8, 44.2, 33.8, 30.2, 15.1 (d, *J* = 3.0 Hz), 6.9. HRMS (ESI) calculated for $C_{21}H_{25}O_3N_5FS$ $[M+H]^+$ 446.1657, found 446.1639.

*1-((1-Cyclopropyl-3-((3-(difluoromethyl)-4-fluorophenyl)amino)-1H-indazol-5-yl)sulfonyl)piperidin-4-ol (**57**)*. 61% yield ^{1}H NMR (400 MHz, DMSO-d_6) δ 9.61 (s, 1H), 8.57 (s, 1H), 7.96 (td, *J* = 8.3, 3.7 Hz, 2H), 7.72 (s, 1H), 7.37 (d, *J* = 10.3 Hz, 1H), 7.23 (t, 1H), 4.67 (d, *J* = 4.0 Hz, 1H), 3.69 (q, *J* = 5.3 Hz, 1H), 3.51 (dt, *J* = 7.9, 3.8 Hz, 1H), 3.16 (p, *J* = 4.7 Hz, 2H), 2.72 (ddd, *J* = 11.8, 8.3, 3.8 Hz, 2H), 1.86 – 1.61 (m, 2H), 1.45 (dp, *J* = 12.5, 4.2 Hz, 2H), 1.14 (d, *J* = 5.2 Hz, 4H). ^{13}C NMR (101 MHz, DMSO-d_6) δ 153.7 (dt, *J* = 242.3, 5.6 Hz), 145.2, 142.0, 139.2 (d, *J* = 2.2 Hz), 126.3, 126.2, 122.6, 121.6 (td, *J* = 22.7, 13.5 Hz), 120.1 (d, *J* = 7.3 Hz), 117.0 (d, *J* = 21.1 Hz), 115.1, 114.0 (dt, *J* = 6.4, 3.5 Hz), 112.3 (td, *J* = 236.0, 3.8 Hz), 110.3, 64.2, 43.7, 33.4, 29.6, 6.8. HRMS (ESI) calculated for $C_{22}H_{24}O_3N_4F_3S$ $[M+H]^+$ 481.1516, found 481.1499.

*1-Cyclopropyl-N-(3-(difluoromethyl)-4-fluorophenyl)-5-(morpholinosulfonyl)-1H-indazol-3-amine (**58**)*. 58% yield, ^{1}H NMR (400 MHz, DMSO-d_6) δ 9.63 (s, 1H), 8.58

(d, *J* = 1.7 Hz, 1H), 8.04 – 7.88 (m, 2H), 7.81 – 7.66 (m, 2H), 7.40 – 7.09 (m, 2H), 3.71 (p, *J* = 5.4 Hz, 1H), 3.68 – 3.58 (m, 4H), 2.91 – 2.82 (m, 4H), 1.20 – 1.08 (m, 4H). ^{13}C NMR (101 MHz, DMSO-d_6) δ 153.7 (dt, *J* = 242.3, 5.7 Hz), 145.3 , 142.1, 139.2 (d, *J* = 2.3 Hz), 126.3, 125.0, 123.1, 121.6 (td, *J* = 22.7, 13.5 Hz), 120.2 (d, *J* = 7.6 Hz), 117.0 (d, *J* = 21.3 Hz), 115.1, 114.0 (t, *J* = 5.7 Hz), 112.2 (td, *J* = 235.9, 3.8 Hz), 110.5, 65.75 , 46.4, 29.7, 6.8. HRMS (ESI) calculated for $C_{18}H_{18}O_3N_4F_3S$ $[M+H]^+$ 467.1359, found 467.1343.

*1-((1-Cyclopropyl-3-((3-(difluoromethyl)-4-fluorophenyl)amino)-1H-pyrazolo[3,4-c]pyridin-5-yl)sulfonyl)piperidin-4-ol (**59**)*. 55% yield, ^{1}H NMR (400 MHz, DMSO-d_6) δ 9.74 (s, 1H), 9.15 (d, *J* = 1.1 Hz, 1H), 8.68 (d, *J* = 1.1 Hz, 1H), 7.94 (dd, *J* = 6.2, 2.8 Hz, 1H), 7.89 (dt, *J* = 8.0, 3.7 Hz, 1H), 7.42 – 7.35 (m, 1H), 7.34 (s, 1H), 4.68 (d, *J* = 3.9 Hz, 1H), 3.92 – 3.81 (m, 1H), 3.54 (tt, *J* = 8.0, 4.0 Hz, 1H), 3.46 – 3.36 (m, 2H), 2.93 (ddd, *J* = 12.3, 8.9, 3.4 Hz, 2H), 1.74 (dp, *J* = 13.3, 3.4 Hz, 2H), 1.41 (dtd, *J* = 12.4, 8.1, 3.5 Hz, 2H), 1.28 – 1.16 (m, 4H). ^{13}C NMR (101 MHz, DMSO-d_6) δ 153.8 (d, *J* = 243.0 Hz), 145.2, 143.6, 138.8 (d, *J* = 2.3 Hz), 137.6, 134.7, 122.3 – 121.2 (m), 120.3 (d, *J* = 7.5 Hz), 118.9, 117.2 (d, *J* = 21.3 Hz), 116.7, 114.1 (d, *J* = 5.6 Hz), 114.9 – 109.5 (m), 64.8, 44.2, 33.8, 30.3, 6.9. HRMS (ESI) calculated for $C_{21}H_{23}O_3N_5F_3S$ $[M+H]^+$ 482.1468, found 482.1453.

*1-Cyclopropyl-N-(3-(difluoromethyl)-4-fluorophenyl)-5-(morpholinosulfonyl)-1H-pyrazolo[3,4-c]pyridin-3-amine (**60**)*. 56% yield, ^{1}H NMR (400 MHz, DMSO-d_6) δ 9.78 (s, 1H), 9.17 (s, 1H), 8.71 (s, 1H), 7.95 (d, *J* = 5.7 Hz, 1H), 7.93 – 7.84 (m, 1H), 7.38 (d, *J* = 8.2 Hz, 1H), 7.36 – 7.09 (m, 1H), 3.86 (q, *J* = 4.7, 3.5 Hz, 1H), 3.63 (t, *J* =

4.4 Hz, 4H), 3.13 (t, *J* = 4.5 Hz, 4H), 1.34 – 1.09 (m, 4H). ^{13}C NMR (101 MHz, DMSO-d_6) δ 152.6 (td), 145.2 , 142.8, 138.8 (d, *J* = 2.2 Hz), 137.7, 134.8, 121.7 (td, *J* = 22.6, 13.2 Hz), 120.3 (d, *J* = 7.5 Hz), 118.9, 117.2, 117.0, 114.1 (d, *J* = 4.3 Hz), 112.2 (td, *J* = 236.1, 3.9 Hz), 66.1, 46.8, 30.3, 6.9. HRMS (ESI) calculated for $C_{20}H_{22}O_3N_5F_3S$ $[M+H]^+$ 468.1312, found 468.1299.

*1-((1-Cyclopropyl-3-((4-fluoro-3-methylphenyl)amino)-1H-pyrazolo[3,4-c]pyridin-5-yl)sulfonyl)piperidin-4-yl dimethylglycinate 2,2,2-trifluoroacetate (**61**).* To the solution of **65** (30 mg) in 1 mL DCM was added 1 mL TFA. The solvent was evaporated under vacuum. Ethyl ether was added to the residue. Precipitate was collected through filtration to afford **61** as yellow solid in quantitative yield. ^{1}H NMR (400 MHz, DMSO-d_6) δ 10.06 (s, 1H), 9.46 (s, 1H), 9.13 (s, 1H), 8.74 (s, 1H), 7.61 (dt, *J* = 8.7, 3.5 Hz, 1H), 7.52 (dd, *J* = 6.9, 2.8 Hz, 1H), 7.12 (t, *J* = 9.2 Hz, 1H), 4.94 (dq, *J* = 7.9, 4.0 Hz, 1H), 4.12 (s, 2H), 3.84 (tt, *J* = 7.0, 3.9 Hz, 1H), 3.45 – 3.36 (m, 2H), 3.18 (ddd, *J* = 12.1, 8.2, 3.6 Hz, 2H), 2.79 (s, 6H), 2.26 (d, *J* = 1.8 Hz, 3H), 2.01 – 1.85 (m, 2H), 1.68 (q, *J* = 9.4 Hz, 2H), 1.26 – 1.13 (m, 4H).

General procedure for the preparation of **62**-**64**. To the solution of **56** (0.1 mmol, 44 mg) in 2 mL DCM was added DCC (0.3 mmol, 62 mg), DMAP (0.12 mmol, 15 mg) and *N*-Boc-*L*-amino acid or *N*,*N*-dimethyl glycine (0.3 mmol). The mixture was stirred for 3 hours at 40 ℃. After cooling to room temperature, the precipitate was removed through filtration. The filtrate was concentrated and purified through column chromatography on silico gel. To the solution of the above product in 1 mL DCM was added 1 mL TFA. The solvent was evaporated under vacuum. Ethyl ether was added to the residue.

Precipitate was collected through filtration to afford **62-64** as yellow solid in quantitative yield.

*1-((1-Cyclopropyl-3-((4-fluoro-3-methylphenyl)amino)-1H-pyrazolo[3,4-c]pyridin-5-yl)sulfonyl)piperidin-4-yl L-valinate 2,2,2-trifluoroacetate (**62**)*. ^{1}H NMR (400 MHz, DMSO-d_6) δ 9.45 (s, 1H), 9.10 (d, J = 1.1 Hz, 1H), 8.73 (d, J = 1.1 Hz, 1H), 8.30 (s, 3H), 7.60 (dt, J = 8.7, 3.6 Hz, 1H), 7.50 (dd, J = 6.9, 2.8 Hz, 1H), 7.11 (t, J = 9.2 Hz, 1H), 4.93 (tt, J = 7.3, 3.6 Hz, 1H), 3.92 – 3.86 (m, 1H), 3.82 (dq, J = 7.0, 4.2, 3.5 Hz, 1H), 3.37 (ddt, J = 14.0, 6.9, 3.8 Hz, 2H), 3.28 – 3.12 (m, 2H), 2.25 (d, J = 1.8 Hz, 3H), 2.14 – 1.98 (m, 1H), 1.91 (s, 2H), 1.75 – 1.57 (m, 2H), 1.29 – 1.13 (m, 4H), 0.89 (t, J = 6.4 Hz, 6H). ^{13}C NMR (101 MHz, DMSO-d_6) δ 168.50, 158.82 (q, J = 32.5 Hz), 155.35 (d, J = 235.7 Hz), 145.67, 143.33, 138.28, 137.65, 134.45, 124.63 (d, J = 18.1 Hz), 119.27 (d, J = 4.1 Hz), 119.06, 117.25 (d, J = 297.5 Hz), 117.03, 115.47 (d, J = 23.4 Hz), 115.28, 70.68, 57.70, 43.55, 40.42, 30.18, 29.93, 29.86, 29.80, 18.65, 17.81, 15.09 (d, J = 3.0 Hz), 6.93.

*1-((1-Cyclopropyl-3-((4-fluoro-3-methylphenyl)amino)-1H-pyrazolo[3,4-c]pyridin-5-yl)sulfonyl)piperidin-4-yl L-alaninate 2,2,2-trifluoroacetate (**63**)*. ^{1}H NMR (400 MHz, DMSO-d_6) δ 9.45 (s, 1H), 9.11 (s, 1H), 8.73 (s, 1H), 8.28 (s, 3H), 7.60 (dt, J = 7.7, 3.4 Hz, 1H), 7.50 (dd, J = 6.9, 2.8 Hz, 1H), 7.11 (t, J = 9.2 Hz, 1H), 4.88 (tt, J = 6.8, 3.4 Hz, 1H), 4.06 (q, J = 7.0 Hz, 1H), 3.82 (tt, J = 6.9, 4.0 Hz, 1H), 3.53 – 3.25 (m, 2H), 3.28 – 3.08 (m, 2H), 2.25 (s, 3H), 1.89 (td, J = 8.8, 4.6 Hz, 2H), 1.67 (p, J = 7.5, 6.7 Hz, 2H), 1.32 (d, J = 7.2 Hz, 3H), 1.27 – 1.13 (m, 4H). ^{13}C NMR (101 MHz, DMSO-d_6) δ 169.65 , 158.76 (q, J = 31.6 Hz), 155.35 (d, J = 235.6 Hz), 145.66, 143.47, 138.29,

137.66, 134.52, 124.63 (d, *J* = 18.1 Hz), 119.27 (d, *J* = 4.1 Hz), 119.05, 116.95, 115.48 (d, *J* = 23.6 Hz), 115.28, 70.55, 48.37, 43.49, 30.19, 29.87, 29.82, 16.12, 15.10 (d, *J* = 3.0 Hz), 6.94.

*1-((1-Cyclopropyl-3-((4-fluoro-3-methylphenyl)amino)-1H-pyrazolo[3,4-c]pyridin-5-yl)sulfonyl)piperidin-4-yl glycinate 2,2,2-trifluoroacetate (**64**)*. ^{1}H NMR (400 MHz, DMSO-d_6) δ 9.46 (s, 1H), 9.12 (d, *J* = 1.1 Hz, 1H), 8.73 (d, *J* = 1.1 Hz, 1H), 8.17 (s, 3H), 7.61 (dt, *J* = 8.7, 3.6 Hz, 1H), 7.51 (dd, *J* = 6.9, 2.8 Hz, 1H), 7.12 (t, *J* = 9.2 Hz, 1H), 4.90 (td, *J* = 7.7, 3.9 Hz, 1H), 3.84 (dq, *J* = 6.7, 3.4, 3.0 Hz, 1H), 3.79 (s, 2H), 3.48 – 3.39 (m, 2H), 3.15 (ddd, *J* = 12.3, 8.3, 3.7 Hz, 2H), 2.25 (d, *J* = 1.9 Hz, 3H), 1.98 – 1.85 (m, 2H), 1.65 (dtd, *J* = 12.1, 7.7, 3.6 Hz, 2H), 1.21 (dddd, *J* = 12.0, 9.5, 6.7, 3.0 Hz, 4H).

*1-((1-Cyclopropyl-3-((4-fluoro-3-methylphenyl)amino)-1H-pyrazolo[3,4-c]pyridin-5-yl)sulfonyl)piperidin-4-yl dimethylglycinate (**65**)*. To the solution of **56** (0.1 mmol, 44 mg) in 2 mL DCM was added DCC (0.3 mmol, 62 mg), DMAP (0.12 mmol, 15 mg) and *N*,*N*-dimethyl glycine (0.3 mmol). The mixture was stirred for 3 hours at 40 ℃. After cooling to room temperature, the precipitate was removed through filtration. The filtrate was concentrated and purified through column chromatography on C18 silico gel afford the product as yellow solid with 90% yield. ^{1}H NMR (400 MHz, Chloroform-*d*) δ 8.43 (dd, *J* = 4.0, 1.1 Hz, 1H), 7.45 (dt, *J* = 8.9, 3.6 Hz, 1H), 7.39 (dd, *J* = 6.6, 3.0 Hz, 1H), 6.98 (t, *J* = 9.0 Hz, 1H), 6.95 (s, 1H), 4.86 (tt, *J* = 7.9, 3.8 Hz, 1H), 3.63 (tq, *J* = 11.6, 3.5 Hz, 3H), 3.18 (ddd, *J* = 12.4, 8.6, 3.5 Hz, 2H), 3.12 (s, 2H), 2.37 – 2.25 (m, 9H), 1.97 – 1.86 (m, 2H), 1.77 – 1.68 (m, 2H), 1.33 – 1.21 (m, 4H). ^{13}C NMR (101

MHz, Chloroform-*d*) δ 169.75, 156.32 (d, *J* = 238.4 Hz), 145.63, 143.61, 137.82, 136.93 (d, *J* = 2.5 Hz), 133.72, 125.19 (d, *J* = 18.4 Hz), 119.96 (d, *J* = 4.4 Hz), 119.41, 116.19, 115.69 (d, *J* = 7.4 Hz), 115.15 (d, *J* = 23.4 Hz), 68.95, 60.21, 45.17, 44.07, 30.23, 29.79, 14.89 (d, *J* = 3.3 Hz), 6.95. HRMS (ESI) calculated for C26H31O4N5F3S $[M+H]^+$ 531.2184, found 531.2169.

*1-((1-Cyclopropyl-3-((4-fluoro-3-methylphenyl)amino)-1H-pyrazolo[3,4-c]pyridin-5-yl)sulfonyl)piperidin-4-yl dimethylglycinate acetate (**66**)*. To the solution of **65** (25 mg) in 1 mL DCM was added 1 mL AcOH. The solvent was evaporated under vacuum. Ethyl ether was added to the residue. Precipitate was collected through filtration to afford **66** as yellow solid in quantitative yield. ^{1}H NMR (400 MHz, DMSO-d_6) δ 11.93 (s, 2H), 9.44 (d, *J* = 3.2 Hz, 1H), 9.12 (d, *J* = 3.2 Hz, 1H), 8.71 (d, *J* = 3.2 Hz, 1H), 7.60 (dd, *J* = 8.6, 4.3 Hz, 1H), 7.55 – 7.44 (m, 1H), 7.11 (td, *J* = 9.3, 3.3 Hz, 1H), 4.78 (s, 1H), 3.82 (dq, *J* = 7.5, 3.8 Hz, 1H), 3.21 – 3.00 (m, 4H), 2.25 (s, 3H), 2.20 (d, *J* = 3.2 Hz, 6H), 1.98 – 1.78 (m, 5H), 1.60 (s, 2H), 1.19 (t, *J* = 7.6 Hz, 4H).

*1-((1-Cyclopropyl-3-((4-fluoro-3-methylphenyl)amino)-1H-pyrazolo[3,4-c]pyridin-5-yl)sulfonyl)piperidin-4-yl dimethylglycinate 2-hydroxypropane-1,2,3-tricarboxylate (**67**)*. The solution of citric acid (230 mg, 1.2 mmol) in ethyl acetate and methanol was added to the solution of **65** (530 mg, 1 mmol) in ethyl acetate dropwise under stirring. The mixture was stirred at room temperature overnight. The mixture was filtered. The cake was washed with ethyl acetate and dried under vacuum to provide the **67** as yellow solid. Yield 91%. ^{1}H NMR (400 MHz, DMSO-d_6) δ 10.99 (s, 2H), 9.43 (s, 1H), 9.12 (s, 1H), 8.71 (s, 1H), 7.60 (dd, *J* = 8.3, 4.1 Hz, 1H), 7.50 (dd, *J* = 6.8, 2.8 Hz, 1H), 7.11

(t, *J* = 9.2 Hz, 1H), 4.82 (dt, *J* = 8.0, 4.4 Hz, 1H), 3.82 (tt, *J* = 6.9, 3.8 Hz, 1H), 3.46 – 3.31 (m, 4H), 3.13 (ddd, *J* = 12.3, 8.5, 3.6 Hz, 2H), 2.70 (d, *J* = 15.3 Hz, 2H), 2.60 (d, *J* = 15.3 Hz, 2H), 2.34 (s, 6H), 2.25 (s, 3H), 1.94 – 1.82 (m, 2H), 1.70 – 1.54 (m, 2H), 1.24 – 1.09 (m, 4H).

*1-((1-Cyclopropyl-3-((4-fluoro-3-methylphenyl)amino)-1H-pyrazolo[3,4-c]pyridin-5-yl)sulfonyl)piperidin-4-yl dimethylglycinate methanesulfonate (**68**)*. ^{1}H NMR (400 MHz, DMSO-d_6) δ 9.84 (s, 1H), 9.45 (s, 1H), 9.12 (s, 1H), 8.73 (s, 1H), 7.68 – 7.24 (m, 3H), 7.11 (t, *J* = 9.2 Hz, 1H), 5.01 – 4.84 (m, 1H), 4.15 (d, *J* = 3.8 Hz, 2H), 3.83 (tt, *J* = 7.0, 4.0 Hz, 1H), 3.38 (q, *J* = 7.2, 6.8 Hz, 2H), 3.17 (t, *J* = 9.2 Hz, 2H), 2.80 (d, *J* = 3.3 Hz, 6H), 2.35 (s, 6H), 2.25 (s, 3H), 1.92 (t, *J* = 9.9 Hz, 2H), 1.69 (s, 2H), 1.27 – 1.13 (m, 4H).

*1-((1-Cyclopropyl-3-((4-fluoro-3-methylphenyl)amino)-1H-pyrazolo[3,4-c]pyridin-5-yl)sulfonyl)piperidin-4-yl dimethylglycinate hydrochloride (**69**)*. The solution of **65** in ethyl acetate was bubbling with HCl gas, which is produced by H_2SO_4 and NaCl, until precipitate appeared. The mixture was filtered and the cake was washed with ethyl acetate. The cake was dried under vacuum to afford **69** as wine red solid. Yield 49% ^{1}H NMR (400 MHz, DMSO-d_6) δ 10.55 (s, 1H), 9.59 (s, 1H), 9.12 (d, *J* = 3.3 Hz, 1H), 8.79 (d, *J* = 3.4 Hz, 1H), 7.69 – 7.58 (m, 1H), 7.58 – 7.49 (m, 1H), 7.11 (td, *J* = 9.4, 3.4 Hz, 1H), 4.93 (s, 1H), 4.15 (s, 2H), 3.90 – 3.77 (m, 1H), 3.39 (t, *J* = 9.6 Hz, 2H), 3.19 (t, *J* = 9.6 Hz, 2H), 2.79 (s, 6H), 2.25 (s, 3H), 1.93 (d, *J* = 12.8 Hz, 2H), 1.68 (d, *J* = 11.3 Hz, 2H), 1.27 – 1.13 (m, 4H).

*1-((1-Cyclopropyl-3-((4-fluoro-3-methylphenyl)amino)-1H-pyrazolo[3,4-c]pyridin-5-yl)sulfonyl)piperidin-4-yl dimethylglycinate maleate (**70**).* The solution of citric acid (14 mg, 0.12 mmol) in ethyl acetate was added to the solution of **65** (53 mg, 0.1 mmol) in ethyl acetate dropwise under stirring. The mixture was stirred at room temperature overnight. The mixture was filtered. The cake was washed with ethyl acetate and dried under vacuum to provide 46 mg **70** as yellow solid 71% yield. ^{1}H NMR (400 MHz, DMSO-d_6) δ 9.46 (s, 1H), 9.13 (s, 1H), 8.73 (s, 1H), 7.60 (dt, *J* = 8.4, 3.6 Hz, 1H), 7.51 (dd, *J* = 6.9, 2.9 Hz, 1H), 7.12 (t, *J* = 9.2 Hz, 1H), 6.06 (s, 2H), 4.92 (tt, *J* = 7.7, 3.8 Hz, 1H), 4.00 (s, 2H), 3.84 (tt, *J* = 6.9, 3.9 Hz, 1H), 3.64 – 3.23 (m, 2H), 3.17 (ddd, *J* = 12.3, 8.2, 3.8 Hz, 2H), 2.71 (s, 6H), 2.32 – 2.18 (m, 3H), 1.93 (ddt, *J* = 11.8, 7.6, 3.7 Hz, 2H), 1.67 (dtd, *J* = 12.3, 7.9, 3.8 Hz, 2H), 1.20 (t, *J* = 6.6 Hz, 4H).

Plasma stability.

2 μL stock solution of compound (50 mM in DMSO) was diluted to 100 μL with the plasma, which was obtained from the mouse fundus vein after centrifugation at 13 000 rpm for 10 min. The mixture was incubated at 37 ℃ under shaking and quenched with 300 μL acetonitrile at different time point. After centrifugation at 10 000 rpm for 10 min, the supernatant was detected in HPLC system. The half-life time was determined based on the peak area.

Solubility

About 1 mg compound was added into 100 μL medium. The mixture was kept at 25 ℃ under shaking overnight. After filtration with 0.22 μm microporous filer, the filtrate was detected in HPLC. The amount of the dissolved compound was determined

by the ratio of the peak area.

Biological method.

Assay for Anti-HBV activity.

HepAD38 cells were seeded into 96-well culture plates at approximately 1×10^4 cells/well in a volume of 100 μL and treated with compounds or DMSO for six days after cells adhered to the well. Medium containing compounds or DMSO were replaced every 3 days. After 6 days, 60 μL cell supernatant was transferred to an eight strip PCR tube using a multichannel pipettor. The samples were heated for 15 min at 95 °C in a PCR amplifier and then centrifuged at 4000 rpm for 10 min. HBV DNA was detected using q-PCR.

Quantitative PCR (q-PCR).

Twenty microliter reaction systems contained 10 μL TaqMan® Gene Expression Master Mix (Applied Biosystems, 4369016), 2μL forward and reverse primers (10 μM), 0.25 μL probe, 5.75 μL dd H_2O and 2 μL treated samples. PCR conditions: 95 °C for 10 min, 95 °C for 15 s, and 60 °C for 1 min for 40 cycles in a real-time 7500 machine. HBV Forward primer: 5'-CCAAATGCCCCTATCCTATCA-3'; and HBV Reverse primer: 5'-GAGGCGAGGGAGTTCTTCTTCTA-3'. HBV probe: 5'-CGGAAACTACTGTT GTTAGACGACGAGGCAG-3'. Pzac-1.2HBV plasmid was used as the standard substance to draw the standard curve, and 80 ng/mL plasmid corresponded to a 10^{13} HBV DNA load. The standard curve contained eight points from 10^{11} to 10^4 with a 10-fold dilution. For anti-HBV EC_{50}, the data for each well was calculated using the following formula: $100\ \%\times(1\text{-}2^{-(C_T\ \text{samples}-C_T\ \text{control})})$, and analyzed using a 3- or 4-

parameter curve fitting algorithm in Graph Pad Prism.

Intracellular DNA and RNA Detection

The comparative C_T ($\Delta\Delta C_T$) quantitation method was used in quantitative PCR (qPCR) or quantitative reverse transcription (qRT-PCR) detection. For intracellular DNA and cccDNA detection, PCR reaction systems were the same as above. In addition, GAPDH was used as a housekeeping gene and 20 μL reaction systems include 10 μL TaqMan® Gene Expression Master Mix (Applied Biosystems, 4369016), 1 μL primer mix (ThermoFisher, Hs02758991_g1), 2 μL DNA samples and 7 μL dd H_2O. cccDNA former primers: 5'-CCCCGTCTGTGCCTTCTC-3'; reverse primers: 5'-CAGCTTGG AGGCTTGAACAGT-3'; cccDNA probes: 5'-FAM-ACTCTCAGCAATGTCAACGA CCGACC-TAM-3'. For intracellular RNA detection, 20 μL reaction systems consist of 10 μL Power SYBR® Green PCR Master Mix (Applied Biosystems, 4367659), 2 μL forward and reverse primers (10 μM), 2 μL DNA samples and 6 μL ddH_2O. GAPDH forward primer: 5'-ACCCACTCCTCCACCTTTG-3'; and reverse primer: 5'-CTGTAGCCAAATTCGTTGTCAT-3'. pgRNA forward primer: 5'-TTTTCACCTCTG CCTAATCATCTCTTG-3'; precore RNA forward primer: 5'-TTGGTCTGCGCACCA GCACC-3'; and their common reverse primer: 5'-GAA GGAAAGAAGTCAGAAGG CAA-3'. The data for each well was calculated using the following formula: $2^{-((C_T \text{ sample}-C_T \text{ sample GAPDH}) - (C_T \text{ control}-C_T \text{ control GAPDH}))}$, and analyzed in Graph Pad Prism.

SEC and EM Analysis.

A recombinant HBV core protein (Cp149) was used in SEC and EM studies. 5μM Cp149 proteins was incubated with 10μM compounds in a buffer containing 150 mM

NaCl, 50 mM HEPES (pH7.4) at 37 °C overnight prior to EM and SEC analysis. Samples were adsorbed to freshly glow discharged carbon coated grids for 30s. The water was removed by filter paper. The grids were stained in fresh 1% (wt/vol) uranyl acetate acid for 1 min. After absorbing excess water by filter paper and drying, the grids were examined with transmission electron microscope. For SEC, samples were analyzed by an Äkta purifier equipped with a size exclusion column (GE Healthcare, Superdex 200 Increase 5/150 GL (micro)). The eluent was pH 7.5 buffer containing 100 mM Tris, 100 mM NaCl, 17g/L Sucrose. The capsids or Cps were detected using UV detector at 280 nm and the ratio of area under the curve (AUC) was calculated to assess capsid formation induced by compounds.

Enzyme-Linked Immunosorbent Assay

HepAD38 or HepG2.2.15 cell culture supernatant was diluted 3-fold for HBeAg detection (Kehua, 20123400740) and 5-fold for HBsAg detection (Kehua, S10910113) according to manufacturer's instructions. Enzyme-Linked immunosorbent assay (ELISA) results are presented as S/VC (S = sample OD value and VC = vehicle control OD value).

***In Vivo* Efficacy in the Hydrodynamic-Injection (HDI) Mouse Model.**

Male C57BL/6 mice (6−8 weeks old) were purchased from Vital River Experimental Animal Co., Ltd. (Beijing, China). All mice were maintained under specific pathogen-free conditions in the animal research center laboratory of Tsinghua University. All animal protocols were approved by the Institute of Animal Care and Use Committee (IACUC) of Tsinghua University, and studies were conducted in compliance with

institutional and national guidelines.

All the mice were weighed and hydrodynamically injected with 8 μg pAAV2-HBV1.3HBV plasmid (genotype D) in a volume of phosphate buffer solution (PBS) to 10% of a mouse's body weight (e.g., 2.0 ml for mouse of 20 g) within 5-7 s through a tail vein. From days 1 to 7, the mice in all the groups were orally dosed with the blank vehicle, 0.05 mg/kg entecavir, 100 mg/kg AB-423, 50 and 100 mg/kg compound 56, and **50** and 100 mg/kg compound **67** at the indicated frequency. Serum and liver samples were collected at the indicated time points for HBV-DNA quantification by real-time PCR.

Pharmacokinetics in mouse.

Male C57BL/6 mice (6−8 weeks old) (Purchased from Vital River Experimental Animal Co., Ltd. (Beijing, China)) were used for pharmacokinetic study. Mice (N=3) were administered with the **56** (i.v. 20 mg/kg and p.o. 100 mg/kg) and **67** (p.o. 100 mg/kg and 200 mg/kg). Compound **56** for i.v. administration was dissolved in normal saline containing 5% (v/v) DMSO and 5% (v/v) Tween 80. Compound **56** for p.o. administration was dissolved in normal saline containing 5% (v/v) DMSO and 0.5% CMC. Compound **67** was dissolved in normal saline containing 5% (v/v) DMSO. Blood samples were collected from the saphenous vein at 5 min, 10 min, 20 min, 30 min, 1 h, 2 h, 4 h, 8 h, 12 h and 24h into heparin-containing microcentrifuge tubes. The blood samples were immediately centrifuged at 4 °C and the plasma was stored at −80 °C. Liver was collected and stored at -80 °C. The compound concentration was determined by HPLC using internal standard method.

Molecule modeling

Molecule modeling of compound **56** and HBV core protein crystal structure (PDB code: 5WRE) was performed with Schrödinger (2017-3) software.

Interference Compounds Examination

All these active compounds are screened with the publicly available filters (http://www.cbligand.org/PAINS/, http://advisor.docking.org) and did not preserve the potential to be PAINS or Aggregators.[53, 54]

Associated Content

Supporting Information

The Supporting Information is available free of charge at XXXXXX.

Anti-HBV activity and cytotoxicity of the compounds, in vivo anti-HBV efficiency of **56** and **67**, procedure for synthesis of the intermediates, NMR spectra for the target compounds, purity data of the compounds and HPLC spectra. (PDF)

Molecular formula strings and some data (CSV)

Author Information

Corresponding author

*For G.L.: Email, gangliu27@tsinghua.edu.cn.

*For Y.M.: Email, mayao@imm.ac.cn.

*For Y.X.: Email, yxiang@mail.tsinghua.edu.cn.

Author Contribution

#These authors contributed equally to this work.

G.L., Y.M. and Y.X. designed this study. C.W. performed the synthesis of the

compounds, evaluation the solubility, and determination of the stability in plasma and pharmacokinetics. Y.P. performed the biological test. L.W. performed the EM and SEC analysis. C.J. and X.T. provide pAAV2-HBV1.3HBV plasmid. S.L performed the HBV infection in Huh7-NTCP cells. Y.X. designed and guided the EM and SEC analysis. G.L., C.W. and Y.P. wrote the manuscript.

Notes

The authors declare no competing financial interest.

Acknowledgements

This work was financially supported by the National Natural Science Foundation of China (81803358), the Beijing Municipal Natural Science Foundation (7202095) of China and Postdoctoral Foundation of Tsinghua-Peking Center for Life Sciences. The authors thank Chinese PLA General Hospital for providing HepG2.A64 and HepG2.1403F cells.

Abbreviations

3TC, Lamivudine; ADME, absorption, distribution, metabolism and excretion; CAMs, capsid assembly modulators; cccDNA, covalently closed circular DNA; CHB, chronic hepatitis B; Cp, core protein; DCC, dicyclohexylcarbodiimide; DMAP, 4-dimethylaminopyridine; EM, electron microscopy; HAP, heteroarylpyrimidines; HBeAg, HBV e antigen; HBsAg, HBV surface antigen; HBV, Hepatitis B virus; HPLC, high performance liquid chromatography; HRMS, high resolution mass spectrum; Hz, hertz; IFN, interferon; MLM, mouse liver microsome; NAs, nucleos(t)ide analogues; NBS, N-bromosuccinimide; PPA, phenylpropenamides; ppm, parts per million; RT,

Reverse transcription; SAR, structure activity relationship; SBA, sulfamoylbenzamide; SEC, size exclusion chromatography; THF, tetrahydrofuran; TFA, trifluoroacetic acid.

References

1. Hepatitis B. https://www.who.int/news-room/fact-sheets/detail/hepatitis-b

2. Seto, W. K.; Lo, Y. R.; Pawlotsky, J. M.; Yuen, M. F., Chronic hepatitis B virus infection. *Lancet* **2018,** *392*, 2313-2324.

3. Zoulim, F.; Durantel, D., Antiviral therapies and prospects for a cure of chronic hepatitis B. *Cold Spring Harb. Perspect. Med.* **2015,** *5*, 21.

4. Tuttleman, J. S.; Pourcel, C.; Summers, J., Formation of the pool of covalently closed circular viral-DNA in hepadnavirus-infected cells. *Cell* **1986,** *47*, 451-460.

5. Werle-Lapostolle, B.; Bowden, S.; Locarnini, S.; Wursthorn, K.; Petersen, J.; Lau, G.; Trepo, C.; Marcellin, P.; Goodman, Z.; Delaney, W. E.; Xiong, S.; Brosgart, C. L.; Chen, S. S.; Gibbs, C. S.; Zoulim, F., Persistence of cccDNA during the natural history of chronic hepatitis B and decline during adefovir dipivoxil therapy. *Gastroenterology* **2004,** *126*, 1750-1758.

6. Lucifora, J.; Xia, Y. C.; Reisinger, F.; Zhang, K.; Stadler, D.; Cheng, X. M.; Sprinzl, M. F.; Koppensteiner, H.; Makowska, Z.; Volz, T.; Remouchamps, C.; Chou, W. M.; Thasler, W. E.; Huser, N.; Durantel, D.; Liang, T. J.; Munk, C.; Heim, M. H.; Browning, J. L.; Dejardin, E.; Dandri, M.; Schindler, M.; Heikenwalder, M.; Protzer, U., Specific and nonhepatotoxic degradation of nuclear hepatitis B virus cccDNA. *Science* **2014,** *343*, 1221-1228.

7. Lau, G. K. K.; Piratvisuth, T.; Luo, K. X.; Marcellin, P.; Thongsawat, S.; Cooksley,

G.; Gane, E.; Fried, M. W.; Chow, W. C.; Paik, S. W.; Chang, W. Y.; Berg, T.; Flisiak, R.; McCloud, P.; Pluck, N.; Peginterferon Alfa, A. H.-P., Peginterferon alfa-2a, lamivudine, and the combination for HBeAg-positive chronic hepatitis B. *N. Engl. J. Med.* **2005,** *352*, 2682-2695.

8. Yang, L.; Liu, F.; Tong, X.; Hoffmann, D.; Zuo, J.; Lu, M., Treatment of chronic hepatitis B virus infection using small molecule modulators of nucleocapsid assembly: recent advances and perspectives. *ACS Infect. Dis.* **2019,** *5*, 713-724.

9. Wynne, S. A.; Crowther, R. A.; Leslie, A. G. W., The crystal structure of the human hepatitis B virus capsid. *Mol. Cell.* **1999,** *3*, 771-780.

10. Zlotnick, A., To build a virus capsid-an equilibrium-model of the self-assembly of polyhedral protein complex. *J. Mol. Biol.* **1994,** *241*, 59-67.

11. Stray, S. J.; Bourne, C. R.; Punna, S.; Lewis, W. G.; Finn, M. G.; Zlotnick, A., A heteroaryldihydropyrimidine activates and can misdirect hepatitis B virus capsid assembly. *Proc. Natl. Acad. Sci. U. S. A.* **2005,** *102*, 8138-8143.

12. Zlotnick, A.; Johnson, J. M.; Wingfield, P. W.; Stahl, S. J.; Endres, D., A theoretical model successfully identifies features of hepatitis B virus capsid assembly. *Biochemistry* **1999,** *38*, 14644-14652.

13. Ceres, P.; Zlotnick, A., Weak protein-protein interactions are sufficient to drive assembly of hepatitis B virus capsids. *Biochemistry* **2002,** *41*, 11525-11531.

14. Lutomski, C. A.; Lyktey, N. A.; Zhao, Z. C.; Pierson, E. E.; Zlotnick, A.; Jarrold, M. F., Hepatitis B virus capsid completion occurs through error correction. *J. Am. Chem. Soc.* **2017,** *139*, 16932-16938.

15. Tan, Z. N.; Pionek, K.; Unchwaniwala, N.; Maguire, M. L.; Loeb, D. D.; Zlotnick, A., The interface between hepatitis B virus capsid proteins affects self-assembly, pregenomic RNA packaging, and reverse transcription. *J. Virol.* **2015,** *89*, 3275-3284.

16. Guo, Y.-H.; Li, Y.-N.; Zhao, J.-R.; Zhang, J.; Yan, Z., HBc binds to the CpG islands of HBV cccDNA and promotes an epigenetic permissive state. *Epigenetics* **2011,** *6*, 720-726.

17. Zlotnick, A.; Venkatakrishnan, B.; Tan, Z. N.; Lewellyn, E.; Turner, W.; Francis, S., Core protein: a pleiotropic keystone in the HBV lifecycle. *Antiviral Res.* **2015,** *121*, 82-93.

18. Feng, S.; Gao, L.; Han, X. C.; Hu, T. S.; Hu, Y. M.; Liu, H. X.; Thomas, A. W.; Yan, Z. P.; Yang, S.; Young, J. A. T.; Yun, H. Y.; Zhu, W.; Shen, H. C., Discovery of small molecule therapeutics for treatment of chronic HBV infection. *ACS Infect. Dis.* **2018,** *4*, 257-277.

19. Corcuera, A.; Stolle, K.; Hillmer, S.; Seitz, S.; Lee, J. Y.; Bartenschlager, R.; Birkmann, A.; Urban, A., Novel non-heteroarylpyrimidine (HAP) capsid assembly modifiers have a different mode of action from HAPs in vitro. *Antiviral Res.* **2018,** *158*, 135-142.

20. Berke, J. M.; Dehertogh, P.; Vergauwen, K.; Van Damme, E.; Mostmans, W.; Vandyck, K.; Pauwels, F., Capsid assembly modulators have a dual mechanism of action in primary human hepatocytes infected with hepatitis B virus. *Antimicrob. Agents Chemother.* **2017,** *6*, e00560-17.

21. Lahlali, T.; Berke, J. M.; Vergauwen, K.; Foca, A.; Vandyck, K.; Pauwels, F.;

Zoulim, F.; Durantel, D., Novel potent capsid assembly modulators regulate multiple steps of the hepatitis B virus life cycle. *Antimicrob. Agents Chemother.* **2018,** *62*, 15.

22. Lam, A. M.; Ren, S. P.; Espiritu, C.; Kelly, M.; Lau, V.; Zheng, L. J.; Hartman, G. D.; Flores, O. A.; Klumpp, K., Hepatitis B virus capsid assembly modulators, but not nucleoside analogs, inhibit the production of extracellular pregenomic RNA and spliced RNA variants. *Antimicrob. Agents Chemother.* **2017,** *61*, e00680-17.

23. Mani, N.; Cole, A. G.; Phelps, J. R.; Ardzinski, A.; Cobarrubias, K. D.; Cuconati, A.; Dorsey, B. D.; Evangelista, E.; Fan, K.; Guo, F.; Guo, H. T.; Guo, J. T.; Harasym, T. O.; Kadhim, S.; Kultgen, S. G.; Lee, A. C. H.; Li, A. H. L.; Long, Q. X.; Majeski, S. A.; Mao, R. C.; McClintock, K. D.; Reid, S. P.; Rijnbrand, R.; Snead, N. M.; Steuer, H. M. M.; Stever, K.; Tang, S.; Wang, X. H.; Zhao, Q.; Sofia, M. J., Preclinical profile of AB-423, an inhibitor of hepatitis B virus pregenomic RNA encapsidation. *Antimicrob. Agents Chemother.* **2018,** *62*, 22.

24. Ko, C.; Bester, R.; Zhou, X.; Xu, Z. H.; Blossey, C.; Sacherl, J.; Vondran, F. W. R.; Gao, L.; Protzer, U., A new role for capsid assembly modulators to target mature hepatitis B virus capsids and prevent virus infection. *Antimicrob. Agents Chemother.* **2020,** *64*, 13.

25. Perni, R. B.; Conway, S. C.; Ladner, S. K.; Zaifert, K.; Otto, M. J.; King, R. W., Phenylpropenamide derivatives as inhibitors of hepatitis B virus replication. *Bioorg. Med. Chem. Lett.* **2000,** *10*, 2687-2690.

26. Campagna, M. R.; Liu, F.; Mao, R. C.; Mills, C.; Cai, D. W.; Guo, F.; Zhao, X. S.; Ye, H.; Cuconati, A.; Guo, H. T.; Chang, J. H.; Xu, X. D.; Block, T. M.; Guo, J. T.,

Sulfamoylbenzamide derivatives inhibit the assembly of hepatitis B virus nucleocapsids. *J. Virol.* **2013,** *87*, 6931-6942.

27. Weber, O.; Schlemmer, K. H.; Hartmann, E.; Hagelschuer, I.; Paessens, A. D.; Graef, E.; Deres, K.; Goldmann, S.; Niewoehner, U.; Stoltefuss, J. D. I., Inhibition of human hepatitis B virus (HBV) by a novel non-nucleosidic compound in a transgenic mouse model. *Antiviral Res.* **2002,** *54*, 69-78.

28. Katen, S. P.; Tan, Z. N.; Chirapu, S. R.; Finn, M. G.; Zlotnick, A., Assembly-directed antivirals differentially bind quasiequivalent pockets to modify hepatitis B virus capsid tertiary and quaternary structure. *Structure* **2013,** *21*, 1406-1416.

29. Klumpp, K.; Lam, A. M.; Lukacs, C.; Vogel, R.; Ren, S. P.; Espiritu, C.; Baydo, R.; Atkins, K.; Abendroth, J.; Liao, G. C.; Efimov, A.; Hartman, G.; Flores, O. A., High-resolution crystal structure of a hepatitis B virus replication inhibitor bound to the viral core protein. *Proc. Natl. Acad. Sci. U. S. A.* **2015,** *112*, 15196-15201.

30. Zhou, Z.; Hu, T. S.; Zhou, X.; Wildum, S.; Garcia-Alcalde, F.; Xu, Z. H.; Wu, D. Z.; Mao, Y.; Tian, X. J.; Zhou, Y.; Shen, F.; Zhang, Z. S.; Tang, G. Z.; Najera, I.; Yang, G.; Shen, H. C.; Young, J. A. T.; Qin, N., Heteroaryldihydropyrimidine (HAP) and sulfamoylbenzamide (SBA) inhibit hepatitis B virus replication by different molecular mechanisms. *Sci Rep* **2017,** *7,* 42374.

31. Liu, H.; Okazaki, S.; Shinoda, W., Heteroaryldihydropyrimidines alter capsid assembly by adjusting the binding affinity and pattern of the hepatitis B virus core protein. *J. Chem. Inf. Model.* **2019,** *59*, 5104-5110.

32. Sari, O.; Boucle, S.; Cox, B. D.; Ozturk, T.; Russell, O. I.; Bassit, L.; Amblard, F.;

Schinazi, R. F., Synthesis of sulfamoylbenzamide derivatives as HBV capsid assembly effector. *Eur. J. Med. Chem.* **2017,** *138*, 407-421.

33. Vandyck, K.; Rombouts, G.; Stoops, B.; Tahri, A.; Vos, A.; Verschueren, W.; Wu, Y. M.; Yang, J. M.; Hou, F. L.; Huang, B.; Vergauwen, K.; Dehertogh, P.; Berke, J. M.; Raboisson, P., Synthesis and evaluation of *N*-phenyl-3-sulfamoyl-benzamide derivatives as capsid assembly modulators inhibiting hepatitis B virus (HBV). *J. Med. Chem.* **2018,** *61*, 6247-6260.

34. Pei, Y. M.; Wang, C. T.; Ben, H. J.; Wang, L.; Ma, Y.; Ma, Q. Y.; Xiang, Y.; Zhang, L. Q.; Liu, G., Discovery of new hepatitis B virus capsid assembly modulators by an optimal high-throughput cell-based assay. *ACS Infect. Dis.* **2019,** *5*, 778-787.

35. Wu, S.; Zhao, Q.; Zhang, P.; Kulp, J.; Hu, L.; Hwang, N.; Zhang, J.; Block, T. M.; Xu, X.; Du, Y.; Chang, J.; Guo, J.-T., Discovery and mechanistic study of benzamide derivatives that modulate hepatitis B virus capsid assembly. *J. Virol.* **2017,** *91*, e00519-17.

36. Vandyck, K.; Verschueren, W. G.; Raboisson, P. J. -M. B., Fused bicyclic sulfamoyl derivatives and the use as medicaments for the treatment of hepatitis B. PCT Int. Appl. WO 2014033167, Mar 6, 2014.

37. Gillis, E. P.; Eastman, K. J.; Hill, M. D.; Donnelly, D. J.; Meanwell, N. A., Applications of fluorine in medicinal chemistry. *J. Med. Chem.* **2015,** *58* , 8315-8359.

38. Ritchie, T. J.; Macdonald, S. J. F.; Young, R. J.; Pickett, S. D., The impact of aromatic ring count on compound developability: further insights by examining carbo- and hetero-aromatic and -aliphatic ring types. *Drug Discov. Today* **2011,** *16*, 164-171.

39. Schaeffer, L., The role of functional groups in drug-receptor interaction: in the practice of medicinal chemistry, 3rd ed, Wermuth, C. -G.; Elsevier, **2008,** pp 464-480.

40. Johnson, T. W.; Gallego, R. A.; Edwards, M. P., Lipophilic efficiency as an important metric in drug design. *J. Med. Chem.* **2018,** *61*, 6401-6420.

41. Tarcsay, A.; Nyiri, K.; Keseru, G. M., Impact of lipophilic efficiency on compound quality. *J. Med. Chem.* **2012,** *55*, 1252-1260.

42. Degorce, S. L.; Bodnarchuk, M. S.; Cumming, I. A.; Scott, J. S., Lowering lipophilicity by adding carbon: one-carbon bridges of morpholines and piperazines. *J. Med. Chem.* **2018,** *61*, 8934-8943.

43. Zafrani, Y.; Sod-Moriah, G.; Yeffet, D.; Berliner, A.; Amir, D.; Marciano, D.; Elias, S.; Katalan, S.; Ashkenazi, N.; Madmon, M.; Gershonov, E.; Saphier, S., CF2H, a functional group-dependent hydrogen-bond donor: is it a more or less lipophilic bioisostere of OH, SH, and CH3? *J. Med. Chem.* **2019,** *62*, 5628-5637.

44. Yan, Z. P.; Wu, D.; Hu, H.; Zeng, J.; Yu, X.; Xu, Z. H.; Zhou, Z.; Zhou, X.; Yang, G.; Young, J. A. T.; Gao, L., Direct inhibition of hepatitis B e antigen by core protein allosteric modulator. *Hepatology* **2019,** *70*, 11-24.

45. Wang, L.; Liu, W.; Liu, Y.; Ji, D.; Si, L.; Zhong, Y.; Xu, D., Establishment of a stable expression and replication cell line transfected with HBV genotype C prevailed in China. *Med. Pharm. J. Chin.* **2010,** *35*, 1425-1428.

46. Serajuddin, A. T. M., Salt formation to improve drug solubility. *Adv. Drug Del. Rev.* **2007,** *59*, 603-616.

47. Yang, P. L.; Althage, A.; Chung, J.; Chisari, F. V., Hydrodynamic injection of viral

DNA: A mouse model of acute hepatitis B virus infection. *Proc. Natl. Acad. Sci. U. S. A.* **2002,** *99*, 13825-13830.

48. Khojasteh, S.C.; Wong, H.; Hop, C., Drug metabolism and pharmacokinetics quick guide. **2011**. DOI 10.1007/978-1-4419-5629-3_2.

49. Sinz, M. W., Avoiding PXR and CAR activation and CYP3A4 enzyme induction. *Top. Med. Chem.* **2013**, *9*, 159−190.

50. Itoh, T.; Mase, T., A general palladium-catalyzed coupling of aryl bromides/triflates and thiols. *Org. Lett.* **2004,** *6*, 4587-4590.

51. Pu, Y. M.; Christesen, A.; Ku, Y. Y., A simple and highly effective oxidative chlorination protocol for the preparation of arenesulfonyl chlorides. *Tetrahedron Lett.* **2010,** *51*, 418-421.

52. Rabe, B.; Vlachou, A.; Pante, N.; Helenius, A.; Kann, M., Nuclear import of hepatitis B virus capsids and release of the viral genome. *Proc. Natl. Acad. Sci. U. S. A.* **2003,** *100*, 9849-9854.

53. Baell, J. B.; Holloway, G. A., New substructure filters for removal of pan assay interference compounds (PAINS) from screening libraries and for their exclusion in bioassays. *J. Med. Chem.* **2010,** *53*, 2719-2740.

54. Irwin, J. J.; Duan, D.; Torosyan, H.; Doak, A. K.; Ziebart, K. T.; Sterling, T.; Tumanian, G.; Shoichet, B. K., An aggregation advisor for ligand discovery. *J. Med. Chem.* **2015,** *58*, 7076-7087.

Table of contents graphic

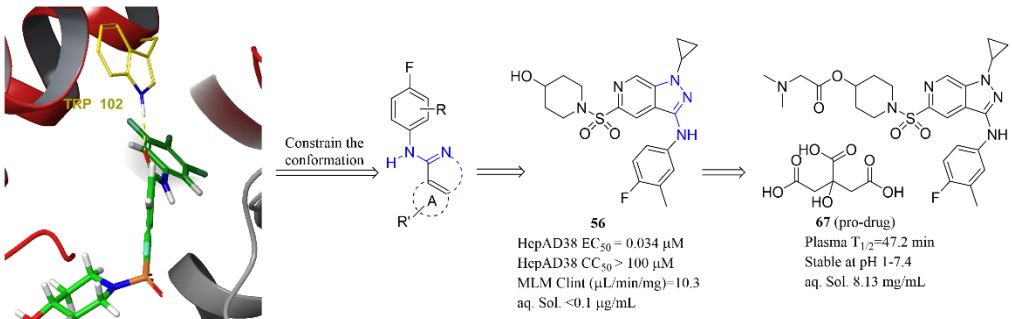

TOC

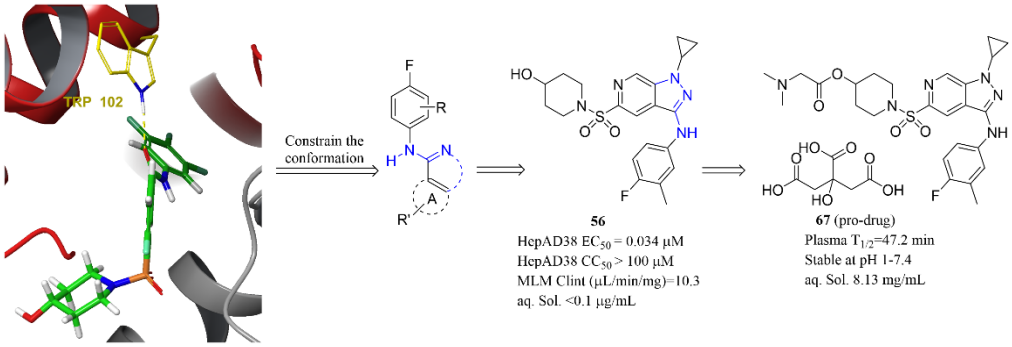
TRP 102
Constrain the conformation
F
R
H
N
N
A
R'
HO
N
S
O
O
NH
F
56
HepAD38 EC50 = 0.034 μM
HepAD38 CC50 > 100 μM
MLM Clint (μL/min/mg)=10.3
aq. Sol. <0.1 μg/mL
O
HO
OH
67 (pro-drug)
Plasma T1/2=47.2 min
Stable at pH 1-7.4
aq. Sol. 8.13 mg/mL